

Dissertation zur Erlangung des Doktorgrades
der Fakultät für Chemie und Pharmazie
der Ludwig-Maximilians-Universität München



Investigation of helenalin-induced cell death in Bcl-2 overexpressing Jurkat cells

Ruth Hoffmann
(geb. Meßmer)
aus Spaichingen

2010

Erklärung

Diese Dissertation wurde im Sinne von §13 Abs. 3 bzw. 4 der Promotionsordnung vom 29. Januar 1998 von Frau Prof. Dr. Angelika M. Vollmar am Lehrstuhl für Pharmazeutische Biologie betreut.

Ehrenwörtliche Versicherung

Diese Dissertation wurde selbstständig, ohne unerlaubte Hilfe erarbeitet.

München, am 20.09.2010

Ruth Hoffmann (geb.Meßmer)

Dissertation eingereicht am:	20.09.2010
1. Gutachter:	Prof. Dr. Angelika M. Vollmar
2. Gutachter:	PD Dr. Manfred Ogris
Mündliche Prüfung am:	29.10.2010

CONTENTS

1 CONTENTS

1	CONTENTS	6
2	INTRODUCTION	10
2.1	Background and aim of the study	10
2.2	Sesquiterpene lactones	11
2.2.1	Helenalin.....	11
2.3	Bcl-2	13
2.3.1	The Bcl-2 family	13
2.3.2	Regulation of Bcl-2 by phosphorylation	13
2.4	Cell death	14
2.5	Apoptosis	14
2.6	Necrosis.....	16
2.7	Autophagy	18
2.7.1	Crosstalk between apoptosis and autophagy	19
2.8	ER stress and autophagy	19
2.8.1	ER stress	19
2.8.2	ER stress - autophagy link.....	20
2.9	Mechanism how Bcl-2 protects from cell death	21
2.9.1	Bcl-2-mediated regulation of mitochondrial membrane permeabilization	21
2.9.2	Bcl-2-mediated regulation of calcium flux in the ER	22
2.10	Significance to overcome Bcl-2-mediated resistance	24
2.10.1	Bcl-2 inhibitors in cancer therapy	24
2.10.2	Overcoming cell death resistance by Bcl-2 overexpression using helenalin	25
3	MATERIALS AND METHODS	28
3.1	Materials	28
3.1.1	Biochemicals, inhibitors, dyes, buffers and cell culture reagents	28
3.1.2	Technical equipment	30
3.2	Cell Culture	30
3.2.1	Cell lines	30
3.2.2	Cell culture.....	31
3.2.3	Seeding for experiments.....	32
3.2.4	Freezing and thawing	32
3.3	Flow cytometry	32
3.3.1	Quantification of Cell death	33
3.3.1.1	Nicoletti assay	33
3.3.1.2	PI exclusion assay.....	33

3.3.1.3	Annexin-V/PI double staining	33
3.3.2	Measurement of ROS generation	34
3.3.3	Measurement of mitochondrial potential dissipation	34
3.4	Clonogenic assay	34
3.5	Western blot	35
3.5.1	Whole lysate preparation	35
3.5.2	Preparation of cytosolic and mitochondrial fractions	36
3.5.3	Immunoprecipitation	36
3.5.4	Protein quantification	37
3.5.5	SDS-PAGE	37
3.5.6	Tank electroblotting	38
3.5.7	Protein detection	39
3.5.7.1	Enhanced chemiluminescence	40
3.5.7.2	Infrared imaging	40
3.5.8	Staining of gels and membranes	41
3.6	Transfection of cells	41
3.6.1	Transfection with Apaf-1 and AIF siRNA	41
3.6.2	Transfection with plasmids	41
3.7	Reporter gene assay	41
3.8	Electrophoretic mobility shift assay (EMSA)	42
3.8.1	Preparation of nuclear extracts	42
3.8.2	Binding reaction and electrophoretic separation	43
3.9	Caspase activity assay	44
3.10	Calcium measurement	45
3.11	Transmission Electron Microscopy	45
3.12	Statistical Analysis	45
4	RESULTS	48
4.1	Helenalin overcomes Bcl-2-mediated resistance	48
4.2	Helenalin does not abrogate mitochondrial function of Bcl-2 and acts independently of the mitochondria and the apoptosome	51
4.2.1	Mitochondrial function	51
4.2.2	Caspase dependency	54
4.3	Mechanisms of helenalin's bypass of Bcl-2-mediated cytoprotection	58
4.3.1	ER stress, autophagy and necroptosis	58
4.3.2	Helenalin inhibits Bcl-2-induced NF- κ B activity	63
4.3.3	Helenalin induces cell death by induction of ROS	66

5	DISCUSSION	70
5.1	Untypical signaling of helenalin-induced cell death	70
5.1.1	Apoptosis	70
5.1.2	Autophagy	71
5.1.3	Helenalin-induced cell death shows necrotic features.....	72
5.2	NF- κ B inhibition and ROS formation are crucial for helenalin-induced cell death ..	72
5.2.1	Increased NF- κ B activity in Bcl-2 overexpressing Jurkat cells is inhibited by helenalin	74
5.2.2	Inhibition of Akt by helenalin.....	74
5.2.3	Helenalin induces ROS generation	75
5.2.4	Overcoming pro-survival pathways via selective NF- κ B inhibition and ROS generation.....	76
6	SUMMARY AND CONCLUSION	78
7	REFERENCES	80
8	APPENDIX	90
8.1	Abbreviations	90
8.2	Publications	94
8.2.1	Original Publications.....	94
8.2.2	Abstracts.....	94
8.3	Curriculum vitae.....	95
8.4	Acknowledgements	96

INTRODUCTION

2 INTRODUCTION

2.1 Background and aim of the study

Cancer-treatment is still one of the biggest challenges in developed countries despite the global efforts and the major steps forward concerning cancer treatment during the last decades. The main problems of cancer therapy are selectivity of chemotherapeutics used and therefore acute and long-term side effects, the probability of relapses and resistance to chemotherapeutic agents. Many standard chemotherapeutics act via targeting mitochondria, thus inducing the release of cytotoxic proteins from mitochondria into the cytosol, which results in induction of cell death by apoptosis¹. Bcl-2 was identified as a proto-oncogene involved in B-cell lymphoma and prevents apoptosis by acting on mitochondria. Overexpression of Bcl-2 often confers chemoresistance and thus is a promising target to combat drug resistance^{2,3}.

Sesquiterpene lactones have been intensively studied concerning their anticancer properties during the last years. Helenalin holds impressive effects on cancer cells *in vitro* and *in vivo*⁴. More importantly, besides its well known capacity to inhibit NF- κ B, our group has shown that helenalin selectively kills human Jurkat T-leukemia cells by targeting the mitochondrial pathway of apoptosis. Interestingly, helenalin was also able to induce cell death in two highly resistant Jurkat cell lines, which overexpress the antiapoptotic proteins Bcl-2 or Bcl-X_L. The mechanism of how helenalin overcomes resistance mediated by Bcl-2 family members has not been studied yet.

Thus, it was the aim of the present work

- **to examine the type of cell death induced by helenalin in Bcl-2 overexpressing Jurkat cells and**
- **to study the underlying mechanisms how helenalin overcomes Bcl-2-mediated cell death resistance in Jurkat cells.**

2.2 Sesquiterpene lactones

Sesquiterpene lactones (STLs) are important secondary metabolites of plants, predominantly found in the sunflower family (Asteraceae). Structurally, they represent C₁₅-terpenoids and their derivatives, which can be further divided into other groups, e.g. the pseudoguaianolide-type STLs, where helenalin belongs to. STLs possess cytotoxic⁵⁻⁸ as well as anti-inflammatory⁹⁻¹⁴ potential. Moreover, they exhibit antibacterial, analgesic, positive inotropic, as well as migraine inhibiting properties^{5,15}. Preparations from flowers of *Arnica montana* are used externally in traditional medicine to treat various inflammatory diseases. The anti-inflammatory activity of STL has been mainly linked to an inhibition of the transcription factor nuclear factor κB (NF-κB).

The biological activity of STLs has been associated with α,β-unsaturated carbonyl structural elements like an α-methylene-γ-lactone or an α,β-unsaturated cyclopentenone moiety^{12,14}. These α,β-unsaturated carbonyl structures can react with nucleophiles, especially cysteine sulfhydryl groups of biological molecules (such as endogenous glutathione) by a Michael-type addition^{4,6,16}. It is therefore not surprising, that STLs have been shown to inhibit a variety of important sulfhydryl-bearing enzymes¹⁶. Existence of a α-methylene-γ-lactone group was essential for their cytotoxic activity and an α,β-unsaturated ester or cyclopentenone strengthened this property⁶. Moreover, cytotoxicity of STLs is strongly dependent on the number and type of alkylating centers. The molecular conformation and the number of H-bond acceptors are also important as noncovalent interactions of STLs with proteins may precede alkylation¹⁴. Importantly, a number of STL-derived drugs are now in phase I-II of clinical trials against a variety of cancer types such as blood-lymph tumors, metastatic breast cancer and nonsmall cell lung cancer¹⁷.

2.2.1 Helenalin

Helenalin is a naturally occurring sesquiterpene lactone extracted from *Arnica montana* and *Arnica chamissonis* ssp. *foliosa* possessing two α,β-unsaturated carbonyl structural elements. The structure of helenalin is shown in Figure 1.

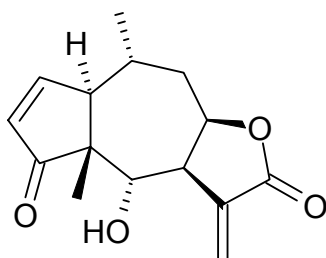


Figure 1 Chemical structure of helenalin.

The antitumoral activity of helenalin was first reported in 1967. Helenalin was the most active constituent of a collection of *Helenium autumnale* screened by the NCI in an *in vivo* assay employing the murine P388 lymphocytic leukaemia¹⁸. Helenalin is cytotoxic to a variety of tumor cells in culture such as human Tmolt3 leukemia, colon adenocarcinoma, cervical adenocarcinoma, osteosarcoma, and glioma cells^{7, 19-21} and has also shown *in vivo* antitumor activity against Walker 256 carcinoma in rats, Ehrlich ascites carcinoma in mice and P388 lymphocytic leukaemia in mice⁴. In contrast to other STLs, studies on helenalin derivatives have shown that the contribution of a cyclopentenone group to its cytotoxicity is considerably higher than that of the methylene lactone group²². The α,β -unsaturated cyclopentenone shows higher reactivity with GSH (glutathione; γ -L-glutamyl-L-cysteinylglycine)¹⁶, and this may probably be the reason why inhibition of GSH synthesis increases cytotoxicity²³, whereas high GSH levels in tumor cells correlate with decreased effects of helenalin²⁴. Helenalin influences a variety of necessary events in the cells by inhibition of Akt (also in preadipocytes)²⁵, protein synthesis (by induction of eIF2 α phosphorylation), DNA synthesis⁴, and telomerase²⁶. It also shows anti-proliferative effects (post-transcriptional nuclear p21 accumulation and inhibition of p27 degradation, protein interactions between p21 and cyclin-dependent kinase 2 (CDK2) are increased, G1 arrest)²⁷. Moreover, helenalin also holds anti-inflammatory properties *in vitro* and *in vivo*. Helenalin reduces edema and chronic-adjuvant-provoked arthritis in the rat²⁸ and it inhibits the migration and chemotaxis of human neutrophils¹², as well as the activities of 5-lipoxygenase and leukotriene C4 synthase²⁹. In line with this, it was shown that helenalin significantly reduces leukocyte infiltration in the mammary gland and decreases *S.aureus* intracellular growth and experimental *S.aureus* infection *in vivo*³⁰. In addition, helenalin induces apoptosis or inhibits proliferation in activated CD4⁺ T cells, and downregulates pro-inflammatory surface receptors and IL-2 production. Thus, helenalin possesses immunosuppressive activity suited for treatment of deregulated and unwanted T cell-mediated immune response³¹. Helenalin inhibits DNA binding of NF- κ B by alkylating p65 at Cys38, but not modifying p50. Although a slight inhibition of I κ B degradation of STLs was also detected, this effect was secondary to alkylation of NF- κ B^{9, 32-35}. Experiments using surface-plasmon resonance method showed that helenalin interacts with the NF- κ B protein RelA (p65) but not with IKK α and IKK β (I κ B kinase α and β), and also not with glutathione at physiological pH to any significant extent, but could bind to reduced form of glutathione at higher pH (pH 8)³⁵.

Previous work of Dirsch et al. showed that helenalin induces caspase-dependent apoptosis in leukaemia Jurkat T-cells (S-Jurkat cells) through the classical mitochondrial pathway, including cytochrome c release preceding caspase activation. The helenalin-induced signaling pathway did not require the death receptor CD95. Interestingly, healthy human

activated blood mononuclear cells were not affected. Although helenalin induces a mitochondria-dependent pathway of apoptosis in S-Jurkat cells, overexpression of the mitochondria protecting proteins Bcl-2 and Bcl-X_L failed to prevent helenalin-induced cell death²¹. Yet, the underlying mechanisms of this phenomenon have not been investigated up to now.

2.3 Bcl-2

2.3.1 The Bcl-2 family

The Bcl-2 family has been grouped into three classes. One class inhibits apoptosis (Bcl-2, Bcl-X_L, Mcl-1, Bcl-B, Bcl-W and A1), whereas the other shows pro-apoptotic properties (Bax, Bak and Bok). Both classes share several regions of sequence homology, BH (Bcl-2 homology) domains (BH1-4 for anti-apoptotic members, BH1-3 for pro-apoptotic members). The third divergent class of BH3-only proteins (Bad, Bik, Bid, HRK, Bim, Bmf, Puma, Noxa) possesses a conserved BH3 domain.

Bax and Bak undergo conformational changes upon activation, oligomerize and form pores in the outer mitochondrial membrane allowing the release of proteins into the cytosol. Despite intensive investigation, the exact mechanism of this process and how antiapoptotic proteins might regulate it, is still controversial. It is thought that Bcl-2 blocks Bax and Bak oligomerisation by binding to the nascent multimers and capping further chain elongation³⁶⁻³⁸. Regardless of the exact mode of activation of Bax and Bak, the ratio of anti-versus pro-apoptotic Bcl-2 proteins rather than the expression levels of one particular molecule of the Bcl-2 family regulates apoptosis sensitivity.

2.3.2 Regulation of Bcl-2 by phosphorylation

Phosphorylation of Bcl-2 in the flexible loop domain is the major regulatory mechanism, modulating the function of Bcl-2. It has been shown that either mono- (S70) or multisite (T69, S70, S87) phosphorylation of Bcl-2 is required for antiapoptotic function of Bcl-2³⁹. Moreover, it has been shown that Bcl-2 functions as an antioxidant⁴⁰, and phosphorylated Bcl-2 slows down G1/S cell cycle transition in association with decreased ROS and increased p27 (CDK2 inhibitor) levels⁴¹. However, other investigators have shown that the multiple-site phosphorylation by JNK abrogates survival function of Bcl-2 in paclitaxel-induced apoptosis⁴². Thus, it seems that the type of stimulus, other regulatory pathways and the degree and duration of the phosphorylation at specific residues of Bcl-2 produce different outcomes⁴³.

2.4 Cell death

Cell death has historically been subdivided into regulated and unregulated forms of cell death but there is emerging evidence that this simple classification does not adequately explain the various cell death mechanisms as there exist multiple non-apoptotic, regulated forms of cell death, some of which overlap apoptosis ⁴⁴.

2.5 Apoptosis

The term apoptosis is based on the morphological characteristics of cells dying from apoptosis, including cellular shrinkage, membrane blebbing and ultimately fragmentation into membrane bound apoptotic bodies ⁴⁵. Apoptosis, which is also called cell death type I, is controlled both positively and negatively by the B-cell lymphoma protein-2 (Bcl-2) family members and involves the sequential activation of caspases ⁴⁴ (although caspase-independent forms of apoptosis can also occur). During apoptosis, the integrity of plasma membrane is conserved but phosphatidylserine (PS) becomes exposed on the cell surface. PS exposure functions as an “eat me” signal for macrophages, which mediate the effective clearance of apoptotic cells. The quick removal of a dying cell is crucial for immune tolerance and tissue homeostasis. Apoptosis is suggested not to trigger inflammation as the immediate clearance of the dying cell prevents the release of intracellular contents. Additionally, the production of anti-inflammatory mediators by phagocytes suppresses inflammation and assists the “immunologically silent” clearance of the cells ⁴⁶.

Apoptosis can be initiated by two types of signals: intracellular stress signals such as DNA damage, oxidative stress or oncogene activation causing the activation of the intrinsic or mitochondrial apoptosis pathway, or extracellular ligands such as Fas ligand, TNF α or TRAIL (INF-related apoptosis-inducing ligand) causing activation of the extracellular or death-receptor apoptosis pathway ⁴⁵. The intrinsic pathway is characterized by the permeabilization of the mitochondrial outer membrane causing the release of pro-apoptotic proteins from the intermembrane space such as cytochrome *c*, AIF (apoptosis inducing factor), EndoG (endonuclease G), Smac/Diablo (secund mitochondria derived activator of caspases/direct IAP binding protein with low pI) and Omi/HtrA2 (high temperature requirement protein A2). This process is tightly regulated by Bcl-2 family members. Release of cytochrome *c*, which is involved in the electron transport, leads to the energy-dependent (ATP/dATP) formation of a complex, the apoptosome, which consists of cytochrome *c*, Apaf-1 (apoptotic protease-activating factor-1) and the initiator caspase-9. Subsequently, caspase-9 is activated which activates further downstream executioner caspases such as caspase-3, which finally leads to cell death ³⁸. Accidental activation of caspases is negatively regulated by inhibitors of apoptosis proteins (IAPs), which are in turn inactivated by Smac and Omi/HtrA2. The latter is

a serine protease and has been reported to cleave cIAPs and to participate in caspase-independent apoptosis. Smac is the best known antagonist of the IAP family and competes with caspase-9 for binding to XIAP and therefore gives rise for induction of apoptosis⁴⁷.

AIF and EndoG both induce caspase-independent cell death. AIF translocates to the nucleus and induces chromatin condensation and high molecular weight DNA fragmentation. Translocation of EndoG to the nucleus also results in internucleosomal DNA fragmentation⁴⁸.

The extrinsic pathway triggers apoptosis by binding of proapoptotic ligands to their cell surface receptors from the tumor necrosis factor receptor (TNFR) family such as TNFR1, TRAIL or CD95 (= Fas, APO-1). This results in the recruitment of intracellular adaptor proteins such as FADD and formation of the death inducing signaling complex (DISC) which brings about activation of procaspase-8. Active caspase-8 can activate effector caspases, which is sufficient to induce apoptosis in type I cells. Moreover, caspase-8 can cleave proapoptotic BH3-only protein Bid into t-Bid, which translocates to mitochondria to induce mitochondrial membrane permeabilisation. This amplification loop is necessary in type II cells, where the sole activation of caspase-8 is not sufficient to induce apoptosis⁴⁹.

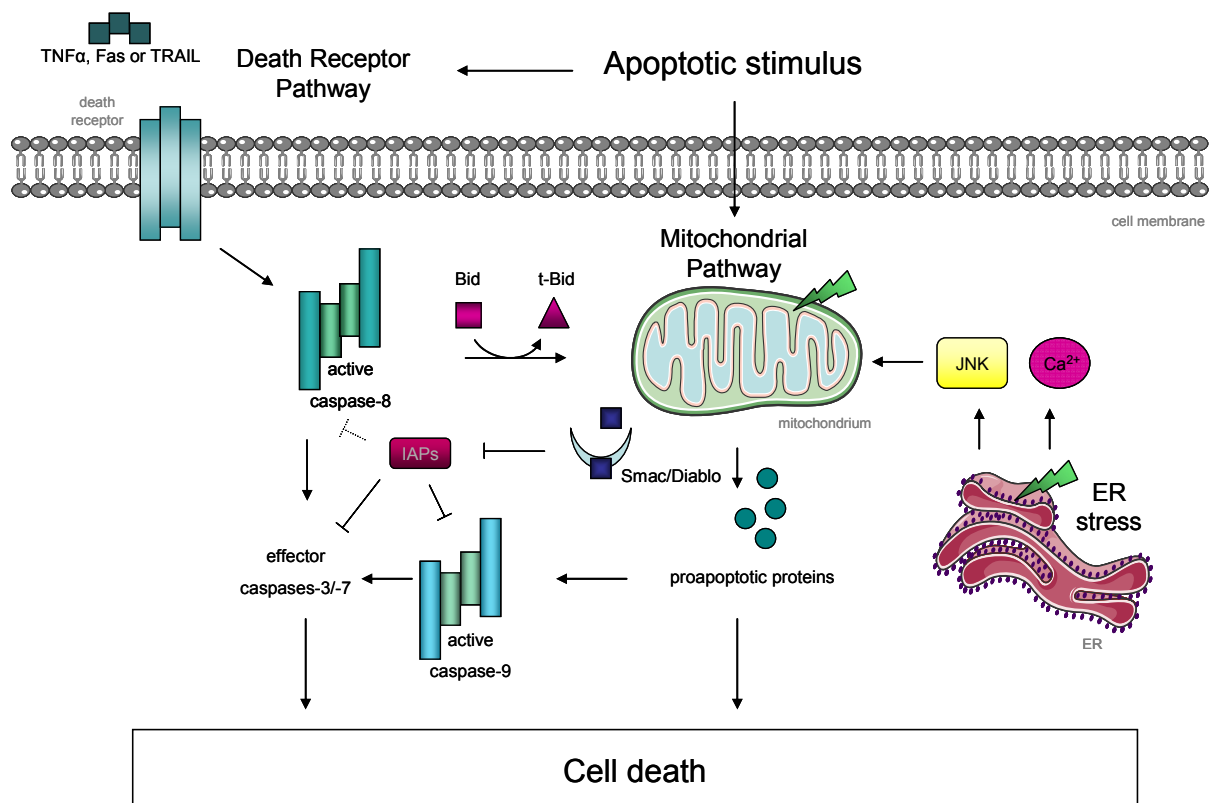


Figure 2 Schematic representation of intrinsic and extrinsic apoptotic pathway. Stimulation of the death receptor initiates the extrinsic pathway by activation of caspase-8. Subsequent activation of executioner caspases leads to cell death. Cleavage of Bid by caspase-8 amplifies the extrinsic pathway by activation of the mitochondrial pathway. The intrinsic pathway of apoptosis is induced by intracellular stress signals and results in the release of several mitochondrial apoptotic mediators. Subsequent formation of the apoptosome leads to activation of caspase-9. Caspases are negatively regulated by IAPs, which in turn are inhibited by Smac/Diablo. ER stress-mediated calcium-release and JNK activation also promote induction of the intrinsic pathway of apoptosis.

2.6 Necrosis

There is now evidence that necrosis, traditionally considered an accidental form of cell death, can be initiated or modulated by programmed control mechanisms. ROS (reactive oxygen species), calcium-ions, poly-ADP-ribose polymerase (PARP), calcium-activated nonlysosomal proteases (calpains) and cathepsins are some of the mediators of necrosis⁵⁰. Yet, several of them are also known to induce apoptosis such as calcium. The identification of an intracellular serpin (protease inhibitor) which prevents necrosis indicates that necrosis can be regulated, programmed and driven by a peptidase stress-response pathway⁵¹.

Necrosis is morphologically characterized by vacuolation of cytoplasm, organelle breakdown, cytoplasmic swelling, breakdown of the plasma membrane^{52, 53} and induction of inflammation due to the release of cellular contents and proinflammatory molecules such as damage-associated molecular pattern (DAMP) molecules, e.g. high-mobility group box 1 (HMGB1) protein, which activate the innate immune cells and thus promote an alerting system for defensive or reparative response⁵⁴. Moreover, processes like mitochondrial swelling, permeability transition (PT) pore opening, loss of mitochondrial membrane potential and ROS production are observed. Necrotic cells can also exhibit changes in nuclear morphology but no organized chromatin condensation and DNA fragmentation as seen in apoptotic processes. Recently, two forms of “programmed necrosis” have been described: necroptosis and PARP1-mediated necrotic death⁴⁴.

Necroptosis has been reported as a form of programmed necrotic cell death under conditions where apoptotic cell death is prevented⁵⁵. Although induction of autophagy has been observed in a number of cell lines by necroptotic signaling, autophagy seems to be a downstream consequence of necroptosis rather than a contributing factor. Moreover, activation of necroptosis requires the kinase activity of RIP1 (receptor interacting protein 1), which is not required for NF- κ B and apoptosis signaling in Jurkat cells⁵⁶. Furthermore, RIP3 has been identified as a crucial upstream activating kinase that regulates RIP1-dependent necroptosis⁵⁷. RIP1 translocates into mitochondria and induces disruption of the bonding of ANT (adenine nucleotide translocase) with cyclophilin D (CypD), a peptidyl-prolyl isomerase, causing rapid mitochondrial dysfunction that is associated with necroptosis. Other execution steps, including activation of phospholipase A2 and lipoxygenases have been described⁴⁴. Necrostatins are well characterized inhibitors of RIP1 and therefore commonly used inhibitors of necroptosis.

PARP1-mediated necrosis is initiated by DNA strand breaks e.g. by alkylating DNA damage, which rapidly activates PARP1. Overactivation of PARP1 mediates depletion of cytosolic NAD⁺ and subsequently induction of necrosis by “energy collapse” in glycolytic cells. PARP1 inhibitors were developed as chemopotentiators of DNA damaging anticancer agents. Moreover, PARP1 activation causes specific release of HMGB1, which can alert immune

cells to the presence of dangerous cells with damaged DNA. But PARP1 also mediates cell death induced by secondary DNA damage. Here, PAR (poly-ADP-ribose) polymer is translocated into the cytosol, which subsequently causes translocation of AIF from mitochondria to the nuclei, where it induces cell death. PARP1-mediated cell death furthermore involves TRAF2-RIP1 (TNF receptor-associated factor 2) dependent JNK activation, which contributes to mitochondrial dysfunction and necrotic death, the relationship between this process and necroptosis remains unclear⁴⁴.

Necrosis often takes place when other cell death programs such as apoptosis or autophagy are blocked⁵⁸, thus necrosis is a mechanism to overcome resistance to apoptosis as observed in several human tumors^{52, 59} and has been observed in apoptosis-defective breast carcinomas treated with anthracycline-based therapy in the clinic⁶⁰. Moreover, the inflammatory component of necrotic death has potential advantage of stimulating an immune response that could increase the efficacy of chemotherapy e.g. of the Abl kinase inhibitor imatinib⁵². On the other hand, sustained inflammatory response can stimulate tumor development. Whether necrosis plays a major role in tumorigenesis is still unclear, as it is almost impossible to experimentally prevent or induce necrosis *in vivo* without affecting other types of cell death.

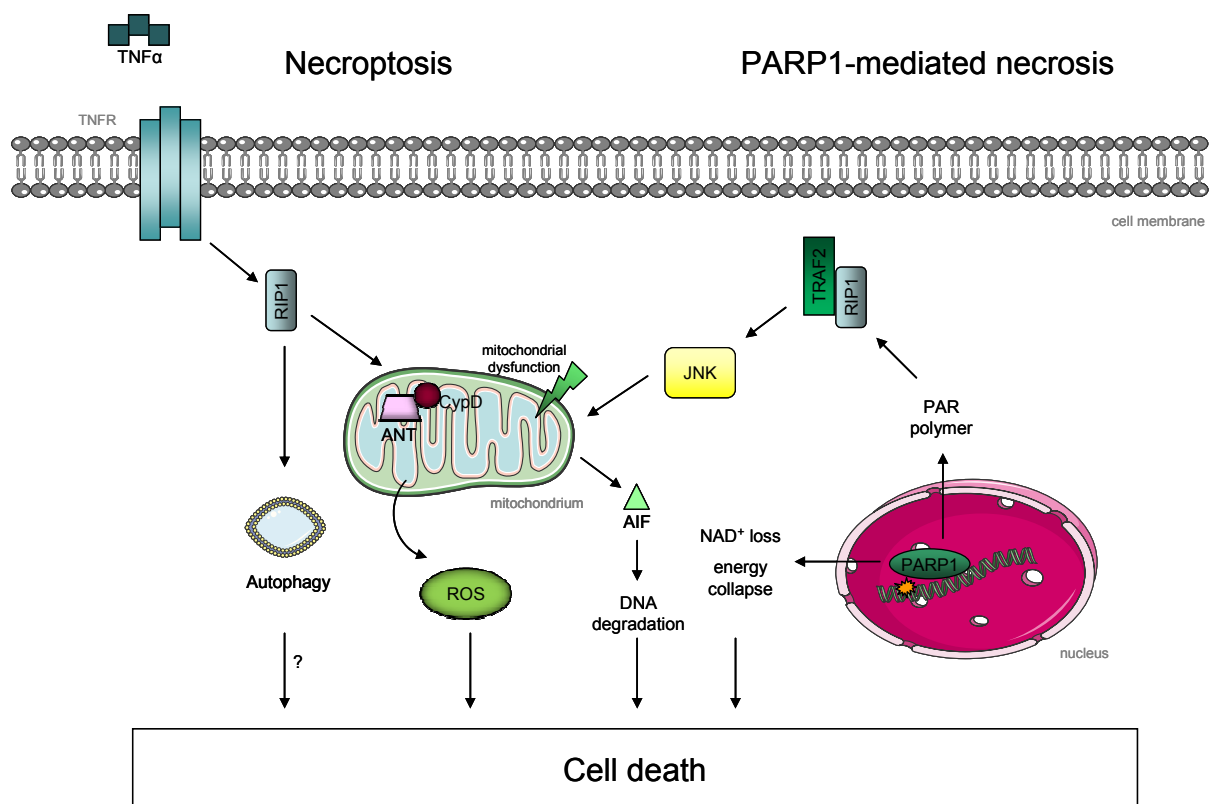


Figure 3 Schematic representation of necrotic signaling. Stimulation of the TNFR leads to activation of RIP1. Through RIP1 kinase activity, the association between ANT and CypD is disrupted and resulting in ATP depletion and the accumulation of ROS. Autophagy can be activated during necroptosis, but it only contributes to cell death in some cell types. DNA damage activates PARP1. Two pathways of PARP1-mediated cell death are shown: energy collapse and AIF translocation. TRAF2-RIP1 dependent JNK activation contributes to mitochondrial dysfunction and necrotic death.

2.7 Autophagy

Macroautophagy, hereafter referred to as autophagy (self eating), which is also called cell death type II, is a multistep process that is characterized by the formation of double- or multi-membraned autophagic vacuoles called autophagosomes. Subsequently, autolysosomes are generated by fusion of the outer membranes of the autophagosomes and late endosomes or lysosomes, which results in vesicular sequestration and degradation of long-lived cytoplasmic proteins and organelles such as mitochondria⁶¹. Autophagy is required for mammalian embryogenesis. It is also observed in cells after exposure to a variety of metabolic and therapeutic stresses such as growth factor deprivation, shortage of nutrients, inhibition of the receptor tyrosine kinase/Akt/mammalian target of rapamycin (mTOR) signaling (e.g. by stimulation with rapamycin), accumulation of intracellular calcium and ER stress. It is still controversial whether autophagy is protective or toxic for cells. Some reports show strong evidence that autophagy prevents inflammation and cancer. Although autophagy serves as tumor suppressor mechanism, autophagy is also a stress survival pathway and inhibition of autophagy could enhance chemotherapy^{62, 63}. The molecular understanding of autophagy was enhanced by the discovery of autophagy-related genes (Atg), which are involved in the control of autophagy. Eighteen yeast Atg, which are required for autophagosome formation have been identified and several mammalian homologues have already been characterized⁴⁴. The initial steps of autophagy induction are the inhibition of the mTOR Ser/Thr kinase, which blocks autophagy and the activation of mammalian Vsp34⁶¹. The formation of the complex consisting of the protein Beclin1, Vps34 (a class III phosphatidylinositol 3-kinase), UVRAG (UV irradiation resistance-associated tumor suppressor gene) and a myristylated kinase (p150 or Vps15) is required for the initiation of the autophagosomes formation as Vps34 becomes activated and catalyzes generation of phosphatidylinositol-3-phosphate, which is necessary for vesicle nucleation. Further downstream, two major conjugation systems are necessary for autophagosomes formation and vesicle elongation as both contribute to the conjugation of phosphatidylethanolamine (PE) to the soluble form of LC3 (named LC3 I) resulting in its conversion to LC3 II, which is associated with peripheral membranes of autophagosomes. These conjugation systems are closely related to ubiquitin-conjugation systems to proteins. The Atg12-Atg5 conjugation pathway results in covalent conjugation of Atg12 to Atg5 and the formation of a larger complex containing oligomerized Atg16. Atg12-Atg5 formation is constitutive and not influenced by autophagy-inducing stimuli⁶²⁻⁶⁴. After maturation to autolysosomes, the inner membrane as well as the luminal content is digested by lysosomal enzymes within the acidic compartment⁶¹.

Inhibition of autophagy can be achieved by the use of 3-MA (3-methyladenine), which is a PI3K inhibitor (inhibiting Vps34) or chloroquine, which inhibits fusion of autophagosomes with

lysosomes. Moreover, small interfering RNAs, which are capable to inhibit Beclin1, Vsp34, Atg5, Atg10, Atg12 or Lamp2 (lysosomal-associated membrane protein 2) can be used. Induction of autophagy is achieved by the use of rapamycin, which inhibits mTOR activity^{61, 65}.

2.7.1 Crosstalk between apoptosis and autophagy

Depending on the circumstances, autophagy can protect cells against cell death but it also can cause cellular demise. The cytotoxic effect of autophagy can be explained by the direct massive self-destructive potential of autophagy or by enabling the induction of apoptosis by the autophagic process. Numerous studies have described an existing cross-talk between apoptosis and autophagy. There are three possibilities how this cross-talk can take place. The first possibility is a kind of apoptosis/autophagy partnership where both, apoptosis and autophagy, can lead to cell death, or, autophagy can occur upstream of apoptosis whereas it also simultaneously modulates independent means of cell death, or, apoptosis may suppress autophagy. The second possibility is that autophagy suppresses apoptosis by promoting cell survival. A third possibility is that autophagy enables apoptosis, which means that autophagy itself does not lead to cell death but enables the apoptotic program by participation in certain morphological changes^{61, 66}.

2.8 ER stress and autophagy

2.8.1 ER stress

Cellular stresses as perturbed calcium homeostasis (calcium overload or depletion of the ER calcium pool⁶⁷), redox state or decreased ATP levels can interfere with protein folding. This causes protein misfolding and activation of an adaptive stress response (UPR), thus trying to increase folding capacity of the ER (endoplasmic reticulum) by induction of proteins involved in chaperoning, protein folding and degradation pathways. Transduction of the UPR (unfolded protein response) is provided by three ER located stress sensors, PKR-like ER kinase (PERK), inositol-requiring enzyme 1 (IRE α and β) and activating transcription factor 6 (ATF6 α and β), which are all bound to glucose-related protein 78 (GRP78) when ER stress is absent. Initiation of UPR is triggered by dissociation of GRP78 from all three sensors. Activated IRE1 recruits TRAF2 that in turn recruits apoptosis signal-regulating kinase 1 (ASK1) which activates JNK (stress-activated c-Jun N-terminal protein kinase). Activated PERK phosphorylates the α -subunit of eukaryotic translocation initiation factor-2 (eIF2 α) which leads to translation suppression. Moreover, the PERK-eIF2 α pathway also induces translation of UPR target genes through selective upregulation of the translation of the transcription factor ATF4.^{62, 68} If the stress, however, is too great, cell death can be induced. Many studies have shown that ER stress can lead to induction of apoptosis through

activation of caspase-12/-4 (which activates caspase-9) and CHOP (transcription factor downstream of PERK and ATF6, which downregulates Bcl-2), IRE1-JNK (targets several Bcl-2 family proteins) and calcium (promotes release of cytochrome c) pathways. Recent reports however, have reported that ER stress can trigger autophagy, as well.

2.8.2 ER stress - autophagy link

ER stress can be a potent inducer of autophagy although it is still not clear whether autophagy in this context is ultimately a cytoprotective mechanism or a precursor to a form of non-apoptotic cell death resembling necrosis^{69, 70}. Continued autophagy is detrimental to cell survival as a consequence of excess organelle and macromolecular catabolism similar to prolonged UPR, which leads to cell death via apoptosis. On the contrary, induction of autophagy shows cytoprotective capacity, as it is important to counteract ER expansion and to degrade protein aggregates during ER stress⁶⁸. Beclin1, located at mitochondria, the ER and the *trans*-Golgi network, is an important inducer of autophagy and has been discovered as a Bcl-2 interacting protein by its BH3 (Bcl-2 homology) domain⁷¹ whereby only ER-tagged Bcl-2 suppresses Beclin1-dependent autophagy⁷². Beclin1 itself fails to induce apoptosis⁷¹. On the other hand, Bcl-2 bound to Beclin1 still maintains its full antiapoptotic capacity. Besides, Bcl-2/Beclin1 interaction can be disrupted by different stimuli subsequently inducing autophagy. Not only the phosphorylation of Bcl-2 (e.g. by JNK) or the phosphorylation of Thr119 in the BH3 domain of Beclin1 (by DAP-kinase) can lead to disruption of the complex, also the competitive distraction by other BH3-only proteins (e.g. Bad) or pharmacological BH3 peptidomimetic agents (e.g. ABT-737) can activate autophagy⁷³.

The ER represents the most important storage site for Ca²⁺ in the cell. Upon ER stress, high amounts of Ca²⁺ can be released into the cytosol, mediating further downstream effects such as apoptosis^{67, 74} or autophagy. Ca²⁺-mediated activation of protein kinase C θ (PKC θ) and of Ca²⁺/calmodulin-dependent kinase kinase- β (CaMKK β) was recently reported to induce autophagy in the context of ER stress^{75, 76}. In addition to the effects of Ca²⁺ released from ER into cytosol, it is also likely that altered concentrations of ER stored Ca²⁺ directly affects UPR signal transduction events that are relevant to cell death regulation⁷⁷.

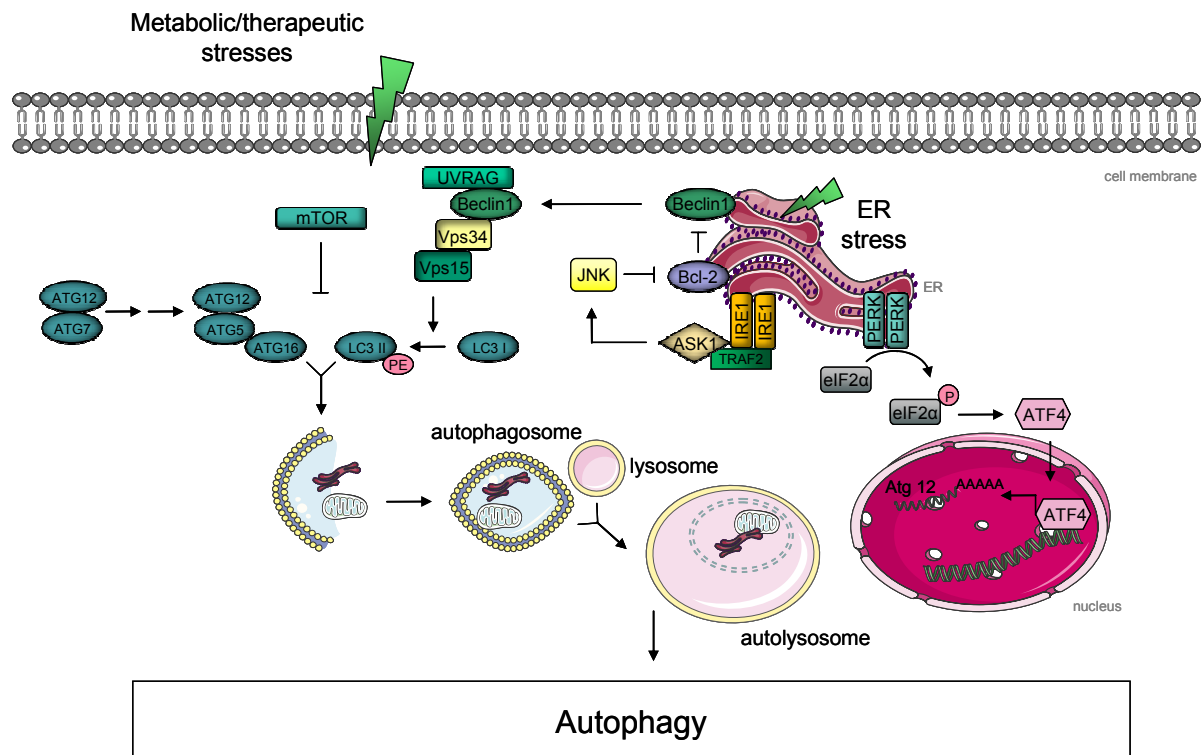


Figure 4 Schematic representation of autophagic signaling. Metabolic and therapeutic stresses as well as ER stress can induce autophagy. Nutrient deprivation suppresses mTOR activity, which in turn inhibits induction of autophagy. Two arms of UPR have been implicated in regulating autophagy during ER stress. The IRE1/JNK pathway enhances autophagy and PERK signaling also potentiates autophagy, possibly via transcriptional upregulation of Atg 12. Bcl-2 is capable of inhibiting autophagy through direct binding to Beclin1. Inhibitory binding of Bcl-2 to Beclin1 is disrupted by JNK mediated phosphorylation of Bcl-2, which results in the formation in the multiprotein complex consisting of Beclin1, UVRAG, Vps15 and Vps34. This leads to activation of the PI3K Vps34, which is necessary for vesicle nucleation. Two ubiquitin-like conjugation systems (LC3 I/II and Atg12-Atg5) are required to form double membrane-walled autophagosomes. Fusion between autophagosomes and lysosomes forms autolysosomes wherein sequestered material is degraded.

2.9 Mechanism how Bcl-2 protects from cell death

Bcl-2 is embedded in the outer mitochondrial membrane (OMM), the ER and the nuclear envelope by a C-terminal hydrophobic membrane-spanning domain, with most of its amino-acids in the cytosol^{78, 79}. Whereas the function of Bcl-2 in the nuclear membrane is not as clear, it exerts its pro-survival activity by acting on mitochondrial pathway of apoptosis and on ER.

2.9.1 Bcl-2-mediated regulation of mitochondrial membrane permeabilization

Bcl-2 counteracts the pro-apoptotic capacity of Bax and Bak and therefore prevents the release of pro-apoptotic factors such as cytochrome c from the mitochondria^{80, 81}. Moreover, mitochondria are also well known mediators of necrotic cell death. The mitochondrial membrane permeability transition (MPT) occurs after opening of a channel complex induced

by calcium overload or oxidative stress. This channel complex has been termed the permeability transition pore (PTP) and is thought to consist of the voltage-dependent anion channel (VDAC:outer membrane channel), the adenine nucleotide translocator (ANT:inner membrane channel), cyclophilin D (CypD) and possibly further molecules. CypD-dependent MTP leads to permeability of both, the inner and the outer mitochondrial membrane finally causing necrosis. As Bcl-2 has the ability to block the MPT probably by inhibiting VDAC activity or other unknown channels involved in MPT, it can therefore block MPT-dependent necrosis in addition to its well established ability to inhibit apoptosis⁸². Additionally, it has been shown that in isolated pancreatic mitochondria PTP mediates loss of mitochondrial membrane potential but not cytochrome c release^{83, 84}. Defects in the electron chain transport in respiring mitochondria causes accumulation of ROS within the cells, causing cellular swelling and plasma membrane rupture, as well as rupture of lysosomes and release of hydrolytic enzymes that destroy proteins, nucleic acids and lipids. MOMP (mitochondrial outer membrane permeabilization) also releases several proteins that contribute to non-apoptotic cell death, including DNase, endonuclease G and AIF⁸⁵.

However, Bcl-2 overexpression cannot always protect from cell death as seen in lymphocytes overexpressing Bcl-2, which are not protected against apoptosis induced by death receptor ligands^{86, 87}. This is due to the fact that in these cell types, also called cell type I, the two apoptotic pathways can be largely independent and caspase-8 activation by the death receptor pathway is sufficient to activate effector caspases without amplification loop mediated by mitochondria.

2.9.2 Bcl-2-mediated regulation of calcium flux in the ER

Even though a lot of research has focused on the actions of Bcl-2 family on the mitochondria, it is long known that Bcl-2 has an antiapoptotic role at the ER. The ER has been identified as a critical early checkpoint that regulates the initiation of mitochondria-dependent pathway of apoptosis in response to severe or prolonged ER stress although the exact mechanisms remain controversial⁶⁸. The ER represents the most important storage site for Ca^{2+} in the cell. Calcium import and export is tightly regulated by two main transporters: the sarcoplasmic/endoplasmic reticulum calcium-ATPase (SERCA) (active import of Ca^{2+}) and the inositol triphosphate (IP_3) receptor (IP_3R) mediating transient release of Ca^{2+} into the cytosol. The release of Ca^{2+} is a critical early event for the initiation of apoptosis induced in many apoptotic signals, as a consequence of organelle disruption, free radical production and activation of Ca^{2+} -dependent phosphatases and proteases such as calcineurin and calpain^{67, 88}. Bcl-2 can interact with both IP_3R and SERCA. Interaction of Bcl-2 with IP_3R leads to permanent leakage of Ca^{2+} , lowering resting state of ER Ca^{2+} -content and also reduces IP_3R -opening upon stress. Parallel blockade of SERCA attenuates active import of Ca^{2+} , which also reduces the amount of Ca^{2+} in the ER. Interestingly, interaction between

Bcl-2 and IP₃R is inhibited by ER localized Bax and Bak and it is also dependent on its phosphorylation status. JNK activation, which is caused by the inositol-requiring enzyme 1 (IRE1)/apoptosis signal regulating kinase 1 (ASK1) kinase arm of the unfolded protein response (UPR), leads to phosphorylation of Bcl-2 probably attenuating Bcl-2-mediated regulation of IP₃R and causing Bcl-2 degradation by proteasome⁶⁸.

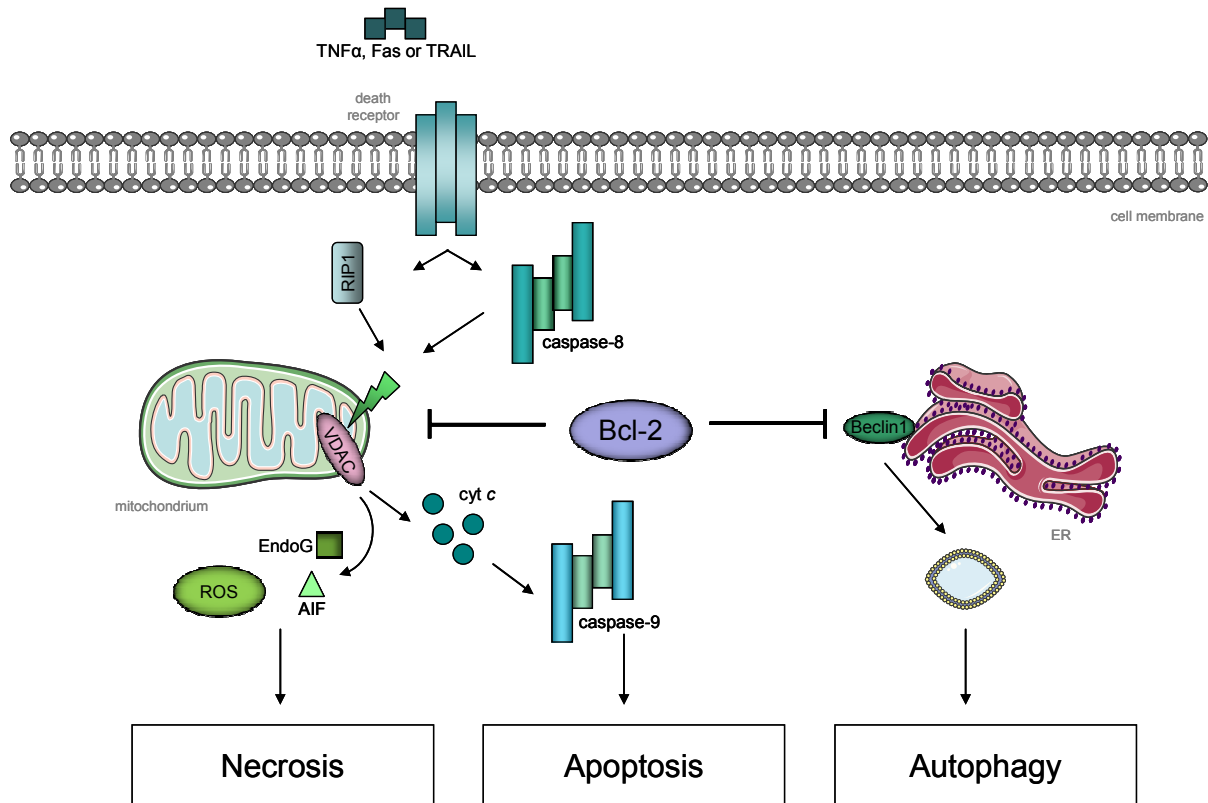


Figure 5 Bcl-2 inhibits different modes of cell death due to close communication with mediators of apoptosis, autophagy and necrosis. Apoptosis and necrosis share the same upstream TNFR. Bcl-2 blocks VDAC and consequent disruption of mitochondrial permeability after RIP1 activation and thus prevents the release of pro-necrotic factors such as endoG and AIF and increase of ROS. Bcl-2 suppresses mitochondrial membrane permeabilization and cytochrome c release downstream of caspase-8. Additionally, autophagy induction is inhibited by Bcl-2 by inhibitory binding to Beclin1, an essential component of the mammalian autophagy system. The image is adapted from⁸¹.

As Bcl-2 blocks cell death by a variety of different mechanisms, it is not surprising that Bcl-2 overexpression has been implicated in tumor survival pathways via its pro-metastatic activity in human non-small cell lung cancer cells and breast cancer cells^{89, 90}, as well as its pro-angiogenic activity as seen in its modulation of vascular endothelial growth factor (VEGF) expression^{91, 92}. Bcl-2 may also act to inhibit the innate antitumor immune response by promoting VEGF production⁹³, as VEGF is known to inhibit the innate antitumor immune response⁹⁴. Bcl-2 has been implicated in immunosilencing and it has been shown that Bcl-2 inhibition provokes antitumor response in activated T cells⁹⁵.

2.10 Significance to overcome Bcl-2-mediated resistance

One hallmark of human cancers is the ability to evade apoptosis. Generally, cell death can be inhibited by an increase of anti-apoptotic molecules and/or by a reduction or defective function of pro-apoptotic proteins. Subsequently, an enhancement in the ratio of anti- to pro-apoptotic Bcl-2 proteins has been observed in a variety of cancers and has been correlated to tumor cell survival and apoptosis resistance⁹⁶. A characteristic feature of follicular lymphoma is the overexpression of Bcl-2, caused by the t(14;18) chromosome translocation, placing the *bcl-2* oncogene into the immunoglobulin heavy chain gene locus, leading to its permanent expression⁹⁷. Moreover, studies on transgenic mice showed, that overexpression of Bcl-2 promotes neoplastic transformation of B and T lymphocytes and also of myeloid cells^{98, 99}. It has been discovered, that overexpression of Bcl-2 is common in many types of human cancer and has frequently been correlated with decreased susceptibility to chemotherapeutics and to increased radioresistance^{2, 96}. Interestingly, Bcl-2 overexpression does not promote cell proliferation as most previously discovered oncogenes do, Bcl-2 overexpression rather inhibits cell death, purging apoptosis as a prominent tumor-suppression mechanism¹⁰⁰. Therefore, the combined overexpression of Bcl-2 and MYC, an oncogene causing increased proliferation, synergize potently in the development of lymphomas and certain other types of cancer¹⁰¹.

2.10.1 Bcl-2 inhibitors in cancer therapy

Interfering with the pro-survival function of Bcl-2 provides suitable means to take aim at tumor cells. Different mechanisms to target and antagonize anti-apoptotic Bcl-2 have been developed and these drugs are already evaluated in several pre-clinical models and early clinical trials. There are different strategies to target Bcl-2. On the one hand there are Bcl-2 inhibitors such as chemical compounds (antisense-oligodeoxynucleotides targeting Bcl-2 mRNA: Genasense, also called G3139/Oblimersen currently used in phase II/III clinical trials e.g. in CLL alone or in combination with other chemotherapeutics) or natural compounds (Gossypol in Phase I/II), on the other hand BH3 mimetics have been developed based on protein-protein interactions between anti- and pro-apoptotic proteins of the Bcl-2 family, which represent non-peptidic compounds such as Bim-like mimetics (Obatoclax) or Bad-like mimetics (ABT-737, oral ABT-263, Phase I). BH3 mimetics competitively bind to the hydrophobic cleft thus displacing pro-apoptotic Bcl-2 family members from the heterodimeric complex, which subsequently can unleash pro-death molecules¹⁰²⁻¹⁰⁴.

2.10.2 Overcoming cell death resistance by Bcl-2 overexpression using helenalin

There is a need to develop additional strategies to overcome Bcl-2-mediated resistance, not only by directly targeting the Bcl-2 protein using Bcl-2 inhibitors, but also by circumventing cell death pathways that are blocked by Bcl-2. As previously mentioned, our group has already shown that helenalin is able to induce cell death despite of Bcl-2 overexpression in Jurkat T-cells. Yet, the type of cell death as well as the underlying mechanisms induced by helenalin in this cell line have not been investigated up to now. As helenalin showed promising effects in these highly resistant cancer cells, it was necessary to find out how helenalin overcomes Bcl-2-mediated resistance.

MATERIALS AND METHODS

3 MATERIALS AND METHODS

3.1 Materials

3.1.1 Biochemicals, inhibitors, dyes, buffers and cell culture reagents

Table 1 Biochemicals and inhibitors, dyes and cell culture reagents

Reagent	Producer
3-MA	Merck , Darmstadt, Germany
Ac-DEVD-AFC (Caspase-3 substrate)	Bachem, Bubendorf, Germany
Ac-LETD-AFC (Caspase-8 substrate)	Bachem, Bubendorf, Germany
BAPTA-AM	Invitrogen, Karlsruhe, Germany
BMS-345541	Sigma-Aldrich, Taufkirchen, Germany
Bradford Reagent™	Bio-Rad, Munich, Germany
Collagen A/G	Biochrom AG, Berlin, Germany
Complete™	Roche diagnostics, Penzberg, Germany
Cycloheximide	Axxora, Lörrach, Germany
DCDHF diacetate	Axxora, Lörrach, Germany
Deferoxamine mesylate (DFO)	Sigma-Aldrich, Taufkirchen, Germany
DMSO	Sigma-Aldrich, Taufkirchen, Germany
CPRG	Roche diagnostics, Penzberg, Germany
Etoposide	Merck , Darmstadt, Germany
FCS gold	PAA Laboratories, Pasching, Austria
Fura-2 AM	BIOTREND GmbH, Cologne, Germany
G418	Merck , Darmstadt, Germany
Helenalin	Axxora, Lörrach, Germany
Human Annexin V-FITC Kit	Bender MedSystems, Vienna, Austria
JC-1 iodide	Axxora, Lörrach, Germany
Na ₃ VO ₄	ICN Biomedicals, Aurora, Ohio, USA
N-acetyl-L-cysteine (NAC)	Sigma-Aldrich, Taufkirchen, Germany
NaF	Merck, Darmstadt, Germany
NEAA	Invitrogen, Karlsruhe, Germany
Necrostatin-1	Merck , Darmstadt, Germany
Paclitaxel (Tax)	Sigma-Aldrich, Taufkirchen, Germany
Page Ruler™ Prestained Protein Ladder	Fermentas, St. Leon-Rot, Germany
Penicillin	PAA Laboratories, Pasching, Austria

PMSF	Sigma Aldrich, Munich, Germany
Polyacrylamide	Roth GmbH, Karlsruhe, Germany
Propidium iodide (PI)	Sigma-Aldrich, Taufkirchen, Germany
Q-VD-OPh	Merck, Darmstadt, Germany
RPMI 1640	PAN Biotech, Aidenbach, Germany
Sodium pyruvate	Merck, Darmstadt, Germany
SP600125	Merck, Darmstadt, Germany
Streptomycin	PAA Laboratories, Pasching, Austria
Thapsigargin (TG)	Sigma-Aldrich, Taufkirchen, Germany
Tris-HCl	Sigma-Aldrich, Taufkirchen, Germany
Triton X-100	Merck, Darmstadt, Germany
Tumor necrosis factor α (TNF α)	Repro Tech GmbH, Hamburg, Germany
UCF101	Merck, Darmstadt, Germany
β -Phenylethyl isothiocyanate (PEITC)	Sigma-Aldrich, Taufkirchen, Germany

Helienalin was dissolved in DMSO and further diluted in PBS. Final DMSO concentration did not exceed 0.1%, a concentration verified not to interfere with the experiments performed.

Table 2 Commonly used buffers

HEPES buffer (pH 7.4)		PBS⁺ Ca²⁺/Mg²⁺ (pH 7.4)	
NaCl	125 mM	NaCl	137 mM
KCl	3 mM	KCl	2.68 mM
NaH ₂ PO ₄	1.25 mM	Na ₂ HPO ₄	8.10 mM
CaCl ₂	2.5 mM	KH ₂ PO ₄	1.47 mM
MgCl ₂	1.5 mM	MgCl ₂	0.25 mM
Glucose	10 mM	H ₂ O	
HEPES	10 mM		
H ₂ O			

PBS (pH 7.4)	
NaCl	132.2 mM
Na ₂ HPO ₄	10.4 mM
KH ₂ PO ₄	3.2 mM
H ₂ O	

3.1.2 Technical equipment

Table 3 Technical equipment

Name	Device	Producer
Culture flasks, plates, dishes	Disposable cell culture material	TPP, Trasadingen, Switzerland
Curix 60	Tabletop film processor	Agfa, Cologne, Germany
Cyclone	Storage Phosphor Screens	Canberra-Packard, Schwadorf, Austria
FACSCalibur	Flow cytometer	Becton Dickinson, Heidelberg, Germany
FACSCanto II	Flow cytometer	Becton Dickinson, Heidelberg, Germany
Mikro 22R	Table centrifuge	Hettich, Tuttlingen, Germany
Nanodrop [®] ND-1000	Spectrophotometer	Peqlab, Wilmington, DE, USA
Nucleofector II	Electroporation device	Lonza GmbH, Cologne, Germany
Odyssey 2.1	Infrared Imaging System	LI-COR Biosciences, Lincoln, NE, USA
Orion II Microplate Luminometer	Luminescence	Berthold Detection Systems, Pforzheim, Germany
SpectraFluor Plus [™]	Microplate multifunction reader	Tecan, Männedorf, Austria
Sunrise [™]	Microplate absorbance reader	Tecan, Männedorf, Austria
Vi-Cell [™] XR	Cell viability analyzer	Beckman Coulter, Fullerton, CA, USA

3.2 Cell Culture

3.2.1 Cell lines

Human leukemia Jurkat T cells transfected with vector control (Neo Jurkat) or Bcl-2 (Bcl-2 Jurkat)¹⁰⁵, kindly provided by Drs. P.H. Krammer and H. Walczak, Heidelberg, Germany, were cultured in RPMI 1640 containing 2 mM L-glutamine (PAN Biotech, Aidenbach, Germany), supplemented with 10% heat inactivated FCS gold (PAA Laboratories, Cölbe, Germany) and 1% pyruvate (Merck, Darmstadt, Germany). Medium of transfected cells was supplemented with 0.5-1 mg/ml G418 (PAA Laboratories, Cölbe, Germany) at least every fifth passage.

Human leukemia Jurkat T cells (J16) (S-Jurkat) were kindly provided by P.H. Krammer and H. Walczak, Heidelberg, Germany. S-Jurkat cells were cultured in RPMI 1640 containing 2 mM L-glutamine, supplemented with 10% FCS gold and 1% pyruvate.

MCF-7 were purchased from DSMZ and cultured (37°C and 5% CO₂) in RPMI 1640 containing 2 mM L-glutamine, supplemented with 10% heat inactivated FCS gold, 1x non-essential amino acids (NEAA), 1 mM pyruvate and 10 µg/ml human insulin. To create stably Bcl-2 overexpressing MCF-7 cells (Bcl-2 MCF-7) and the empty-vector control cell line (Neo MCF-7), 2 x 10⁶ MCF-7 cells were transfected with 3 µg of pcDNA3 Bcl-2 vector (Addgene plasmid 8768⁴²) or empty vector pcDNA3 (Invitrogen, Karlsruhe, Germany) using the Nucleofector[®] II device (program P-020) in combination with the Amaxa[®] Cell Line Nucleofector Kit[®] V (both from LONZA Cologne AG, Cologne, Germany), according to the manufacturer's instructions, respectively. Subsequently, cells were permanently cultivated with G418 (500 µg/ml) to select for stable expression.

The human pancreatic cancer cell line L3.6pl was kindly provided by Christiane J. Bruns (Department of Surgery, Klinikum Großhadern, LMU Munich, Germany). The cells were cultivated on 0.001% Collagen G-coated culture flasks and stimulation plates in RPMI 1640 containing 2 mM L-glutamine, supplemented with 10% heat inactivated FCS gold, 1x non-essential amino acids (NEAA) and 1 mM pyruvate. To create stably Bcl-2 overexpressing L3.6pl cells (Bcl-2 L3.6pl) and the empty vector control cell line (Neo L3.6pl), 4 x 10⁶ L3.6pl cells were either transfected with 3 µg of pcDNA3 Bcl-2 vector or empty vector pcDNA3 (Invitrogen, Karlsruhe, Germany) using the Nucleofector[®] II device (program C-019) in combination with the Amaxa[®] Cell Line Nucleofector Kit[®] V (both from LONZA Cologne AG, Cologne, Germany), according to the manufacturer's instructions. Subsequently, cells were permanently cultivated with G418 (250 µg/ml) to select for stable expression.

3.2.2 Cell culture

Cell lines were cultivated at 37°C with 5% CO₂ in a humidified incubator. Jurkat cell lines were maintained at the density below 1 x 10⁶ and used up to passage 25. All adherent cells were passaged after reaching 80-90% confluency. MCF-7 cells were used up to passage 25 and L3.6pl cells were used up to passage 35. For splitting and seeding, adherent cells were washed once with pre-warmed PBS, T/E was added and cells were incubated at 37°C and the enzymatic reaction was stopped by adding new medium as soon as cells were detached. Subsequently, cells were centrifuged and supplied with fresh medium.

The cell density and viability was determined using ViCELL[™] cell viability analyzer (Beckman Coulter, Krefeld, Germany).

Table 4 Solutions and reagents for cell culture

Trypsin/EDTA (T/E)		Collagen G	
Trypsin	0.05%	Collagen G	0.001%
EDTA	0.20%	PBS	
PBS			

For heat inactivation, FCS gold was partially thawed for 30 min at room temperature. Subsequently, it was totally thawed at 37°C. Finally, FCS was inactivated at 56°C for 30 min. FCS was aliquoted and stored at -20°C.

3.2.3 Seeding for experiments

Only G418 free medium was used for experiments. Unless indicated otherwise, cells were seeded as follows:

Jurkat cells were seeded at 7×10^5 cells/ml (for experiments up to 24 h) or at 3.5×10^5 (for stimulation time for 48 h) at least 5 h before stimulation or at 5×10^5 cells/ml the day before (about 16 h before stimulation) in 24-well plates, respectively.

L3.6pl cells were seeded at $0.7-1 \times 10^5$ cells/well in Collagen G coated 24-well plates or at 2.5×10^5 cells/well in 6-well plates about 16 h before stimulation, respectively.

MCF-7 cells were seeded at 1×10^5 cells/well in 24-well plates about 16 h before stimulation.

3.2.4 Freezing and thawing

From all cell lines nitrogen stocks were prepared. After centrifugation (180 x g, 10 min, 4°C) cells were resuspended in the appropriate freezing medium (70% normal medium for each cell line, 10% DMSO and 20% additional FCS gold) and cells were transferred to cryovials ($2-4 \times 10^6$ cells in 1.5 ml per vial) and frozen overnight at -20°C. Cells were then kept at 80°C and if desired, transferred to liquid nitrogen (-196°C) after two days for long-term storage.

3.3 Flow cytometry

Flow cytometry (FCM) has been used for the analysis of cell death, ROS generation and mitochondrial membrane dissipation. Measurements were performed on a FACSCanto II or on a FACSCalibur (Becton Dickinson, Heidelberg, Germany), respectively. Cells were illuminated by a blue argon laser (488 nm).

Table 5 FACS buffer for FACSCalibur

Sheath fluid (pH 7.37)	
NaCl	8.12 g
KH ₂ PO ₄	0.26 g
Na ₂ HPO ₄	2.35 g
KCl	0.28 g
Na ₂ EDTA	0.36 g
LiCl	0.43 g
NaN ₃	10 mM
H ₂ O	ad 1,000 ml

3.3.1 Quantification of Cell death

Quantification of cell death was either performed according to Nicoletti et al.¹⁰⁶, labeled as Nicoletti assay, by propidium iodide (PI) exclusion assay or by Annexin-V/PI double staining.

3.3.1.1 Nicoletti assay

Briefly, cells were seeded in 24 well-plates. Growth medium was exchanged (for MCF-7 and L3.6pl) and cells were stimulated with desired substances for the indicated times. After stimulation, cells were washed with PBS and incubated in a buffer containing 0.1% sodium citrate, 0.1% Triton X-100 and 50 µg/ml PI overnight at 4°C and analyzed by flow cytometry on a FACS Calibur (Becton Dickinson, Heidelberg, Germany). Nuclei to the left of the G1-peak containing hypodiploid DNA were considered dead. If indicated, specific cell death was calculated as: [(absolute cell death of compound-treated cells – absolute cell death of untreated cells) / (100 – absolute cell death of untreated cells) x 100].

3.3.1.2 PI exclusion assay

After stimulation, cells were washed with PBS and incubated with a solution of PBS and PI (5 µg/ml) for 30 min at room temperature in the dark. PI stained cells were detected by flow cytometry using FACS Calibur (Becton Dickinson, Heidelberg, Germany). Cell death was analyzed employing histogram plots except experiments with stimulation time for 24 h and 48 h, which were analyzed employing dot plots.

3.3.1.3 Annexin-V/PI double staining

Bcl-2 Jurkat and Neo Jurkat cells were either left untreated (Co) or treated with helenalin 20 µM for the indicated time points. Cells were double stained with Annexin V-FITC/Propidium iodide (PI) using human Annexin V-FITC Kit (Bender MedSystems, Vienna,

Austria) according to the manufacturer's protocol. Briefly, stimulated cells were collected in FACS tubes, centrifuged (600 x g, 5 min, room temperature), washed with PBS and resuspended in 195 μ l binding buffer (10 mM Hepes/NaOH pH 7.4, 140 mM NaCl, 2.5 mM CaCl_2) with 5 μ l of the provided Annexin V-FITC solution. After incubation at room temperature under light protection for 10 minutes, samples were washed with PBS and resuspended in 190 μ l of binding buffer and 10 μ l of PI stock solution (20 μ g/ml) and subsequently analyzed by flow cytometry using FACS Canto II (Becton Dickinson, Heidelberg, Germany).

3.3.2 Measurement of ROS generation

Bcl-2 Jurkat cells were left untreated (Co) or treated with helenalin (20 μ M) for the indicated times, centrifuged (600 x g, 5 min, room temperature) and resuspended in PBS. Samples were stained with the oxidation-sensitive dye 2',7'-dichlorodihydrofluorescein diacetate (DCDHF diacetate, 10 μ M) for 30 minutes at 37°C in the dark. Subsequently, cells were centrifuged, diluted in fresh PBS and analyzed by flow cytometry using FACS Calibur (Becton Dickinson, Heidelberg, Germany).

3.3.3 Measurement of mitochondrial potential dissipation

Bcl-2 Jurkat cells left untreated (Co) or treated with helenalin 20 μ M for the indicated time point. Subsequently, 5,5',6,6'-tetrachloro-1,1',3,3'-tetraethylbenzimidazol-carbocyanine iodide (JC-1) was directly added into the wells at a final concentration of 1.25 μ M and cells were incubated for 15 min at 37°C. After centrifugation (600 x g, 5 min, room temperature), samples were resuspended in PBS and analyzed by flow cytometry using FACS Canto II (Becton Dickinson, Heidelberg, Germany). An increase in green fluorescence (FITC-A channel) indicates loss of mitochondrial membrane potential.

3.4 Clonogenic assay

Neo Jurkat and Bcl-2 Jurkat cells were left untreated or treated with helenalin (20 μ M) or etoposide (2 μ M) for 2 h. Subsequently, cells were washed with PBS and resuspended in culture medium (5×10^5 cells/ml). Cell suspensions were diluted 1:10 with methylcellulose (0.52%) medium containing 40% FCS. Cells were seeded in 96-well plates (100 μ l) and colonies were scored after 7 days of culture using the S.CORE-colony forming assay Online Imaging Analysis System from S.CO LifeScience (Garching, Germany).

Neo L3.6pl and Bcl-2 L3.6pl cells were seeded in 6-well plates (2.5×10^5 cells/well) and either left untreated (Co) or treated with helenalin (5, 10, 20 μ M) or paclitaxel (Tax; 500 nM) for 2 h. Subsequently, cells were collected by trypsinization, centrifuged (1000 rpm, 5 min) and supported with fresh medium. Cells were then seeded in 6 well-plates (1×10^4 cells/well)

and allowed to grow for 6 days. Afterwards, cells were stained with crystal violet (0.5% crystal violet in 20% methanol) for 15 min., unbound crystal violet was removed by washing with water and the plates were air dried. Pictures of the wells were taken. Afterwards, intracellular crystal violet was solved with sodium citrate solution (0.05 M Na₃-citrate, 50% ethanol) and absorption was measured at 550 nm in a SpectraFluor Plus™ (Tecan). Untreated cells (Co) were set as 100% viable cells.

3.5 Western blot

3.5.1 Whole lysate preparation

For Western blot analysis, cells were treated as indicated and at least 2 wells of a 24-well plate per sample were pooled. Cell samples were collected by centrifugation, washed with ice-cold PBS and lysed in the appropriate lysis buffer for 30 min at 4°C. Lysates were homogenized with an ultrasonic device and centrifuged at 10,000 x g for 10 min at 4°C and supernatants were collected into new tubes. One part of the lysate was used for determination of protein concentration (Bradford), the rest was diluted with 5x SDS sample buffer (4 parts lysate, 1 part buffer) or with 3x Laemmli buffer (2 parts lysate, 1 part buffer) and boiled for 5 min at 95°C. Samples were used immediately or stored at -20°C.

Table 6 Buffers for the preparation of total cell lysates

Lysis buffer		Lysis buffer for phospho-proteins	
Tris-HCl, pH 7.5	30 mM	Tris-Base	20 mM
NaCl	150 mM	NaCl	137 mM
EDTA	2 mM	EDTA	2 mM
Triton X-100	1%	Triton X-100	1%
Complete™		C ₃ H ₇ Na ₂ O ₆ P	20 mM
		NaF	10 mM
		Na ₃ VO ₄	2 mM
		Na ₄ P ₂ O ₇	2 mM
		PMSF	1 mM
		Glycerol	10%
		Complete™	

Table 7 Sample buffer

5x SDS sample buffer		3x Laemmli buffer	
Tris-HCl, pH 6.8	3.125 M, 100 μ l	Tris-HCl	187.5 mM
Glycerol	500 μ l	Glycerol	30%
SDS 20%	250 μ l	SDS	6%
DTT 16%	125 μ l	Bromphenolblue	0.025%
Pryonin Y 5%	5 μ l	β -Mercaptoethanol	12.5%
H ₂ O	ad 1,000 μ l	H ₂ O	

3.5.2 Preparation of cytosolic and mitochondrial fractions

Release of cytochrome *c* from mitochondria was analyzed according to Leist et al. ¹⁰⁷. Briefly, cells were treated as indicated and cell samples were collected by centrifugation and washed with ice-cold PBS. Subsequently, the cell pellet was resuspended in permeabilization buffer and incubated for 20 min at 4°C. Permeabilized cells were centrifuged (230 x g, 10 min, 4°C), the supernatant was removed and centrifuged again (10 min, 20,000 x g) to clear from any remaining cell fragments. The obtained cytosolic fraction was separated by SDS-PAGE and probed for mitochondrial proteins as described below. The remaining pellet of the first centrifugation was resuspended in 0.1% Triton/PBS (15 min, 4°C), centrifuged (20,000 x g, 4°C, 10 min) and the supernatant containing mitochondrial fraction was analyzed by SDS-PAGE. Purity of cytosolic fractions was assessed by incubating membranes with VDAC.

Table 8 Permeabilization buffer

Permeabilization buffer	
Mannitol	210 mM
Sucrose	70 mM
Hepes, pH 7.2	10 mM
EGTA	0.2 mM
Succinate	5 mM
BSA	0.15%
Digitonin	60 μ g/ml
H ₂ O	

3.5.3 Immunoprecipitation

Bcl-2 Jurkat cells were left untreated (Co) or treated with helenalin (20 μ M) for 2 h or 6 h. At least 4 wells of a 24-well plate per sample were pooled. One additional well was left untreated (whole cell lysate sample). After stimulation, cells were lysed in general lysis buffer

and the amount of protein was determined. The whole cell lysate sample was immediately frozen at -85°C . The other samples were treated as follows: For each sample, 300-400 μg protein was filled up to a final volume of 250 μl with lysis buffer and 2.5 μl of Beclin1 antibody was added. The samples were gently shaken over night at 4°C by end over end rocking. In the next step, 50 μl Protein A Agarose Beads (50%v/v, Sigma) for each sample were centrifuged (14,000 rpm, 1 min, 4°C), washed and resuspended in lysis buffer and added to the samples. Subsequently, samples were gently inverted at 4°C for approximately 3 h. The precipitates were centrifuged (14,000 rpm, 1 min, 4°C), and 40 μl of the supernatant were kept as binding control (BC). The remaining pellet was carefully washed three times with 500 μl lysis buffer. After completely removing the last wash solution, samples were mixed with β -mercaptoethanol containing 3x Laemmli buffer and boiled at 95°C for 5 minutes. Also 20 μl of the whole cell lysate, 2 μl of Beclin1 antibody (antibody control) and 20 μl of the binding controls (BC) were boiled with 3x Laemmli buffer, respectively. All samples were analyzed by Western blot.

For a selective detection of Beclin1 protein without hindrance by interfering immunoprecipitating immunoglobulin heavy and light chains, the Rabbit TrueBlot™: HRP anti-rabbit IgG antibody (NatuTec GmbH, Frankfurt a.M., Germany) was used.

3.5.4 Protein quantification

In order to employ equal amounts of proteins in all samples for Western blot analysis, protein concentrations were determined using Bradford assay. After measurement, protein concentration was adjusted by adding 1x SDS sample buffer.

Bradford Assay (Bradford solution, Bio-Rad, Munich, Germany) was performed as described previously¹⁰⁸. Coomassie Brilliant Blue as a dye is used, which binds to proteins. 10 μl protein samples (1:10 dilution in water) were incubated with 190 μl Bradford solution for 5 min. Thereafter, absorbance was measured photometrically at 592 nm using Tecan Sunrise™ Microplate absorbance reader (TECAN, Männedorf, Austria). Protein standards were obtained by diluting a stock solution of bovine serum albumin (BSA, 2 mg/ml). Linear regression was used to determine the actual protein concentration of each sample.

3.5.5 SDS-PAGE

Proteins were separated by discontinuous SDS-polyacrylamid gel electrophoresis (SDS-PAGE) according to Laemmli¹⁰⁹. Equal amounts of protein were loaded on discontinuous polyacrylamide gels, consisting of a separation and stacking gel, and separated using the Mini-PROTEAN 3 electrophoresis module (Bio-Rad, Munich, Germany). The concentration of Rotiphorese™ Gel 30 (acrylamide) in the separating gel was adjusted for an optimal separation of the proteins depending on their molecular weights. Electrophoresis was carried out at 100 V for 21 min for protein stacking and 200 V for 45 min for protein separation. The

molecular weight of proteins was determined by comparison with the prestained protein ladder PageRuler™.

Table 9 Acrylamide gels and acrylamide concentration in the separation gel

Stacking gel		Separation gel (10%)	
Rotiphorese™ Gel 30	1.7 ml	Rotiphorese™ Gel 30	5 ml
Tris-HCl 1.25 M, (pH 6.8)	1 ml	Tris-HCl 1.5 M, (pH 8.8)	3.75 ml
SDS 10%	100 µl	SDS 10%	150 µl
TEMED	20 µl	TEMED	15 µl
APS 10%	100 µl	APS 10%	75 µl
H ₂ O	7.0 ml	H ₂ O	6.1 ml

Acrylamide concentration	Proteins
7.5%	70-120 kDa
10%	70-30 kDa
12%	60-20 kDa
15%	10-45 kDa

Table 10 Electrophoresis buffer

Electrophoresis buffer	
Tris	4.9 mM
Glycine	38 mM
SDS	0.1%
H ₂ O	

3.5.6 Tank electroblotting

After protein separation, proteins were transferred onto a nitrocellulose membrane (Hybond-ECL™, Amersham Bioscience, Freiburg, Germany) by electro tank blotting¹¹⁰. A blotting sandwich was prepared in a box filled with 1x tank buffer to avoid bubbles as follows: cathode – pad – blotting paper – separating gel (from SDS-PAGE) – nitrocellulose membrane – blotting paper – pad – anode. The membrane was equilibrated with 1x tank buffer 45 minutes prior to running the tank blot. Sandwiches were mounted in the Mini Trans-Blot® system (Bio-Rad, Munich, Germany), ice-cold 1x tank buffer was filled into the chamber and a cooling pack was inserted to avoid excessive heat. Transfers were carried out at 4°C, either at 100 V for 90 min or at 23 V over night.

Table 11 Tank blotting buffer

5x Tank buffer		1x Tank buffer	
Tris base	240 mM	5x Tank buffer	20%
Glycine	195 mM	Methanol	20%
H ₂ O		H ₂ O	

3.5.7 Protein detection

Prior to the immunological detection of the relevant proteins, unspecific protein binding sites were blocked. Therefore, the membranes were incubated in non-fat dry milk powder (Blotto) 5% or BSA 5% for 2 h at room temperature. Afterwards, detection of the proteins was performed by incubating the membrane with the respective primary antibody at 4°C overnight (Table 12). After three washing steps with PBS containing 0.1% Tween (PBS-T), the membrane was incubated with the secondary antibody, followed by 3 additional washing steps. All steps regarding the incubation of the membrane were performed under gentle agitation. In order to visualize the proteins, two different methods have been used depending on the labels of the secondary antibodies: enhanced chemiluminescence or infrared imaging.

Table 12 Primary antibodies

Antigen	Source	Provider
AIF	Rabbit polycl.	Chemicon
Akt	Rabbit polycl.	Cell Signaling
Apaf-1	Mouse IgG1	BD Biosciences
Bcl-2	Goat polycl.	Santa Cruz
Bcl-2	Mouse monocl.	Merck
Beclin1	Rabbit polycl.	Cell Signaling
BiP/GRP78	Mouse IgG2a	BD
caspase-3	Rabbit polycl.	Santa Cruz
caspase-9	Rabbit polycl.	Cell Signaling
cytochrome c	Rabbit polycl.	Cell Signaling
eIF2 α (D-3)	Mouse IgG1	Santa Cruz
GADD153/CHOP10	Rabbit polycl.	Sigma
I κ B α	Rabbit polycl.	Cell Signaling
JNK	Rabbit polycl.	Cell Signaling
LC3B (G40)	Rabbit polycl.	Cell Signaling
mTOR	Rabbit polycl.	Cell Signaling
phos.-Akt ^{S473}	Mouse IgG2b	Cell Signaling

phos.-c-Jun ^{S63}	Rabbit polycl.	Cell Signaling
phos.-eIF2 α ^{S51}	Rabbit polycl.	Cell Signaling
phos.-I κ B α ^{S32}	Rabbit polycl.	Santa Cruz
phos.-JNK ^{T183/Y185}	Rabbit polycl.	Cell Signaling
phos.-mTOR ^{S2448}	Rabbit polycl.	Cell Signaling
Smac	Mouse IgG1	Cell Signaling
VDAC	Rabbit polycl.	Cell Signaling
β -actin	Mouse monocl.	Chemicon

Antibodies were diluted according to the manufacturer's instructions.

3.5.7.1 Enhanced chemiluminescence

Membranes were incubated for 2 h with HRP-conjugated secondary antibodies (Table 13). For detection, luminol was used as a substrate. The membranes were incubated with ECL (enhanced chemiluminescence) solution for 1 minute (ECL Plus Western Blotting Detection Reagent RPN 2132, GE Healthcare, Munich, Germany). The appearing luminescence was detected by exposure of the membrane to an X-ray film (Super RX, Fuji, Düsseldorf, Germany) and subsequently developed with a Curix 60 Developing system (Agfa-Gevaert AG, Cologne, Germany).

3.5.7.2 Infrared imaging

Secondary antibodies coupled to IRDyeTM 800 and Alexa Fluor[®] 680 with emission at 800 and 700 nm, respectively, were used. Membranes were incubated for 1 h. Protein bands of interest were detected using the Odyssey imaging system (Li-COR Biosciences, Lincoln, NE). Secondary antibodies used for this type of protein detection are listed in (Table 13).

Table 13 Secondary antibodies

Antibody	Dilutions in Blotto 1%	Provider
Goat anti-mouse IgG1: HRP	1:1,000	Biozol
Goat anti mouse IgG: HRP	1:1,000	Southern Biotechnology
Goat anti-rabbit: HRP	1:1,000	Dianova
Donkey anti-goat: HRP	1:1,000	Santa Cruz
TrueBlot TM : HRP anti-rabbit IgG	1:1,000	NatuTec GmbH
Alexa Fluor [®] 680 Goat anti-mouse IgG	1:10,000	Molecular Probes
Alexa Fluor [®] 680 Goat anti-rabbit IgG	1:10,000	Molecular Probes
IRDye TM 800CW Goat anti-mouse IgG	1:20,000	LI-COR Biosciences
IRDye TM 800CW Goat anti-rabbit IgG	1:20,000	LI-COR Biosciences

3.5.8 Staining of gels and membranes

Gels were stained for 30 minutes in the Coomassie staining solution and destained with the Coomassie destaining solution to control equal loading of the gel and the performance of the transfer. A 0.2% Ponceau S in 5.0% acetic acid solution was used to stain membranes. Destaining was performed in distilled water.

Table 14 Gel staining solution

Coomassi staining solution		Coomassi destaining solution	
Coomassie blue	3.0 g	Glacial acetic acid	100 ml
Glacial acetic acid	100 ml	Ethanol	333 ml
Ethanol	450 ml	H ₂ O	ad 1,000 ml
H ₂ O	ad 1,000 ml		

3.6 Transfection of cells

For transient transfection with the indicated siRNA and plasmids, respectively, cells were electroporated using the Nucleofector[®] II device in combination with the Amaxa[®] Cell Line Nucleofector Kit[®] V (both from LONZA Cologne AG, Cologne, Germany) according to the manufacturer's instructions.

3.6.1 Transfection with Apaf-1 and AIF siRNA

Sense and antisense siRNA oligonucleotides corresponding to nucleotides 978-998 of Apaf-1 (AATTGGTGCACCTTTTACGTGA)¹¹¹, to the AIF nucleotides GGAAATATGGGAAAGATCCdTdT¹¹² and oligonucleotides corresponding to a scrambled sequence were purchased from Biomers.net GmbH (Ulm, Germany) and annealed to create the double-stranded siRNAs. Bcl-2 Jurkat cells were transfected with 3 µg of scrambled, Apaf-1 or AIF siRNAs. Cells were stimulated 48 h after transfection.

3.6.2 Transfection with plasmids

Bcl-2 and Neo Jurkat cells as well as MCF-7 and L3.6pL cells were transfected with plasmids as indicated in the appropriate experiments.

3.7 Reporter gene assay

Bcl-2 and Neo Jurkat cells (4×10^6) were co-transfected with 4 µg of plasmid containing 5.7 kB of human NF-κB promoter driving a firefly luciferase gene (pNF-κB-Luc, Stratagene, La Jolla, CA, USA) and 506 ng of a β-galactosidase plasmid (pβ-Gal, 6.83 kB, Promega, Mannheim, Germany) using the Nucleofector[®] II device (program C-019) in combination with

the Amaxa[®] Cell Line Nucleofector Kit[®] V (both from LONZA Cologne AG, Cologne, Germany), according to manufacturer's instructions, respectively. 100 μ l of cells suspension (5×10^5 cells/ml) was seeded in 96-well plates (round bottom; TPP Trasadigen, Switzerland). 12 h after transfection, cells were left untreated (Co) or treated with helenalin 20 μ M for the indicated times. Subsequently, plates were centrifuged (1500 rpm, 10 min, 4°C), cells were washed once with ice-cold PBS and 80 μ l/well of passive lysis buffer (Cat#E194A; Promega, Mannheim, Germany) was added and samples were frozen at -85°C over night. Afterwards, plates were incubated for 15 min under gentle agitation at room temperature and subsequently, 50 μ l of the lysate per sample were transferred into white 96-well plates. Luciferase activity was measured with Orion II Microplate Luminometer (Berthold Detection Systems, Pforzheim, Germany) using luciferase assay buffer.

As a control, β -galactosidase activity was measured in a plate-reading multifunction photometer SpectraFluor Plus[™] (Tecan, Männedorf, Austria) at 505 nm. Briefly, 20 μ l of cell lysate per sample was transferred into 96-well plates and 180 μ l of substrate buffer was added (200 μ l of 50nM CPRG, 20 μ l β -mercaptoethanol in 20 ml Z-buffer). The enzyme activity of β -galactosidase was calculated as the difference between fluorescence at 0 h to 48 h. Luciferase activity was normalized to β -galactosidase activity and NF- κ B activity thus obtained is expressed as x-fold activity referring to untreated Neo Jurkat cells.

Table 15 Buffers for reportergene assay

Z-buffer (pH 7.01)		Luciferase assay buffer (pH 7.8)	
Na ₂ HPO ₄	60 mM	D-Luciferin	470 μ M
NaH ₂ PO ₄	40 mM	Coenzym A	270 μ M
KCl	10 mM	DTT	33.3 mM
MgCl ₂	10 mM	ATP	530 μ M
H ₂ O		MgSO ₄	2.67 mM
		Tricine	20 mM
		EDTA	0.1 mM
		H ₂ O	

3.8 Electrophoretic mobility shift assay (EMSA)

3.8.1 Preparation of nuclear extracts

Nuclear extracts were prepared from either untreated or stimulated Neo Jurkat and Bcl-2 Jurkat cells, respectively. In order to gain a usable amount of nuclear protein, 1×10^6 cells were used per sample. Following stimulation, cells were scraped on ice after washing twice with ice-cold PBS. After centrifugation (1,500 rpm, 5 min, 4°C), the supernatant was

discarded and 400µl of nuclear extraction buffer A was added to the remaining pellet. Samples were incubated at 4°C for 15 min on ice, 25 µl NP-40 10% were added and samples were centrifuged (12,000 rpm, 1 min, 4°C) immediately. The supernatant was removed and the remaining pellet was suspended in 50 µl buffer B. Samples were incubated at 4°C for 15 min with continuous shaking. After centrifugation (12,000 rpm, 5 minutes, 4°C) supernatants were frozen at -80°C and nuclear proteins were kept until used for protein quantification (by Bradford assay) and electro mobility shift assay (EMSA).

Table 16 Extraction buffers for nuclear proteins

Extraction Buffer A		Extraction Buffer B	
HEPES, pH 7.9	10 mM	HEPES, pH 7.9	20 mM
KCl	10 mM	NaCl	0.4 mM
EDTA	0.1 mM	EDTA	0.1 mM
EGTA	0.1 mM	EGTA	0.1 mM
DTT	1.0 mM	DTT	1.0 mM
PMSF	0.5 mM	PMSF	0.5 mM
H ₂ O		Glycerol	25%
		H ₂ O	

3.8.2 Binding reaction and electrophoretic separation

The oligonucleotide for NF-κB with the consensus sequence 5'-AGT TGA GGG GAC TTT CCC AGG C-3' was purchased from Promega. Using the T4 polynucleotide kinase the oligonucleotides were 5' end-labeled with [γ -³²P]-ATP. Equal amounts of nuclear protein (1-2 µg) were incubated with 2 µg poly(dIdC) and 3 µl of freshly prepared reaction buffer for 10 min at room temperature. For the supershift assay, 1 µl of the respective antibody, p65 or p50 (both goat polyclonal antibody, 200 µg/0.1 ml, Santa Cruz Biotechnology, Heidelberg, Germany), was added before incubation at room temperature. The binding reaction was started by adding 1 µl of the radioactive-labeled oligonucleotide and carried out for 30 min at room temperature. The protein-oligonucleotide complexes were separated by gel electrophoresis (Power Tec™ HC, BioRad) with 0.25 x TBE buffer at 100 V for 60 min using non-denaturing polyacrylamide gels (5% PAA, 20% glycerol). After electrophoresis, gels were exposed to Cyclone Storage Phosphor Screens (Canberra-Packard, Schwadorf, Austria) for 24 hours, followed by analysis with a phosphor imager station (Cyclone Storage Phosphor System, Canberra-Packard).

Table 17 Buffers and gels for EMSA

5x Binding Buffer		Loading Buffer	
Tris/ HCl	50 mM	Tris/HCl	250 mM
NaCl	250 mM	Glycerol	40%
MgCl ₂	5.0 mM	Bromphenolblue	0.2%
EDTA	2.5 mM		
Glycerol	20%		

Reaction buffer		10x TBE, pH 8.3	
5x binding buffer	90%	Tris	890 mM
Loading buffer	10%	Boric acid	890 mM
DTT	2.6 mM	EDTA	20 mM
		H ₂ O	

Non-denaturing PAA gels 4.5%	
10 x TBE	5.3%
Rotiphorese™ Gel 30	15.8%
Glycerol	2.6%
TEMED	0.05%
APS	0.08%
H ₂ O	

3.9 Caspase activity assay

Jurkat cells were left untreated (Co) or stimulated with helenalin or PEITC, respectively. PEITC has been described to induce caspase activity in Bcl-2 Jurkat cells^{113, 114}. Afterwards, cells were collected by centrifugation, washed with ice cold PBS and stored with 70 µl/sample of lysis buffer (Buffer A: 5 mM MgCl₂, 1 mM EGTA, 0.1% Triton-X-100, 25 mM HEPES pH 7.5) at -85°C over night. Afterwards, lysates were centrifuged (10,000 x g, 10 min, 4°C), supernatants were collected and incubated in a black 96-well plate with Buffer B (HEPES 50 mM, sucrose 1%, CHAPS 0.1%, pH 7.5) and caspase substrates, Ac-LETD-AFC for caspase-8 or Ac-DEVD-AFC (Bachem, Bubendorf, Germany) for caspase-3, respectively. The reading was performed in a plate-reading multifunction photometer (SpectraFluor Plus™, Tecan, Männedorf, Austria) at 37°C. The caspase activity was calculated from the difference between fluorescence 0 h to 2 h of substrate incubation. Protein concentration of samples was used for normalisation. Caspase activity is expressed as x-fold increase of caspase activity compared to the control.

3.10 Calcium measurement

Changes in intracellular calcium levels were analyzed with Fura-2 AM. Fura-2 free of Ca^{2+} ions emits fluorescence upon excitation at 380 nm, but after binding to Ca^{2+} , fluorescence shifts to 340 nm. Therefore, the 340:380 nm ratio of fluorescence intensity provides a parameter for calcium release. Briefly, Jurkat cells were centrifuged (180 x g, 5 min, 23°C), washed once with HEPES buffer and resuspended at 2×10^6 cells per ml in HEPES buffer containing 3 μM Fura-2 AM. Cell suspension was incubated for 30 min at 37°C; later, a volume of 300 ml cell suspension was transferred to an Adhesion Slide (Marienfeldt) and incubated at 37°C for further 15 min. After three washing steps with HEPES buffer, cells were stimulated with helenalin or thapsigargin for 10 min and fluorescence was assayed by microscopy (Axiovert 200). Ratio was calculated by TILLVision software.

3.11 Transmission Electron Microscopy

S-Jurkat and Bcl-2 Jurkat cells were left untreated (Co) or treated with helenalin for 8 hours, collected by centrifugation, resuspended and fixed in fixing solution (2.5% glutaraldehyde in fixative buffer: 75 mM cacodylate, 75 mM NaCl, 2 mM MgCl_2 , pH 7.0) for 1 h. Subsequently, cells were washed several times for increasing periods in fixative buffer, postfixed in 1% OsO_4 in fixative buffer and washed with buffer and aqua dest. Cells were dehydrated with a graded series of acetone. Cells were infiltrated with Spurr low-viscosity epoxyresin and polymerized at 65°C. Pictures were taken with a Zeiss EM 912 transmission electron microscope with integrated Ω -filter, operated in “zero-loss-mode”.

3.12 Statistical Analysis

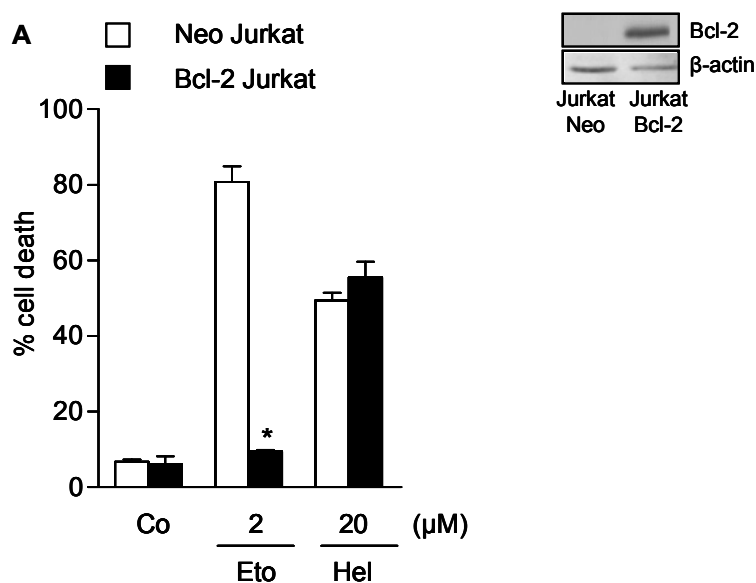
All experiments were performed at least three times. Results are expressed as mean value SEM. Statistical analysis was performed with GraphPad Prism™ version 3.0 for Windows (GraphPad Software, San Diego California, USA). One-way ANOVA with Bonferroni multiple comparison post-test or unpaired two-tailed Student's t-test were performed. P values < 0.05 were considered significant.

RESULTS

4 RESULTS

4.1 Helenalin overcomes Bcl-2-mediated resistance

Based on the data of Dirsch et al., showing that helenalin also induces cell death in Bcl-2 overexpressing Jurkat cells ²¹, we compared helenalin to the classical chemotherapeutic agent etoposide concerning cell death induction and clonogenic survival after treatment of Bcl-2 Jurkat cells and the vector control cell line (Neo Jurkat cells). We could confirm that overexpression of the antiapoptotic protein Bcl-2 does not protect from cell death induced by helenalin. Moreover, helenalin almost completely inhibited colony growth in both Jurkat cells overexpressing Bcl-2 and the control cell line (Figure 6 A-B). In contrast, the classical chemotherapeutic agent etoposide is not able to induce cell death and does not suppress the clonogenic survival of Bcl-2 overexpressing cells, whereas it shows clear effects in Neo Jurkat cells.



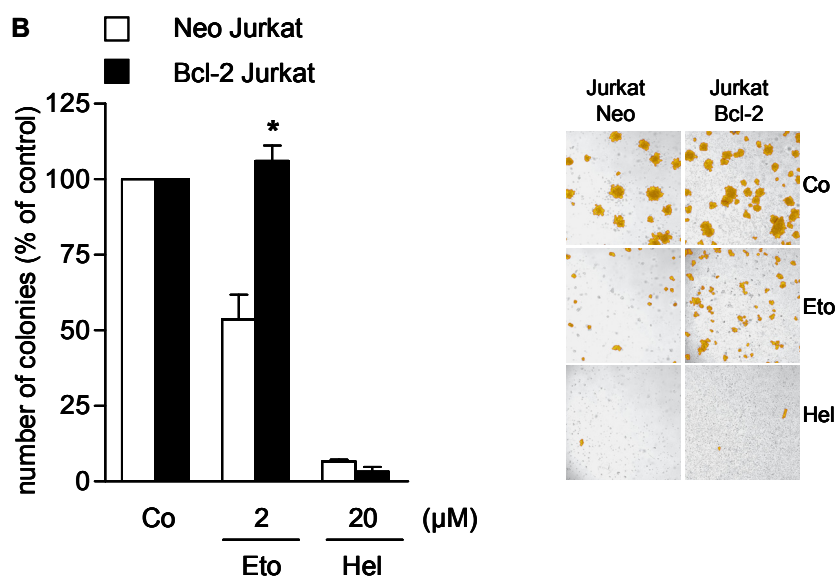
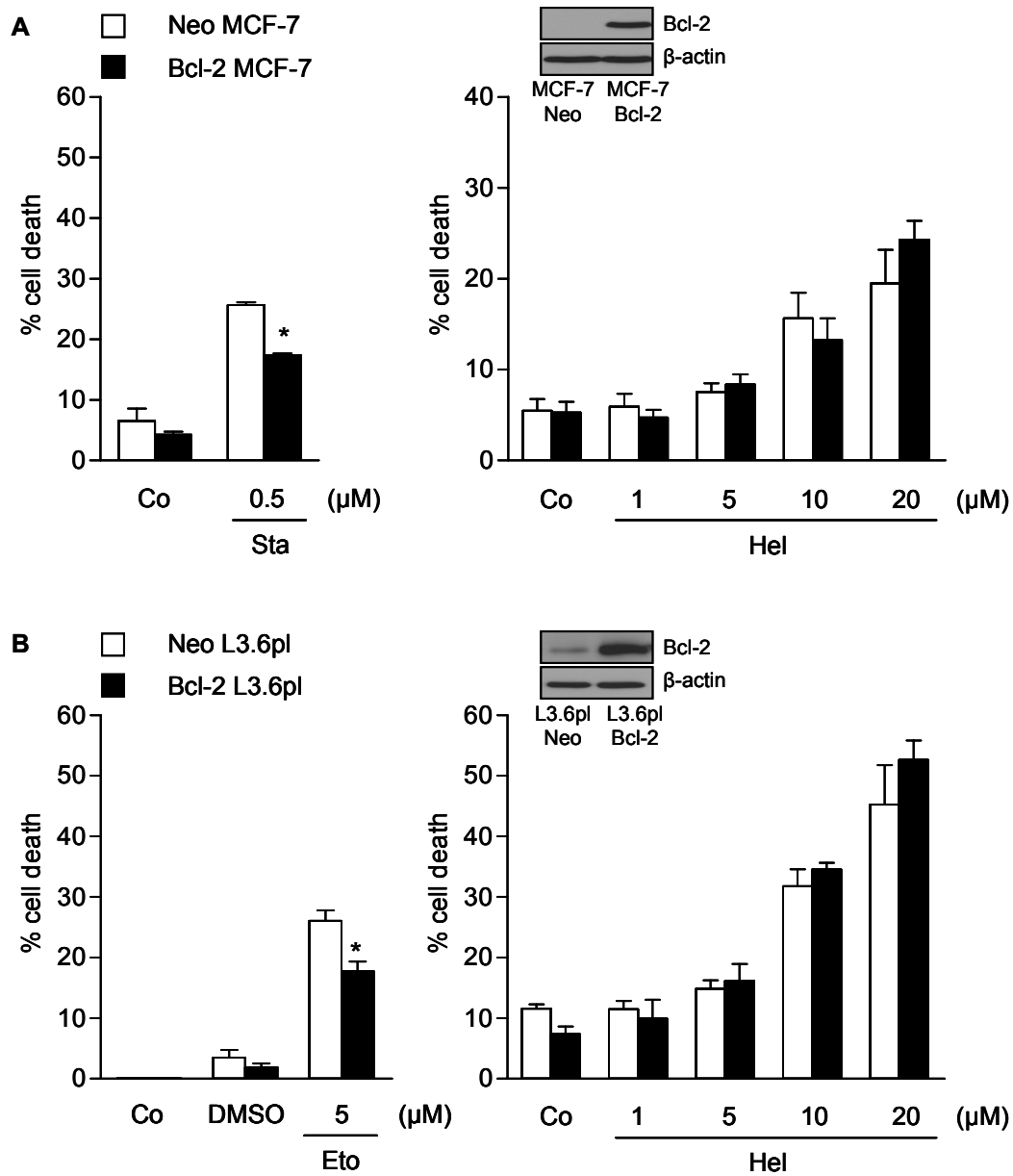


Figure 6 Helenalin overcomes Bcl-2-mediated resistance in Jurkat cells. A, Neo Jurkat or Bcl-2 Jurkat cells were either left untreated (Co) or treated with helenalin (Hel) or etoposide (Eto) with the indicated concentrations for 24 h. Cell death was quantified by Nicoletti assay. B, Neo Jurkat and Bcl-2 Jurkat cells were left untreated (Co) or stimulated with helenalin (Hel) or etoposide (Eto) with the indicated concentrations for 2 h and a clonogenic assay was performed. Results are represented as the number of colonies referred to untreated cells (Co). Data are expressed as mean \pm SEM (n=3). *, $p < 0.001$ (ANOVA, Bonferroni). Protein extracts from Neo/Bcl-2 Jurkat cells were prepared and Bcl-2 protein levels were analyzed by Western blot. Experiments for Figure 6 were performed by N. López Antón.

To verify that helenalin not only affects resistant leukaemia cells, we stably overexpressed Bcl-2 in two further cell lines, the breast cancer cell line MCF-7 and the highly metastatic human pancreatic carcinoma cell line L3.6pl. As shown in Figure 7, helenalin induces cell death and abrogates clonogenic survival despite of elevated Bcl-2 levels in both cell lines, whereas other classical chemotherapeutic agents like etoposide, staurosporine or paclitaxel affected the vector control cells in a more significant way than the Bcl-2 protected cells. These results underline the anti-resistance potential of helenalin also in solid tumors overexpressing Bcl-2.



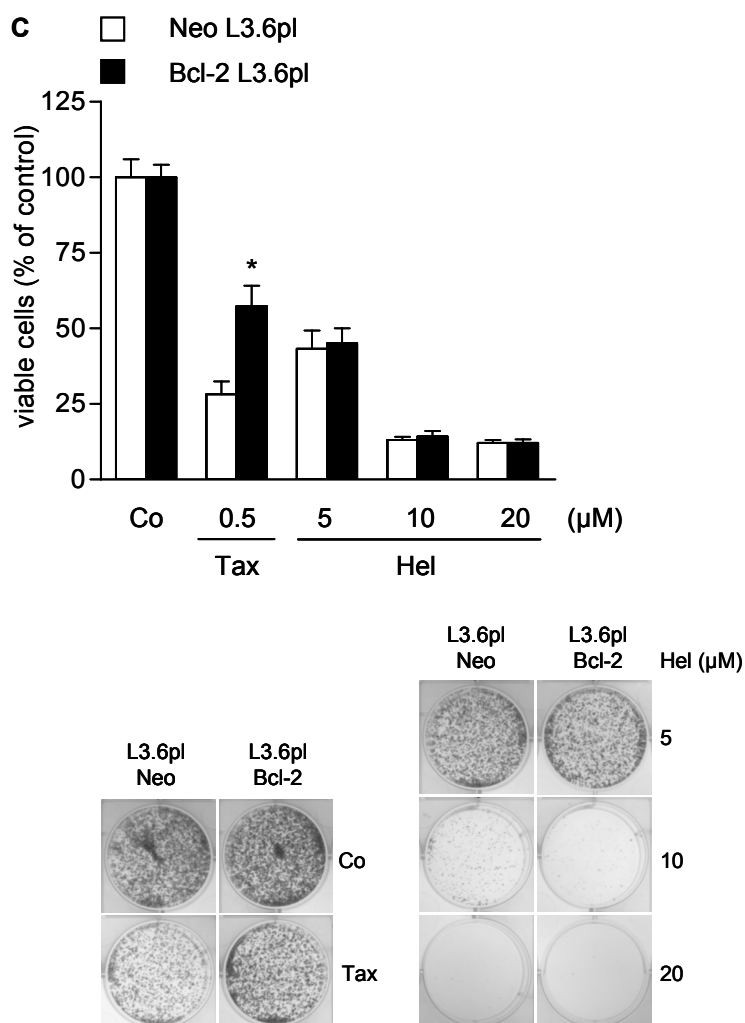


Figure 7 Helenalin overcomes Bcl-2-mediated resistance in MCF-7 and L3.6pl cells. A, Neo MCF-7 or Bcl-2 MCF-7 cells were treated with staurosporine (Sta; 48 h) or helenalin (Hel; 24 h) with the indicated concentrations and cell death was quantified by Nicoletti assay. Data are expressed as mean \pm SEM (n=3). *, $p < 0.01$ (ANOVA, Bonferroni). B, Neo L3.6pl or Bcl-2 L3.6pl were treated with etoposide (Eto), solvent (DMSO) or helenalin (Hel) with the indicated concentrations for 24 h. Cell death was either quantified by Nicoletti assay (Eto; quantified as specific cell death as described in "Material and Methods") or PI exclusion assay for helenalin-treated cells. Data are expressed as mean \pm SEM (n=3). *, $p < 0.001$ (ANOVA, Bonferroni). C, For the clonogenic assay, Neo L3.6pl and Bcl-2 L3.6pl cells were either left untreated (Co) or treated with paclitaxel (Tax) or helenalin (Hel) with the indicated concentrations for 2 h. Data are expressed as mean \pm SEM (n=3). *, $p < 0.001$ (ANOVA, Bonferroni). Protein extracts from Neo/Bcl-2 MCF-7 cells and Neo/Bcl-2 L3.6pl cells were prepared and Bcl-2 protein levels were analyzed by Western blot.

4.2 Helenalin does not abrogate mitochondrial function of Bcl-2 and acts independently of the mitochondria and the apoptosome

4.2.1 Mitochondrial function

Focus was now put on the mechanisms leading to cell death in Bcl-2-overexpressing Jurkat cells. As shown in the Western blot, helenalin did neither alter Bcl-2 protein level nor induce its phosphorylation as observed by treatment with paclitaxel (Figure 8 A). In line with this, helenalin did not abrogate the function of Bcl-2 on mitochondria as the mitochondrial

membrane potential (MMP) was kept nearly intact yet after 6 h of helenalin-treatment and only minute amounts of cytochrome *c* are released into the cytosol in Bcl-2 overexpressing compared to vector control cells treated with helenalin (Figure 8 B-C).

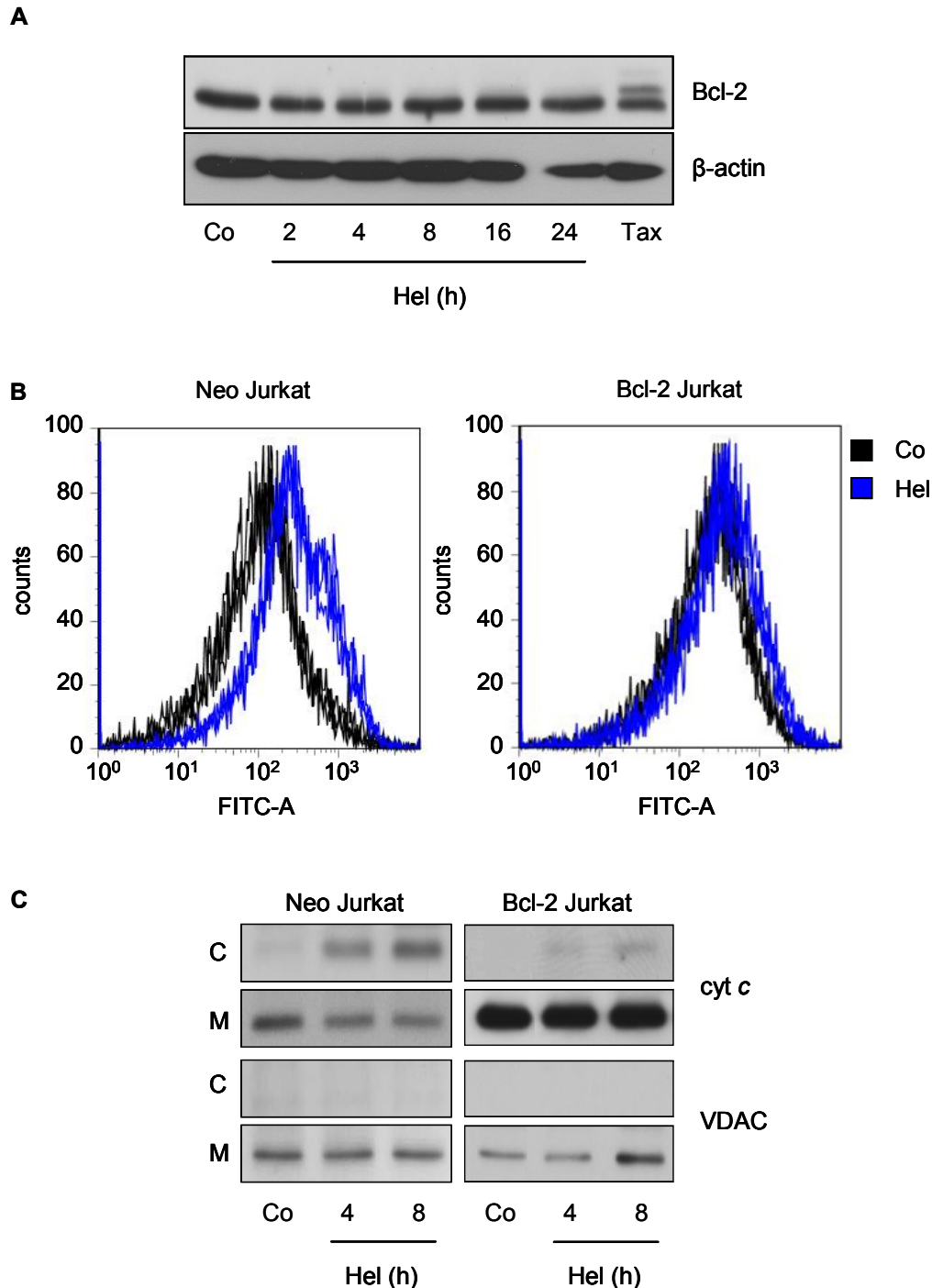


Figure 8 Helenalin does not abrogate mitochondrial function of Bcl-2. A, Bcl-2 Jurkats were treated with helenalin (Hel; 20 μ M) for the indicated times or as a control inducing Bcl-2 phosphorylation, with paclitaxel (Tax; 1 μ M, 16 h) and Western blot analysis was performed. B, Neo Jurkat and Bcl-2 Jurkat cells were treated with helenalin (Hel; 20 μ M, 6 h) and the loss of mitochondrial membrane potential (MMP) was determined by staining cells with JC-1. Histograms of one representative experiment out of triplicates of untreated (Co) and helenalin-treated cells (Hel) are shown. C, For Western blot analysis of cytochrome *c* release, Neo Jurkat and Bcl-2 Jurkat cells were treated with helenalin (Hel; 20 μ M) for the indicated times. Cytosolic and membrane fractions were prepared.

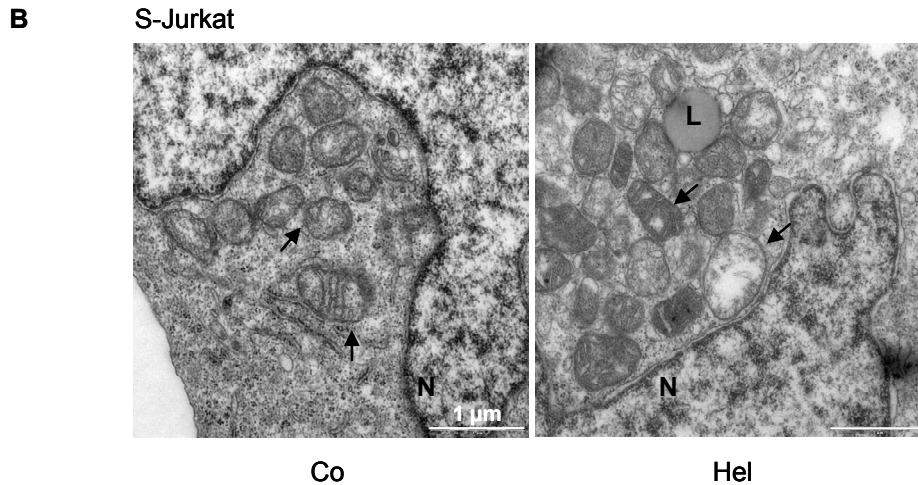
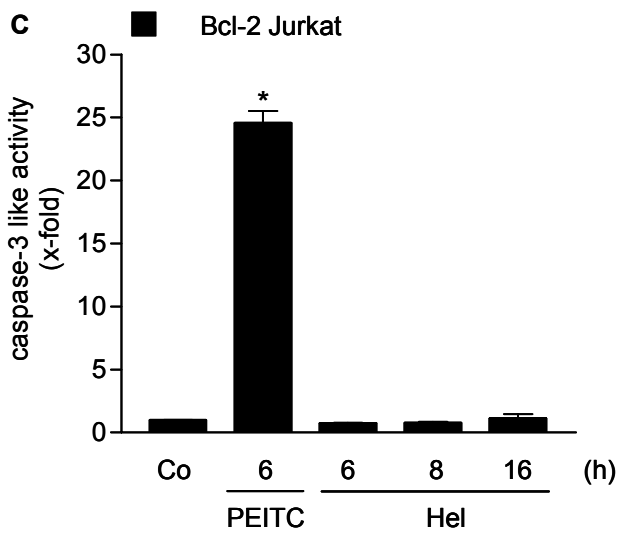
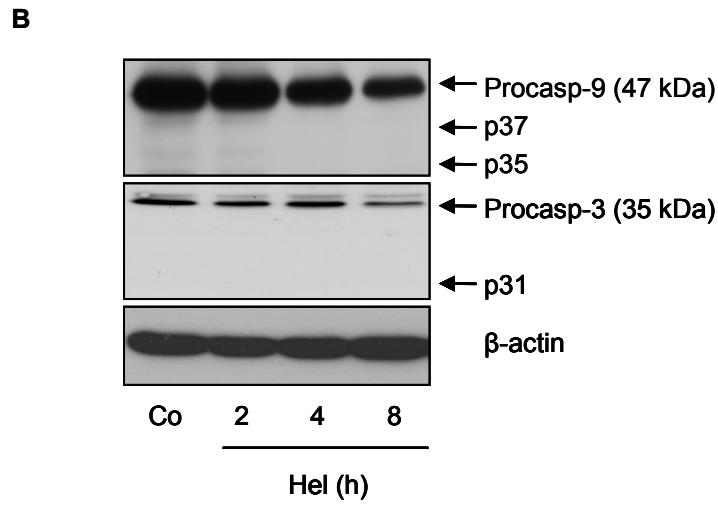
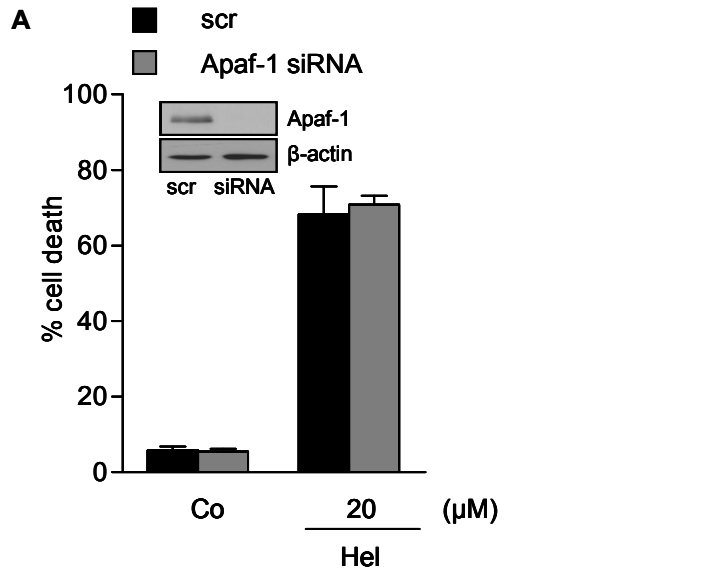


Figure 9 Influence of helenalin on mitochondrial morphology. A, Bcl-2 Jurkat cells were treated with helenalin (Hel; 20 μ M) for 8 h and samples were prepared for TEM microscopy. B, As a control for the induction of apoptosis, wild type S-Jurkat cells were treated with helenalin (Hel; 10 μ M, 8 h). Black arrows indicate mitochondria. N: nucleus, L: lipid body, V: vacuole.

4.2.2 Caspase dependency

As a next step the participation of the classical apoptosome pathway was investigated. The apoptosome consist of cytochrome *c*, Apaf-1 and the initiator caspase-9. Silencing of Apaf-1 *via* siRNA did not influence the induction of cell death by helenalin (Figure 10 A) suggesting that helenalin-induced cell death occurs independently of the apoptosome and the mitochondrial pathway of apoptosis. Along this line, Western blot analysis (Figure 10 B), as well as measurement of caspase-3 like and caspase-8 activity (Figure 10 C-D) and employment of the pan-caspase inhibitor Q-VD-OPh (Figure 10 E) revealed no involvement of caspases in helenalin-induced cell death in Bcl-2 overexpressing cells. The chemical β -phenylethyl isothiocyanate (PEITC) was used as positive control, known to induce caspase-dependent cell death in Bcl-2 Jurkat cells^{113, 114}.



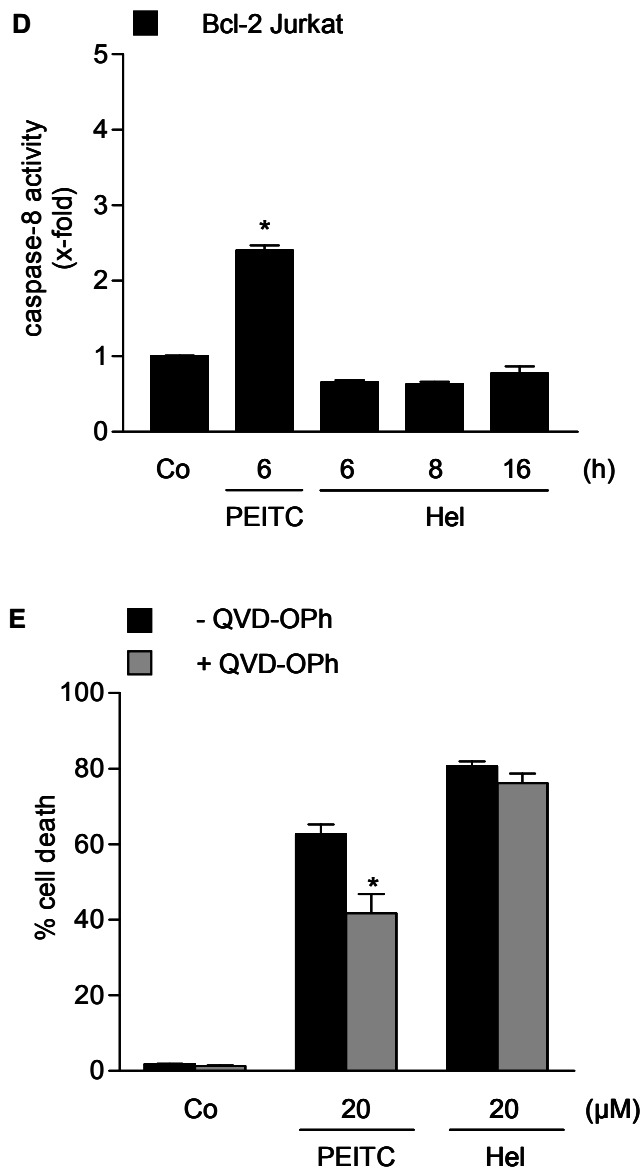
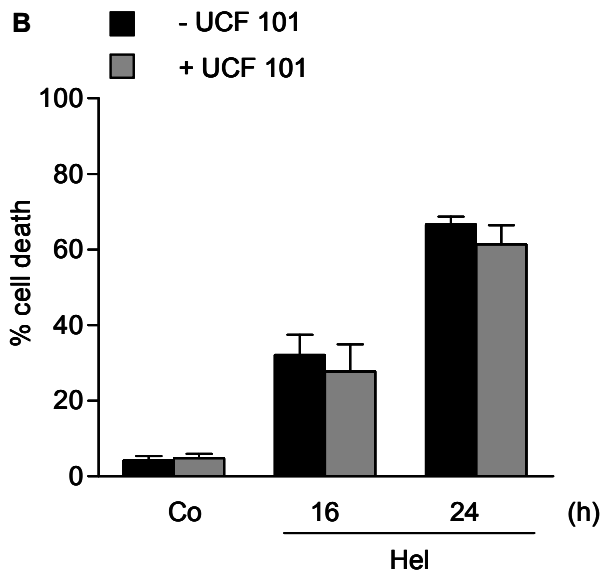
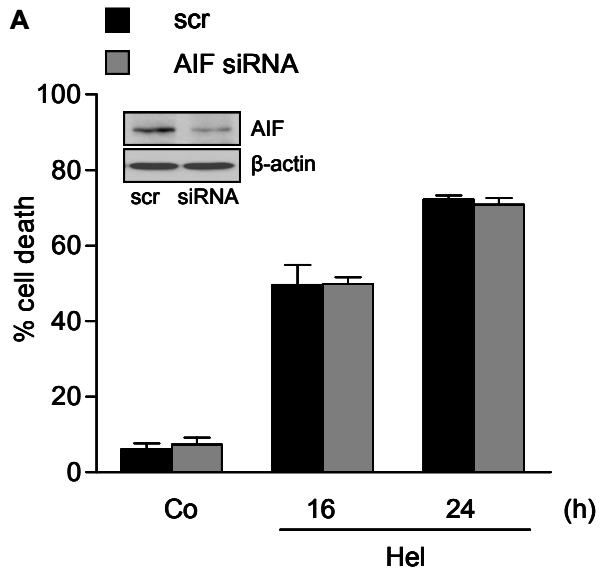


Figure 10 Classical mitochondrial pathway and caspases are not involved in helenalin-induced cell death. A, Bcl-2 Jurkat cells were transiently transfected with scrambled (scr) or Apaf-1 siRNA oligonucleotides and treated with helenalin (Hel; 20 μ M, 24 h). Cell death was quantified by Nicoletti assay. Apaf-1 protein levels in transfected cells were analyzed by Western blot. B, Western blot analysis of caspase activation in Bcl-2 Jurkat cells after incubation with helenalin (Hel; 20 μ M) for the indicated times. Arrows indicate proforms of caspase-9 and -3 and location of their active, cleaved forms, respectively. C and D, Determination of caspase-3 like and caspase-8 activity in Bcl-2 Jurkat cells. Cells were treated with helenalin (Hel; 20 μ M) or β -phenylethyl isothiocyanate (PEITC; 20 μ M) for the indicated time points and caspase activity was determined. E, Bcl-2 Jurkat cells were treated with β -phenylethyl isothiocyanate (PEITC; 20 μ M) or helenalin (Hel; 20 μ M) for 16 h and cell death was measured by PI exclusion. If indicated, cells were pre-incubated with the pan-caspase inhibitor Q-VD-OPh (10 μ M) for 1 h. Data are expressed as mean \pm SEM (n=3). *, p < 0.001 (ANOVA, Bonferroni). Experiments for Figure 10 A and B were performed by N. López Antón.

Since caspases are not the main players in helenalin-mediated cell death in Bcl-2 overexpressing Jurkat cells, the role of the caspase-independent apoptotic factors such as the serine protease Omi/HtrA2 and the endonuclease AIF were investigated. Silencing of AIF and use the Omi inhibitor UCF (Figure 11 A-B) revealed that these caspase-independent mediators are unlikely to be involved in helenalin evoked cell death. Evidence for a non-

apoptotic cell death signaling of helenalin was finally provided by analysis of phosphatidylserin at the outer cell membrane (Annexin V staining), a classical sign of early apoptosis. Interestingly, the Bcl-2 overexpressing cells did not show significant translocation of phosphatidylserin after helenalin-treatment for 8 h, whereas the vector control cells (Neo Jurkat cells) were clearly Annexin V positive (Figure 11 C).



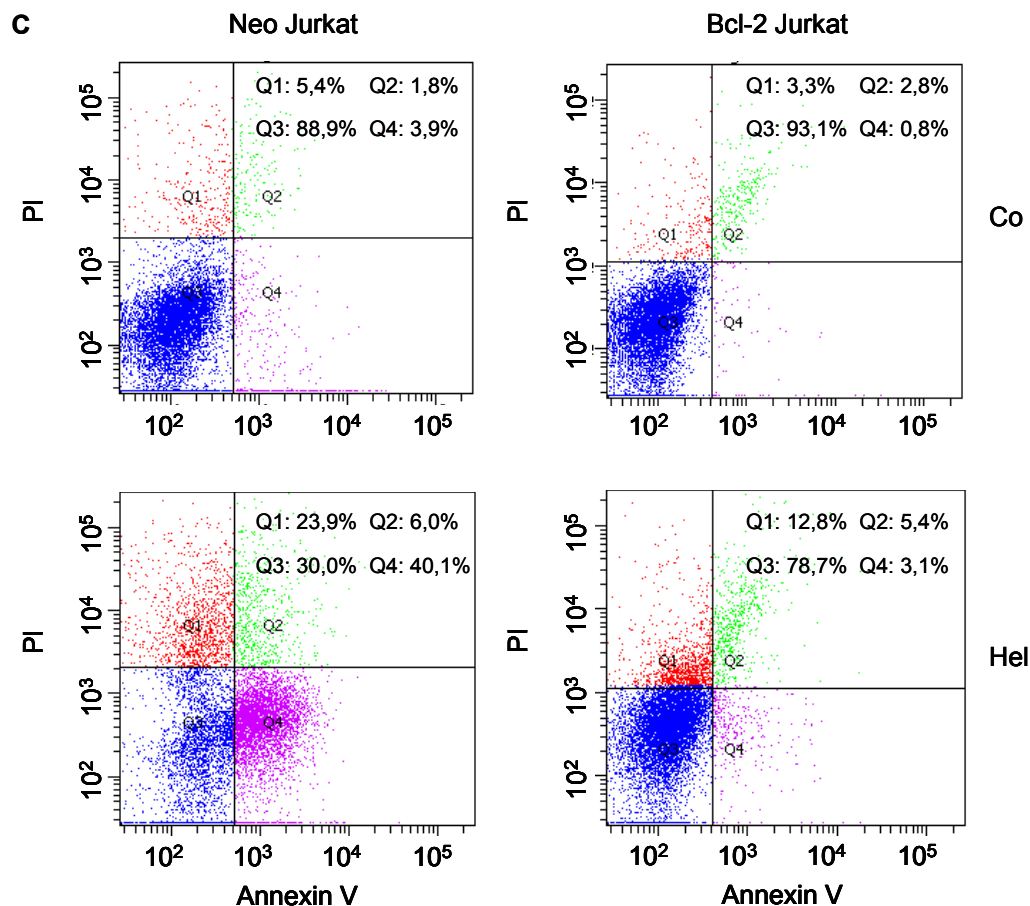


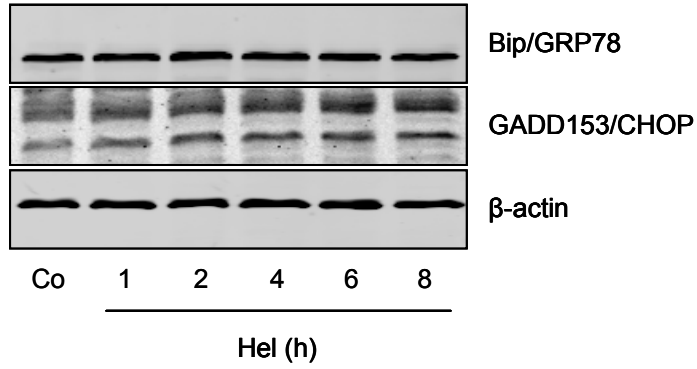
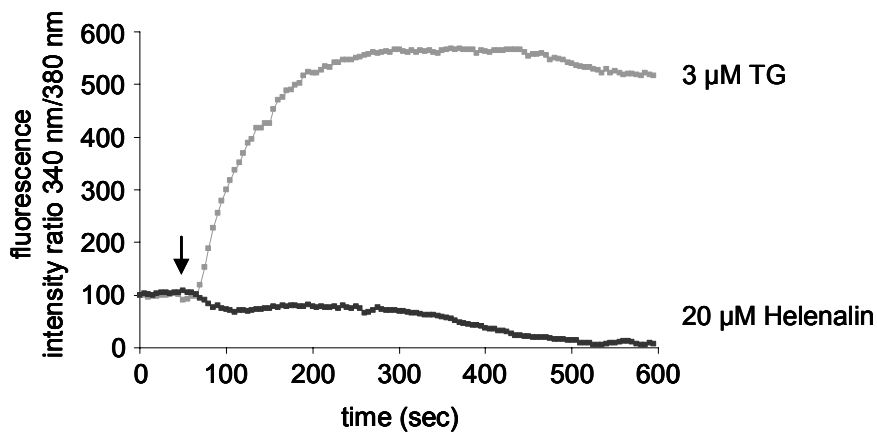
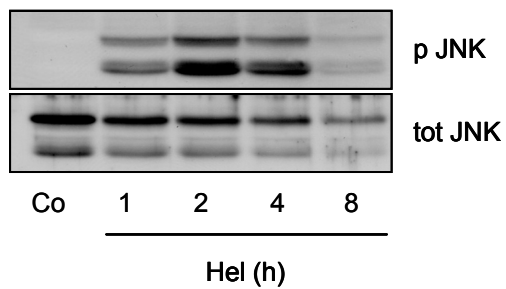
Figure 11 Diverse mitochondria-derived caspase-independent apoptotic factors are not involved in helenalin-induced cell death. A, Bcl-2 Jurkat cells were transfected with scrambled (scr) or AIF siRNA oligonucleotides and cells were treated with helenalin (Hel; 20 μ M) for the indicated times. Cell death was measured by Nicoletti assay. Western blot showing AIF protein levels in scramble (scr) or AIF siRNA transfected cells. B, Bcl-2 Jurkat cells were left untreated (Co) or preincubated with the Omi/HtrA2 inhibitor UCF101 (10 μ M) for 1 h and then treated with helenalin (Hel; 20 μ M) for 16 h or 24 h, respectively. Cell death was quantified by Nicoletti assay. C, Neo Jurkat and Bcl-2 Jurkat cells were left untreated (Co) or treated with helenalin (Hel; 20 μ M) for 8 h and PI/Annexin V-FITC staining was performed. Dot plots of one representative experiment are shown. Data are expressed as mean \pm SEM (n=3). Experiments for Figure 11 A and B were performed by N. López Antón.

4.3 Mechanisms of helenalin's bypass of Bcl-2-mediated cytoprotection

4.3.1 ER stress, autophagy and necroptosis

In search for nonapoptotic events leading to cell death, we first focused on autophagy. Depending on the context, autophagy enhances cell survival or commits the cell to non-apoptotic cell death. ER stress induction has recently been linked to induction of autophagy^{69, 118}. Nevertheless, no evidence for ER stress-induced by helenalin is given since helenalin did not affect the expression of BiP/GRP78 and GADD153/CHOP, two major UPR-upregulated proteins during ER stress (Figure 12 A). Furthermore, increased Ca^{2+} -levels, as seen after treatment with thapsigargin, an inhibitor of the endoplasmic reticulum Ca^{2+}

ATPase (SERCA), was not observed after incubation with helenalin (Figure 12 B). However, a strong induction of JNK, a rapid phosphorylation of eIF2 α and dephosphorylation of mTOR in Bcl-2 overexpressing cells were observed upon helenalin-treatment (Figure 12 C-E).

A**B****C**

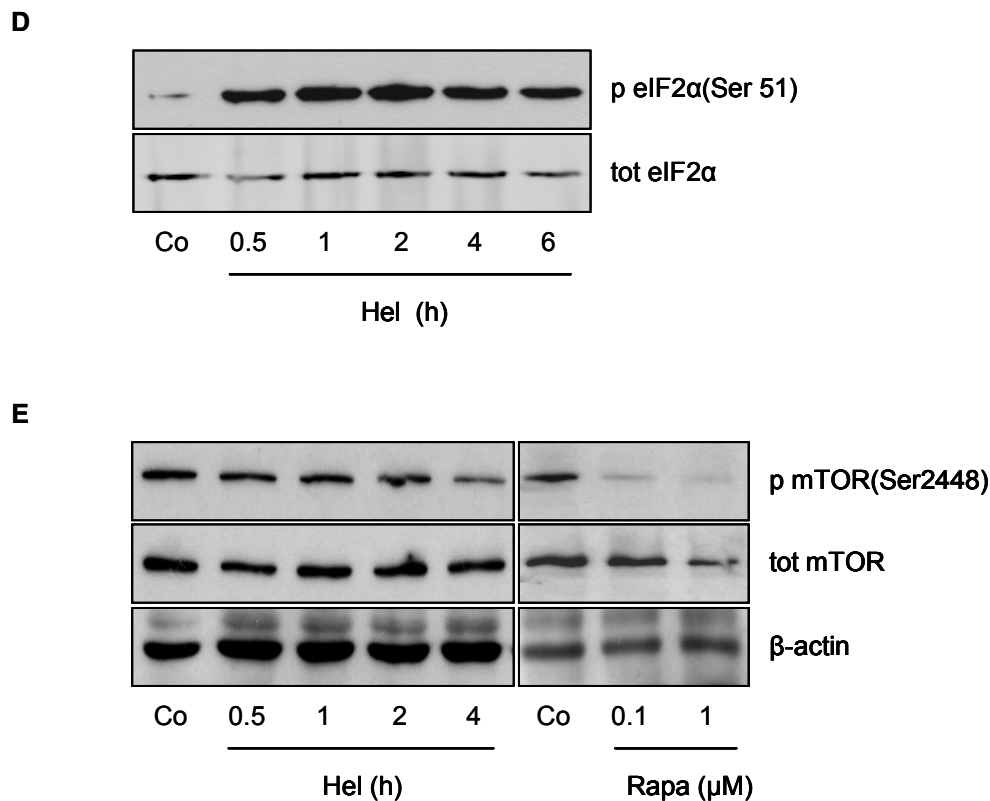
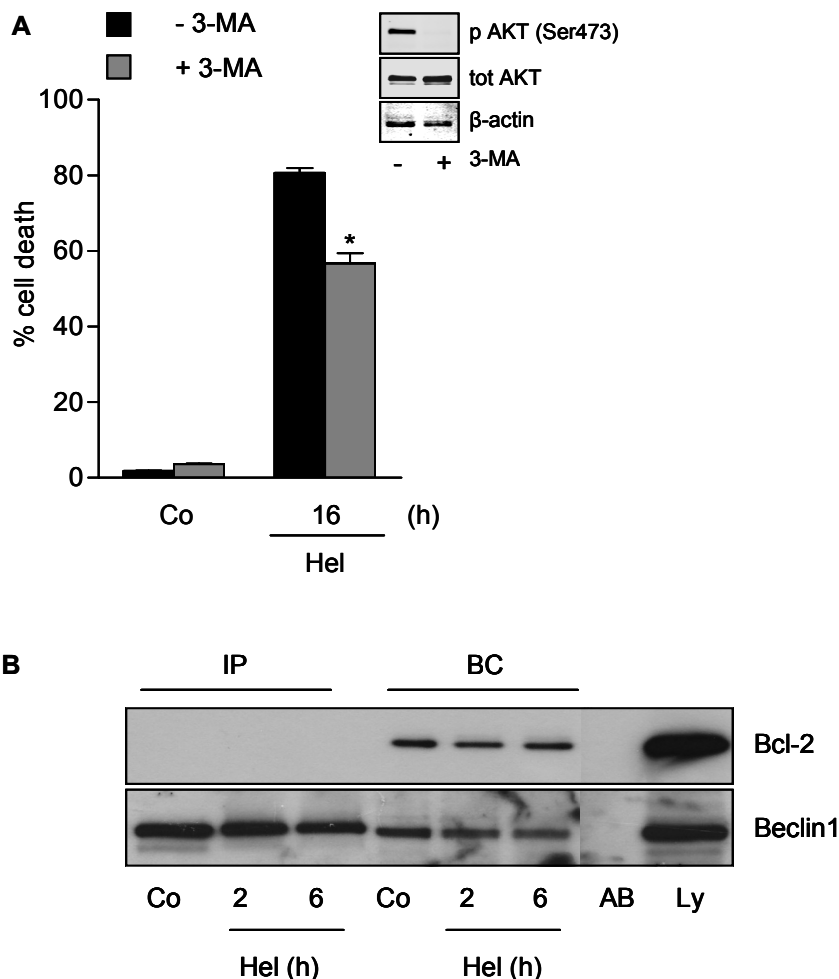


Figure 12 Helenalin does not cause ER stress. A, For the Western blot analysis of proteins involved in ER stress, Bcl-2 Jurkat cells were treated with helenalin (Hel; 20 μM) for the indicated time points. B, Intracellular calcium-levels were determined. Thapsigargin (TG) was used as a control for rapid increase of intracellular calcium-levels. The average-value curve of 3 independent experiments is shown. C-E, Levels of phosphorylation status of JNK, eIF2α and mTOR were determined by Western blot analysis. Rapamycin (Rapa; 6 h) was used as a control to induce dephosphorylation of mTOR at Ser2448. Experiments for Figure 12 C were performed by N. López Antón.

Activation of JNK, phosphorylation of eIF2α and inhibition of mTOR have been linked to induction of autophagy^{69, 118}. By the use of 3-MA (3-methyladenine), a well established inhibitor of autophagy⁶⁵, we wanted to investigate if helenalin induces autophagy. Although the PI3K inhibitor 3-MA partly diminishes helenalin-induced cell death after 16 h of stimulation (Figure 13 A), it could not prevent cell death by helenalin after a longer stimulation time (also see Figure 15 C). Activity of 3-MA was confirmed by analysis of the phosphorylation status of the PI3K downstream target Akt (insert). Bcl-2 is an important inhibitor of autophagy by binding Beclin1 and thus preventing the induction of autophagy. The Bcl-2/Beclin1 complex can be disrupted by activated JNK. Investigation of the interaction of Bcl-2 with Beclin1 by immunoprecipitation assay in our cells revealed, that there was no interaction detectable neither in the controls nor in helenalin-treated cells (Figure 13 B). Furthermore, no accumulation of LC3 II, commonly observed during autophagy, could be detected by Western blot (Figure 13 C). Most importantly, electron microscopic examination did not reveal characteristic autophagolysosomes within helenalin-treated Bcl-2 overexpressing cells (data not shown).

We next focused on mediators involved in signaling events of programmed necrosis. Necrostatin-1 (Nec-1) inhibits RIP1 and acts as a specific inhibitor of necroptotic cell death¹¹⁹. Exposure of Bcl-2 Jurkat cells to Nec-1 before helenalin-treatment did not prevent cell death arguing against necroptosis as a mode of cell death in these cells. In contrast, Nec-1 abrogated necroptosis induced by TNF- α in the presence of cycloheximide and the pan-caspase inhibitor Q-VD-OPh in S-Jurkat cells (positive control)^{55, 120} (Figure 13 D and insert). As already mentioned, helenalin induced early JNK activation and this has also been associated with programmed necrosis⁴⁴. Yet, JNK activation by helenalin does not contribute to cell death as indicated by the employment of SP600125, a commonly used JNK inhibitor (activity was confirmed by analyzing the phosphorylation of the JNK downstream target c-Jun) (Figure 13 E and insert).



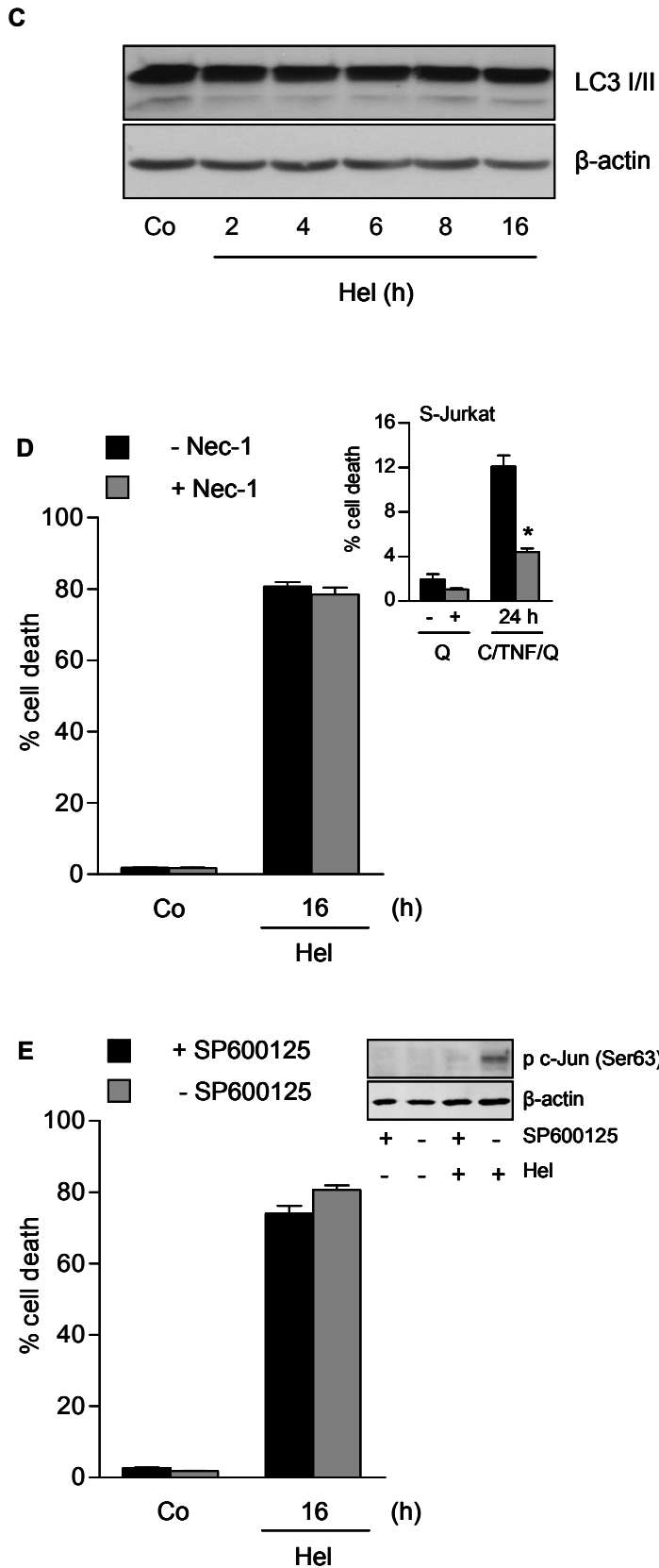
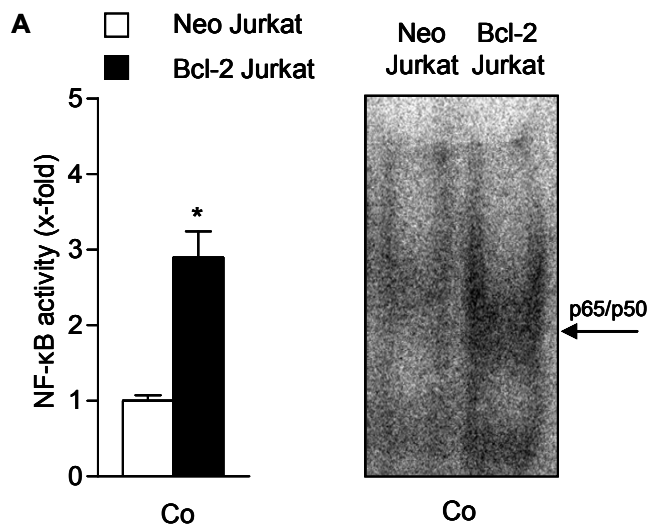


Figure 13 Helenalin induces neither autophagy nor necroptotic cell death. A, Bcl-2 Jurkat cells were treated with helenalin (Hel; 20 μ M) either with or without a 1 h-pretreatment with the autophagy inhibitor 3-MA (10 mM). Cell death was quantified by PI exclusion assay. Insert shows Western blot analysis of phosphorylation status of Akt after treatment with the PI3K inhibitor 3-MA (10 mM; 24h). B, Bcl-2 Jurkat cells were treated with helenalin (20 μ M) for the indicated times. Beclin1 was immunoprecipitated and the amount of co-precipitated Bcl-2 was detected by Western blot analysis. IP: immunoprecipitated samples, BC: binding control, Ly: whole cell lysate

sample, AB: antibody control. C, For the Western blot analysis of the autophagy-induced conversion of LC3 I to LC3 II, Bcl-2 Jurkat cells were treated with helenalin (Hel; 20 μ M) for the indicated times. D, If indicated, Bcl-2 Jurkat cells were incubated with necrostatin-1 (Nec-1; 30 μ M) 1 h before treatment with helenalin (Hel; 20 μ M, 16 h). Insert: Induction of necroptotic cell death in S-Jurkat cells with a combination of TNF α (10ng/ml), cycloheximide (C; 1 μ g/ml) and pan-caspase inhibitor Q-VD-OPh (10 μ M), which is reduced by a 1 h-pretreatment with Nec-1 (30 μ M). Cell death was quantified by PI exclusion assay, respectively. E, Bcl-2 Jurkat cells were treated with helenalin (Hel; 20 μ M, 16 h) either with or without a 1 h-pretreatment with the specific JNK inhibitor SP600125 (10 μ M). Cell death was quantified by PI exclusion assay. Western blot analysis of JNK downstream target p cJun(Ser63) after helenalin- and SP600125-treatment of Bcl-2 Jurkat cells. Data are expressed as mean \pm SEM (n=3). *, $p < 0.001$ (ANOVA, Bonferroni).

4.3.2 Helenalin inhibits Bcl-2-induced NF- κ B activity

Since a link between Bcl-2 and the nuclear factor κ B signaling pathway has been described for other cell lines¹²¹, we next examined if Bcl-2 overexpressing Jurkat cells show increased NF- κ B activity and if helenalin is able to interfere. In fact, as seen in Figure 14 A, nuclear shift as well as a NF- κ B activity assay clearly show that Bcl-2 overexpression leads to increased constitutive NF- κ B activity, known to be mediator of survival and death resistance in leukemia cells¹²². Helenalin significantly reduces NF- κ B binding and activity in Bcl-2 overexpressing cells (Figure 14 B). The subunit composition of NF- κ B was investigated by a supershift assay. The shift of the band or decreased binding activity indicate that the upper band consist of p65 and p50 both, in the control and TNF α -treated cells.



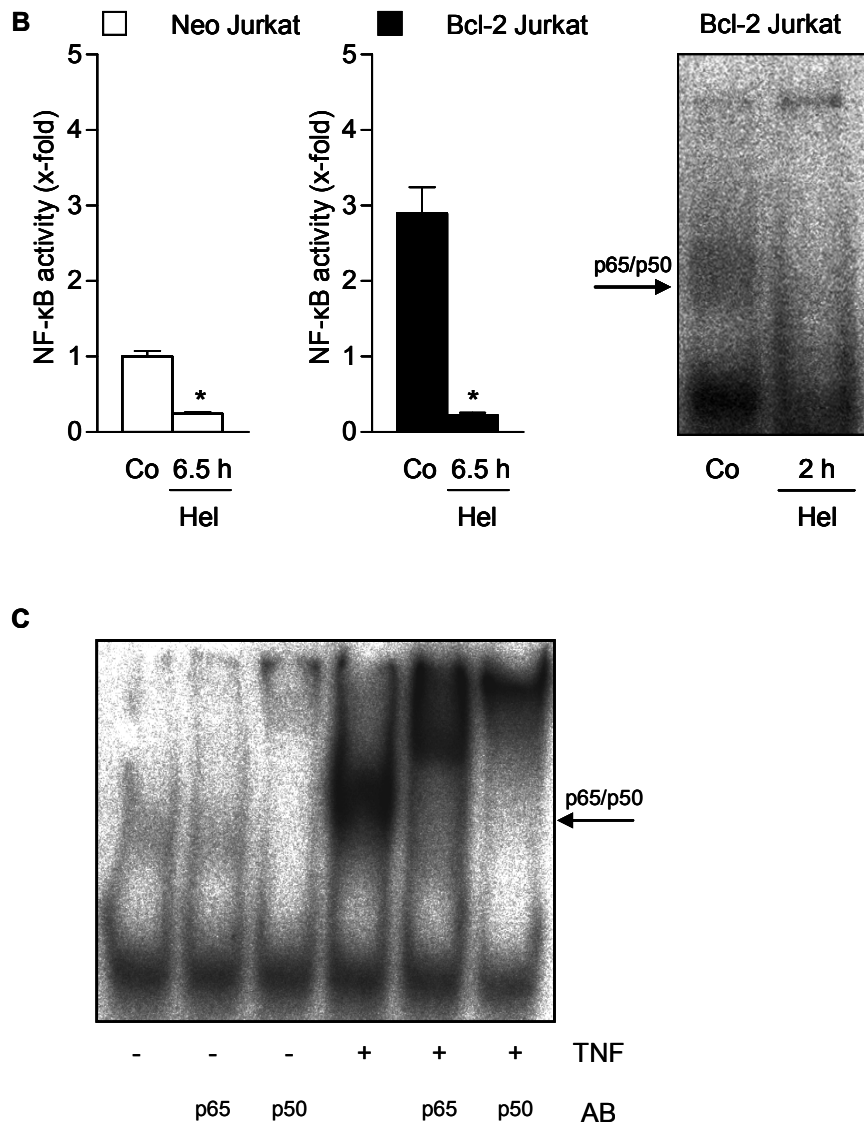
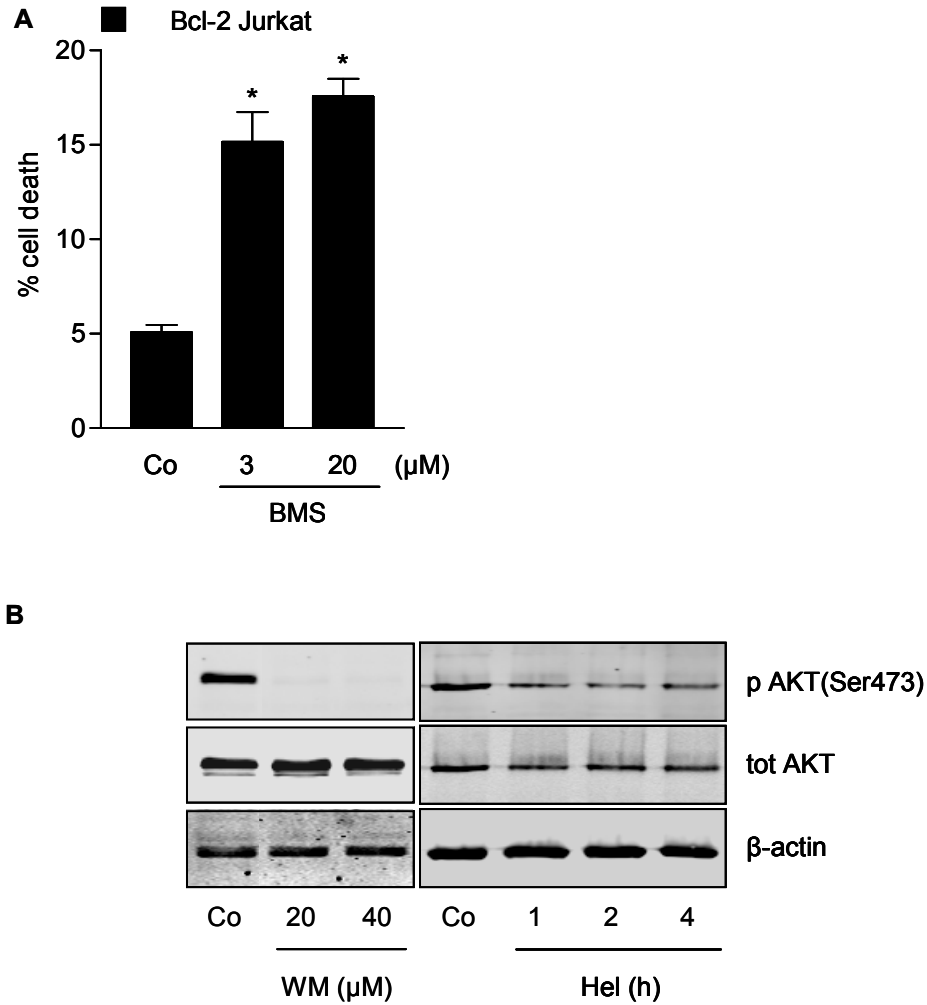


Figure 14 Helenalin overcomes Bcl-2-mediated resistance by inhibition of protective NF- κ B activity. A, In order to determine the basic NF- κ B activity in untreated Neo Jurkat and Bcl-2 Jurkat cells (Co), a reporter gene assay, as well as electrophoretic mobility shift assay (EMSA) were performed. NF- κ B activity is diagrammed as x-fold activity referring to untreated Neo Jurkat cells. Data are expressed as mean \pm SEM (n=3). *, p < 0.001 (Student's t-test). B, Helenalin's capacity to inhibit NF- κ B promoter activity and DNA binding capacity was proved by reporter gene assay (left panel) and EMSA (right panel). For the reporter gene assay, Neo Jurkat and Bcl-2 Jurkat cells were either left untreated (Co) or treated with helenalin (Hel; 20 μ M) for 6.5 h. Data are expressed as mean \pm SEM (n=3). *, p < 0.0001 (Student's t-test) versus controls, respectively. For the electrophoretic mobility shift assay, Bcl-2 Jurkat cells were left untreated (Co) or treated with helenalin (Hel; 20 μ M, 2 h). Nuclear proteins were isolated, P³²-labeled NF- κ B consensus sequence oligonucleotides were added. C, Subunit composition of NF- κ B was determined by supershift assay. EMSA was performed without or with specific antibodies (AB) against p65 and p50 (2 μ g per sample) which were added to the binding reactions before performance of EMSA. Nuclear protein was prepared from untreated or TNF α (TNF)-treated (10 ng/ml; 30 min) cells.

The NF- κ B inhibitor BMS-345541 (N-(1,8-Dimethylimidazo[1,2-a]quinoxalin-4-yl)-1,2-ethanediamine hydrochloride), acting on the I κ B kinase complex¹²³, was also able to induce cell death in Bcl-2 protected cells (Figure 15 A), yet to a minor extent in comparison with helenalin. Moreover, as shown by Western blot analysis (Figure 15 B), helenalin also reduced phosphorylation of Akt, which is another important factor in cancer cells concerning

cell growth and survival¹²⁴. However, the PI3K inhibitors 3-MA and wortmannin, which both efficiently inhibit Akt downstream of PI3K, neither induced cell death in Bcl-2 overexpressing cells themselves nor added to the cytotoxicity of helenalin or BMS in Bcl-2 overexpressing Jurkat cells. As shown before, 3-MA rather reduced or delayed cell death induction by helenalin.



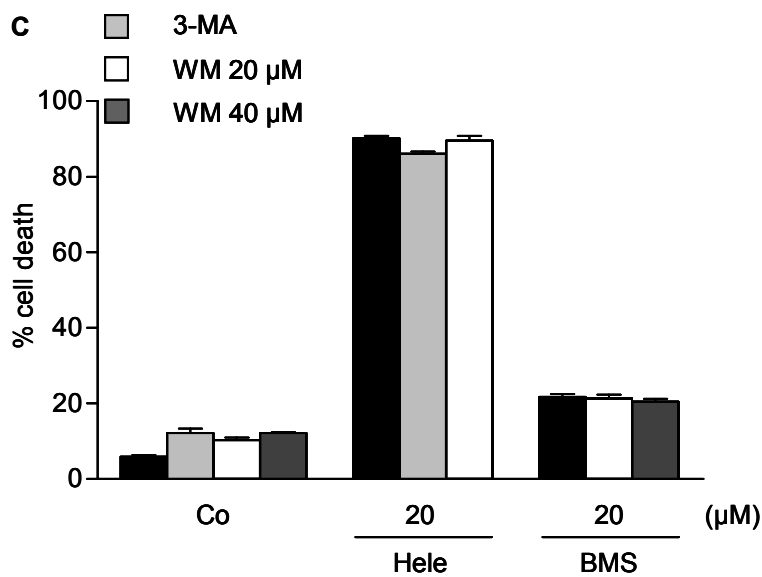


Figure 15 Helenalin overcomes Bcl-2-mediated resistance by inhibition of protective NF- κ B activity. A, Bcl-2 Jurkat cells were treated with increasing concentrations of the NF- κ B inhibitor BMS-345541 (BMS) for 48 h. Cell death was measured by PI exclusion assay. B, The level of phosphorylation status of Akt at Ser473 after treatment of Bcl-2 Jurkat cells with helenalin (Hel; 20 μ M) or with the positive control wortmannin (WM; 6 h) was analyzed by Western blot. C, Bcl-2 Jurkat cells were incubated with the PI3K inhibitor 3-MA (10 mM) or wortmannin (WM 20 μ M or 40 μ M) 1 h before treatment with helenalin (20 μ M) or BMS-345541 (BMS; 20 μ M) and cell death was measured after 48 h using PI exclusion assay. Data are expressed as mean \pm SEM (n=3). *, p < 0.001 (ANOVA, Bonferroni).

4.3.3 Helenalin induces cell death by induction of ROS

The focus on NF- κ B inhibition and cell death induction asks for further mediators. Factors downstream of NF- κ B inhibition leading to cell death are increased levels of free iron. This process is mediated by downregulation of iron storage protein FHC and in turn ROS production¹²². As shown in Figure 16 A, helenalin induced ROS synthesis comparable to the positive control H₂O₂, measured by increase of fluorescence of the ROS-sensitive dye 2',7'-Dichlorodihydrofluorescein diacetate (DCDHF) and the use of antioxidants such as NAC or Tiron completely prevents cell death. Moreover, cell death by helenalin involves iron-ions as the use of the iron chelator desferrioxamine (DFO) inhibited cell death by helenalin (Figure 16 B-C).

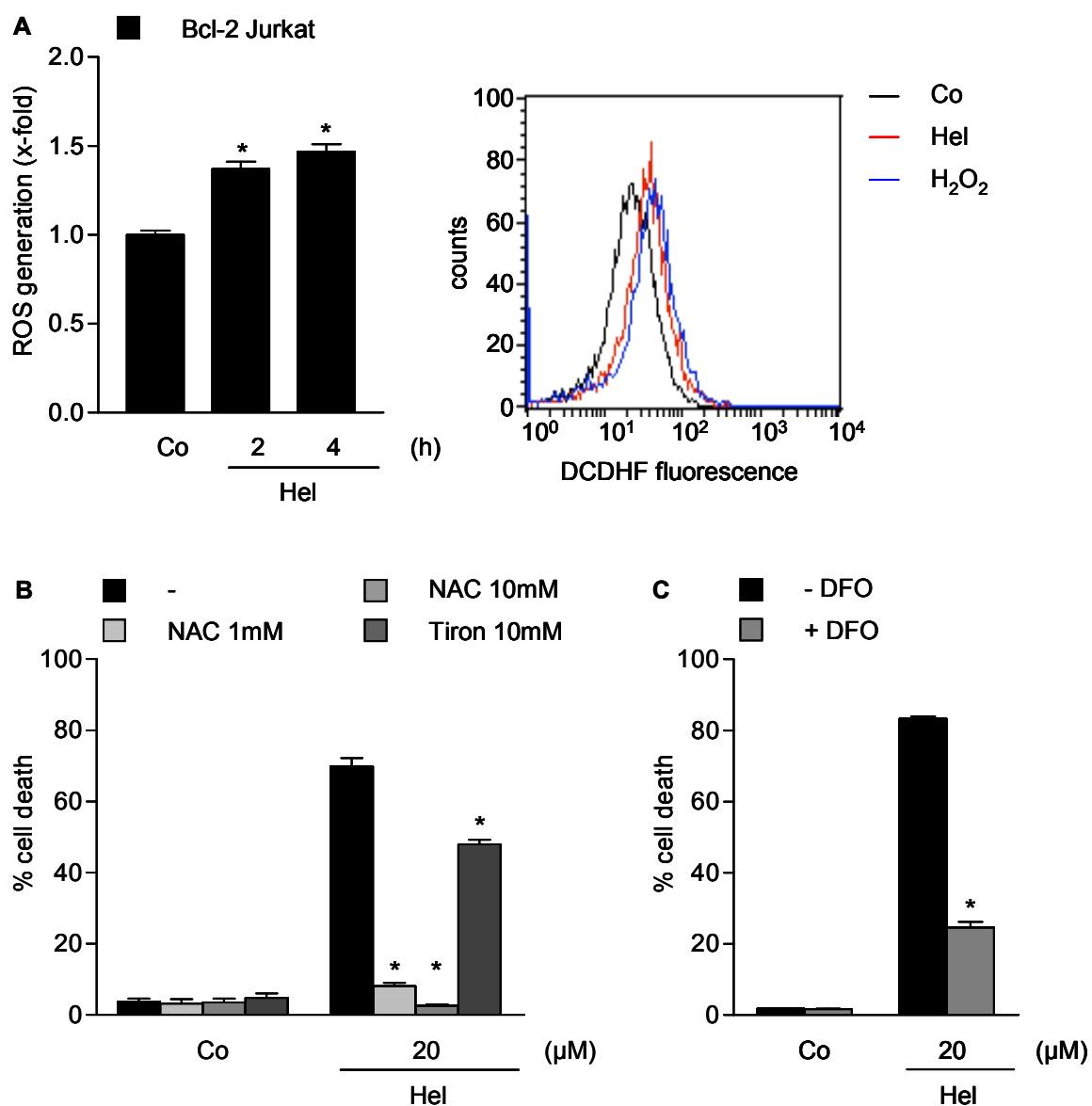


Figure 16 Helenalin induces cell death by generating ROS. A, After incubation with helenalin (Hel; 20 μ M) for the indicated times, Bcl-2 Jurkat cells were stained with DCDHF diacetate and analyzed by flow cytometry. The x-fold increase of ROS generation compared to untreated (Co) cells is shown (left panel). An increase of DCDHF fluorescence correlates with augmented levels of ROS after treatment with helenalin (Hel; 20 μ M) or H₂O₂ (17.6 μ M, 30 min). Representative histogram plot is shown (right panel). B, Bcl-2 Jurkat cells were pretreated with NAC or Tiron for 1h before incubation with helenalin (Hel; 20 μ M) for 24 h or treated with solvent as a control. Cell death was measured by Nicoletti assay. C, To investigate the influence of iron on helenalin-induced formation of ROS, Bcl-2 Jurkat cells were treated with helenalin alone (Hel; 20 μ M), or in combination with deferoxamine mesylate (DFO; 20 μ M) for 16 h and cell death was measured by PI exclusion. Data are expressed as mean \pm SEM (n=3). *, p <0.001 (ANOVA, Bonferroni). Experiments for Figure 16 B were performed by N. López Antón.

DISCUSSION

5 DISCUSSION

Evasion of cell death of cancer cells is still a challenging problem for the efficacy of cancer treatment and the development of new anticancer therapies. Many chemotherapeutic agents induce apoptosis via the intrinsic or the extrinsic pathway. Thus, one possibility for cancer cells to evade cell death, especially apoptosis, is the overexpression of anti-apoptotic proteins such as Bcl-2, which is frequently observed in many types of human cancer. New strategies have to be found to overcome Bcl-2-mediated resistance, by directly targeting the Bcl-2 protein e.g. by the use of Bcl-2 inhibitors, or by circumventing cell death pathways that are blocked by Bcl-2. Helenalin has been proofed to be effective in a variety of tumor cells^{7, 19, 20} and has also shown *in vivo* antitumor activity⁴. Interestingly, helenalin has recently gained considerable attention as lead structure for treatment of inflammation^{9, 30, 31} whereas the related STL parthenolide has been preferentially appreciated as experimental tumor drug¹²⁵⁻¹²⁷. However, own and others work attribute antitumor activity even *in vivo* also to helenalin^{4, 7, 19-21, 128, 129}.

5.1 Untypical signaling of helenalin-induced cell death

5.1.1 Apoptosis

First, the common players and downstream effects of apoptosis signaling such as release of cytochrome *c* and subsequently apoptosome-formation as well as caspase activation were investigated. By overcoming Bcl-2-mediated resistance, helenalin does not behave like a specific Bcl-2 inhibitor since neither typical mitochondrial activation features such as cytochrome *c* release, disruption of mitochondrial membrane potential and caspase activation nor classical apoptosis have been observed for helenalin in comparison to specific Bcl-2 inhibitors such as the compound ABT-737¹⁰⁴. Phosphorylation of Bcl-2 in the flexible loop domain is the major regulatory mechanism, which modulates the function of Bcl-2. Other investigators have shown that the multiple-site phosphorylation by JNK abrogates survival function of Bcl-2 in paclitaxel-induced apoptosis⁴². Although JNK is activated as an early event after helenalin-treatment, we do not observe phosphorylation of Bcl-2, suggesting that Bcl-2 remains unaffected. This assumption is underlined by the fact that mitochondrial membrane potential is conserved in Bcl-2 overexpressing Jurkat cells even after 6 h of helenalin-treatment. Other reports have shown that sustained JNK activation, e.g. induced by ROS, is responsible for induction of apoptosis and necrosis¹³⁰⁻¹³³ and JNK activation has also been described in the context of autophagy^{134, 135}. Yet, by the use of a JNK inhibitor we could exclude that helenalin-induced JNK activation is responsible for cell death induction, suggesting that the observed activation of JNK might rather be a stress response.

5.1.2 Autophagy

We focused on autophagy in an attempt to characterize the type of cell death induced by helenalin in Bcl-2 overexpressing cells since this process is linked and influenced by Bcl-2 and NF- κ B. Besides, autophagy has recently been described to be a downstream event of ER stress^{69, 118, 136}. Therefore we first focused on important events during ER stress such as upregulation of BiP/GRP78 and CHOP/GADD153, JNK activation, Ca²⁺-release and phosphorylation of eIF2 α ^{77, 137, 138}. Yet, no evidence for ER stress is given since helenalin did not affect the expression of BiP/GRP78 and CHOP/GADD153. Others have shown that ER stress induces caspase-4/12 activation upstream of mitochondria leading to caspases-9/3 activation and apoptosis^{139, 140}, thus, the fact that caspases are not involved in helenalin-induced cell death supports the finding that ER stress is not induced. The ER represents the most important storage site for Ca²⁺ in the cell. Upon ER stress, high amounts of calcium ions can be released into the cytosol, mediating further downstream effects such as apoptosis^{67, 74} or autophagy by calcium-mediated activation of PKC θ and of CaMKK β ^{75, 76}. It is believed that also the source and the amount of increased calcium ions may induce different types of cell death. The influx of calcium across the plasma membrane triggers necrosis, whereas the release of calcium from the ER might rather induce apoptosis⁵⁰. We could not observe increased calcium-levels after helenalin-treatment, although helenalin has been reported to decrease cellular glutathion levels^{141, 142}, which is frequently associated with an increase of resting intracellular calcium-levels, which finally is responsible for cytotoxicity¹⁴³. Yet, increase of intracellular calcium-levels was also not observed after stimulation with helenalin alone in other studies^{143, 144}. Phosphorylation of eIF2 α leads to impaired protein synthesis as a result of UPR. It has already been described that helenalin inhibits protein synthesis^{4, 145} by activating eIF2 α -kinase causing phosphorylation of eIF2 α and inhibition of eIF3. Indeed, we do observe early phosphorylation of eIF2 α , but this is unlikely to be caused by UPR in our model. Phosphorylation of eIF2 α is rather caused by a direct influence of helenalin on protein-synthesis in Bcl-2 overexpressing cells. Although we observe reduction of cell death to a certain extend after 16 h when cells were pre-treated with 3-MA, we could not see an entire prevention of helenalin-induced cell death by 3-MA especially after longer stimulation times. These findings suggest that cell death induction by helenalin is just delayed but not prevented by 3-MA. We do not observe an influence on helenalin-induced cell death by the use of wortmannin, another PI3K and autophagy inhibitor. Although 3-MA is a commonly used autophagy inhibitor, recent reports have shown that it also inhibits other processes, which are not specific for macroautophagy (e.g. other degradative pathways or 3-MA mediated inhibition of UPR activation by ER stress). Thus, results obtained by the singular use of 3-MA to implicate autophagy, should be interpreted with caution^{65, 118}. To exclude that cell death induced by helenalin is accompanied or caused

by autophagic signaling, it was necessary to investigate other markers for autophagy such as the conversion of LC3 I to membrane-bound LC3 II. After helenalin-treatment, no increase of LC3 II in the Western blot analysis could be observed. Weak processing of LC3 in WT Jurkat clones has been described before, probably due to hyperactive mTOR signaling that results in these PTEN (phosphatidylinositol(3,4,5)-triphosphate phosphatase)-deficient cells¹⁴⁶. Consequently, no evidence for autophagy is given since we could not detect increase of LC3 II levels or typical formation of autophagosomes after helenalin-treatment.

5.1.3 Helenalin-induced cell death shows necrotic features

Our investigations show that apoptosis and autophagy are not induced by helenalin. This fact led us consider necrosis as the type of cell death caused by helenalin in Bcl-2 Jurkat cells. Although necrosis has always been considered as an accidental form of cell death, recent studies showing that initiation of necrosis could be blocked by inhibition of discrete cellular processes led to the idea that necrosis could be "programmed". Likewise, programmed necrosis takes place in patients treated with chemotherapeutics and an important physiologic role for programmed necrosis in response to viral infection has been suggested⁵². Two forms of programmed necrosis have been described, necroptosis and PARP1-mediated necrotic death. Necroptosis depends on the kinase activity of RIP1, which can be inhibited by necrostatin-1. The inhibition of cell death by necrostatin-1 thus proves the induction of necroptosis. Moreover, induction of autophagy during necroptosis has also been observed⁴⁴. Since the use of RIP-1 inhibitor necrostatin-1 does not influence helenalin-induced cell death and we do not observe induction of autophagy, helenalin-induced necrosis can not be linked to necroptotic pathways. Other forms of programmed necrosis such as PARP1-mediated necrosis have also to be taken into consideration. However, it is unlikely that helenalin induces PARP1-mediated necrosis in Bcl-2 overexpressing Jurkat cells, as the two major players of this pathway, AIF and JNK, are not involved (shown by use of AIF siRNA experiments and the use of JNK inhibitor).

Yet, helenalin-induced cell death is characterized by necrotic features, as Bcl-2 overexpressing cells lack PS exposure and show an early onset becoming PI positive. The theory, that necrosis is the type of cell death induced by helenalin in this cell line is also supported by the fact that characteristics of other possible pathways leading to cell death, such as apoptosis or autophagy, cannot be detected.

5.2 NF- κ B inhibition and ROS formation are crucial for helenalin-induced cell death

Helenalin has been shown to interfere with the signal transduction through nuclear factor NF- κ B^{9, 34} playing a pivotal role in inflammation, tumorigenesis and cancer^{147, 148}. Persistent

NF- κ B signaling can facilitate the six hallmarks of cancer: self-sufficient growth, insensitivity to growth-inhibitory signals, evasion of apoptosis, limitless replicative potential, sustained angiogenesis, and tissue invasion and metastasis. Several NF- κ B proteins are found to be overexpressed in several cancers¹⁴⁹. Thus, NF- κ B is another crucial player for cell survival and apoptosis resistance in many cancer types, especially in lymphomas^{150, 151}. Therefore, several small inhibitors of NF- κ B activation such as I κ B kinase (IKK α or IKK β inhibitors, NEMO peptide, thalidomide or antisense oligonucleotides and small interfering RNAs targeting IKK or NF- κ B subunits) and the proteasome (bortezomib) or of the DNA binding of NF- κ B (oligonucleotides that mimic the NF- κ B consensus binding site) are under intensive investigation¹⁵⁰. Malignant cells that exhibit constitutive NF- κ B activation are relatively resistant to radio- or chemotherapy, and NF- κ B inhibitors increase their sensitivity to such anticancer treatments¹⁵², most likely by downregulating antiapoptotic NF- κ B target genes such as c-IAPs, c-FLIP, Bcl-2, and Bcl-X_L. These publications and numerous other recently published data on NF- κ B in hematological malignancies indicate that there is high probability that indirect or direct NF- κ B inhibitors will be used as cancer therapeutics in the future¹⁵⁰.

Interestingly, besides mitochondria-protecting effects of Bcl-2, a link between Bcl-2 and constitutive activation of NF- κ B has been described in a number of recent reports. Bcl-2 mediates phosphorylation of I κ B α at Ser 32 and Ser 36 followed by its proteasomal degradation. This mechanism is mediated by the N-terminal BH4 domain of Bcl-2¹⁵³. Further investigation showed that Bcl-2 signals through Raf-1/MEKK-1 signaling complex to activate IKK β ¹⁵⁴. In line with this, it has been found that downregulation of Bcl-2 attenuates NF- κ B activation because Bcl-2-mediated degradation of the cytoplasmic inhibitor I κ B α is essential for NF- κ B activation¹⁵⁴. This mechanism causes resistance to TNF α -induced apoptosis. In another study it has been shown that Bcl-2 overexpression leads to increased activity of Akt as well as IKK (as a downstream target), by direct interaction of Bcl-2 with Akt¹⁵⁵. Therefore it is not surprising, that also in other tumor cells, an overexpression of Bcl-2 causing increased NF- κ B activity leads to higher risk of tumor metastasis mediated by higher expression of MMP-9¹²¹.

Moreover, also NF- κ B can influence Bcl-2 expression. Lymphoma cells with the t(14;18) translocation show high levels of nuclear NF- κ B proteins, which activate the expression of Bcl-2. This activation is mediated by the CRE (cAMP response element) and the SP1 binding site¹⁵⁶. Another report shows that p50 homodimers of NF- κ B, which act downstream of MEK/ERK, contribute to transcription of the Bcl-2 oncogene^{157, 158}. Additionally, it could be shown that p50 and p52 homodimers, in collaboration with Bcl-3, transactivate the Bcl-2 promoter and that in breast cancer and leukemic (CLL) cells, high NF- κ B expression was associated with high Bcl-2 expression¹⁴⁹. Although helenalin inhibits transcriptional activity of NF- κ B in Bcl-2 Jurkat cells, we did not observe an influence on Bcl-2 expression levels in the

Western blot analysis after helenalin-treatment. Due to vector-driven overexpression of Bcl-2 in Jurkat cells, the reduction of NF- κ B activity by helenalin does not influence Bcl-2 levels in our model. However, as discussed below, we do observe that Bcl-2 overexpression leads to increased NF- κ B activity in Jurkat cells.

5.2.1 Increased NF- κ B activity in Bcl-2 overexpressing Jurkat cells is inhibited by helenalin

For the first time we show that Bcl-2 overexpressing Jurkat cells possess increased NF- κ B activity, which might be additionally beneficial for the cells to survive chemotherapy. Therefore, targeting the NF- κ B pathway in this cell line by the use of NF- κ B inhibitors such as helenalin might be a promising strategy to overcome chemo-resistance. The impact of targeting NF- κ B in cancer therapy is underlined by other studies on STLs showing that normal cells are normally not sensitive to the tested STLs. This is due to only basal NF- κ B activity in normal cells, which is required for differentiation rather than for oncogenesis. Further, in contrast to normal hematopoietic stem cells, NF- κ B signaling is elevated in leukaemia stem cells. This renders cancer stem cells (which are the reason for relapses after chemotherapy) sensitive to the STL parthenolide. Here, effective eradication of leukaemic stem and progenitor cells is due to inhibition of NF- κ B and increase in ROS¹⁷.

The use of the NF- κ B inhibitor BMS-345541 shows that cell death is induced due to inhibition of NF- κ B in Bcl-2 overexpressing Jurkat cells. Yet, helenalin shows superior activity in comparison to BMS-345541. This might be due to the fact that helenalin binds to the transcriptional active p65 subunit of NF- κ B in the nucleus^{9, 32} whereas BMS-345541 only inhibits the upstream activator I κ B-kinase complex¹²³. This means, that helenalin blocks NF- κ B activation pathway at the very end. It remains speculative that the IKK mediated NF- κ B activation pathway does not play a major role in Bcl-2 overexpressing Jurkat cells, but it would explain the fact that BMS-345541 is not as potent as helenalin.

5.2.2 Inhibition of Akt by helenalin

Highly phosphorylated amounts of Akt have been found in type II cell lines, such as Jurkat cells, known to be deficient of PTEN, an upstream inhibitor of the Akt pathway⁴⁹. As shown by Western blot analysis, helenalin also strongly reduces phosphorylation of Akt, which has important function in cancer cells concerning cell growth and survival¹²⁴. PI3K inhibitors such as 3-MA and wortmannin, which both efficiently inhibit Akt downstream of PI3K, neither induce cell death in Bcl-2 overexpressing cells themselves nor add to the cytotoxicity of helenalin or BMS-345541 in Bcl-2 overexpressing Jurkat cells. Thus, helenalin-mediated Akt inhibition does not play a major role in cell death induction.

5.2.3 Helenalin induces ROS generation

Increased ROS generation is commonly observed in cancer cells due to increased metabolic activity and holds cancer-promoting effects as ROS play an important role in stimulating cell growth and proliferation. Yet, high levels of ROS can also induce cellular damage, depending on the levels and also the duration of ROS stress. This fact and the assumption that cancer cells highly depend on their antioxidant systems to counteract increased ROS may provide an opportunity to kill tumor cells, as they might be highly vulnerable to further oxidative insults by exogenous agents ¹⁵⁹. Bcl-2 is localized to the membranes of mitochondria, ER and nuclear envelope, which are all major sites of ROS production. While Bcl-2 has been described as an antioxidant because of its inhibitory effect on H₂O₂ induced lipid peroxidation ⁴⁰, there is also evidence that Bcl-2 may promote a pro-oxidant intracellular milieu as ectopic expression of Bcl-2 caused elevated constitutive level of superoxide anion and intracellular pH in leukaemia cells ¹⁶⁰. Elevated COX activity and oxygen consumption and correlating O₂⁻-production has been observed in Bcl-2 overexpressing tumor cells. This is probably due to heightened mitochondrial respiration suggesting an increased tendency to leak electrons for the generation of O₂⁻ as a by-product ¹⁶¹. Yet, it is interesting that separate studies illustrate that Bcl-2 overexpressing cells have higher levels of total cellular GSH ¹⁶².

We could show that helenalin induces early ROS generation and cell death induced in Bcl-2 Jurkat cells is mediated by ROS as helenalin-mediated cell death is attenuated by treatment with antioxidants such as NAC and Tiron. Interestingly, the NF-κB pathway has been reported to regulate the expression of proteins or enzymes with antioxidative capacities preventing accumulation of toxic ROS ¹⁶³⁻¹⁶⁵. Ferritin heavy chain (FHC), a subunit of the iron storage protein Ferritin, has been found to be a target for constitutive NF-κB signaling in malignant lymphomas without additional stimuli. FHC owns ferroxidase activity converting toxic Fe²⁺ into non-toxic Fe³⁺. As iron plays an important role in the Fenton reaction generating toxic hydroxyl anions and hydroxyl radicals, the proper sequestration of intracellular iron (e.g. by FHC) is highly critical to avoid generation of oxidative stress. Inhibition of the constitutively active NF-κB pathway caused an increase in free intracellular iron by downregulation of ferritin heavy chain in CTCL cells and T cells from Sézary patients but not in T cells from normal healthy donors. This in turn induces massive production of ROS, which finally leads to cell death ¹²². Our own data support this notion also for Bcl-2 overexpressing leukemia cells as helenalin-induced cell death is significantly decreased after treatment with the iron chelator DFO.

Thus, clearly the inhibition of NF-κB, free intracellular iron and ROS are the main mediators of helenalin-induced cell death in Bcl-2 overexpressing Jurkat cells.

5.2.4 Overcoming pro-survival pathways via selective NF- κ B inhibition and ROS generation

Massive ROS generation can lead to both, apoptosis and necrosis. Apoptosis induction by H₂O₂ for instance is mediated by the release of cytochrome *c* and the activation of transcription factors like NF- κ B which may upregulate death proteins or produce inhibitors of survival proteins⁶². Further effects of ROS on mitochondria have been described such as DNA damage, facilitation of Ca²⁺-induced permeability transition pore opening, induction of dissociation of cardiolipin from cytochrome *c*, which then exits the mitochondria and activates mitochondrial pathway of apoptosis¹⁶⁶. As in our setting Bcl-2 overexpression protects cells from cytochrome *c* release and helenalin inhibits NF- κ B, cells might be forced to switch to necrosis. A switch from apoptosis to necrosis can also occur due to inhibition of caspases¹⁶⁷ or a drop in cellular levels of ATP caused by failure of mitochondrial energy production by oxidants/ROS^{168, 169}. Nevertheless, ROS represent important mediators that are involved in the transduction of the necrotic signal e.g upon stimulation with TNF α where ROS may be generated by mitochondria and glycolysis⁶². Further, helenalin affects the antioxidative system by decreasing intracellular GSH levels^{141, 142}. Hence, by inhibiting NF- κ B, helenalin probably constrains counterregulation by NF- κ B-mediated upregulation of antioxidatives, confirming the assumption that helenalin might therefore cause ROS-stress which the cells cannot handle. To this end, helenalin-induced ROS production as shown here in parallel with impaired antioxidative properties of tumor cells treated with helenalin might account for this success. NF- κ B inhibition by helenalin can act upstream of ROS generation or ROS generation after helenalin-treatment can contribute to inhibition of NF- κ B (as ROS have been shown to inactivate NF- κ B as it is sensitive to oxidative modifications of essential cystein residues¹⁵⁹). It seems that the increase of ROS occurs earlier than the inhibition of NF- κ B by helenalin. Hence, it is possible that the upregulation of ROS levels is not primarily caused by impaired NF- κ B activity, rather the damage caused by ROS generation might be increased by NF- κ B inhibition as NF- κ B acts as a transcription factor for antioxidatives which neutralize ROS.

Several studies showed that helenalin influences a variety of necessary events in the cells by inhibition of Akt²⁵, protein synthesis (by induction of eIF2 α phosphorylation) as well as DNA synthesis⁴, and telomerase²⁶. It also shows anti-proliferative effects²⁷. In this study, we revealed a high chemotherapeutic potential of helenalin, as we were able to add a new way of helenalin's influence on cell signaling by overcoming pro-survival pathways via selective NF- κ B inhibition together with ROS generation.

SUMMARY AND CONCLUSION

6 SUMMARY AND CONCLUSION

The present study highlights the plant compound helenalin to overcome Bcl-2-mediated chemoresistance of tumor cells. Thereby inhibition of Bcl-2-induced upregulation of NF- κ B activity and ROS generation are major players in helenalin provoked non-apoptotic cell death in Bcl-2 overexpressing Jurkat cells.

Interestingly, also with regard to our work, a link between Bcl-2 and constitutive activation of nuclear factor κ B (NF- κ B) has been described in other cells^{153, 154}. For the first time we show here that Bcl-2 overexpressing Jurkat T cells possess increased NF- κ B activity as compared to empty vector control cells. Thus, Bcl-2 might not only prevent apoptosis by inhibition of pro-apoptotic Bax/Bak and subsequently abrogating the intrinsic mitochondrial pathway but also prevents cell death by inducing a NF- κ B driven survival machinery. Using helenalin as tool we could in fact confirm this notion.

In summary, helenalin abrogates Bcl-2-mediated chemoresistance not by impairing the Bcl-2-induced mitochondrial resistance but via inhibition of augmented NF- κ B activity in Bcl-2 overexpressing tumor cells and production of ROS leading to necrosis. Thus, helenalin circumvents classical pathways that are blocked by Bcl-2 overexpression. While other chemotherapeutic agents like etoposide or BMS-345541 are not able to considerably induce cell death in Bcl-2 overexpressing Jurkat cells, this uncommon mode of action seems to be the key for the success of helenalin. Helenalin therefore represents a promising compound to overcome chemoresistance by directly targeting survival strategies of cancer cells like NF- κ B.

In conclusion, we showed that

- **Jurkat cells overexpressing Bcl-2 possess increased NF- κ B activity, which contributes to cell death resistance**
- **by inhibition of NF- κ B through helenalin this resistance can be overcome**
- **ROS generation is crucial for cell death induced by helenalin**
- **among all tested agents and inhibitors it is to emphasize that only helenalin is able to considerably induce cell death in these cells and this fact might be restricted to its unique mode of action.**

Therefore, helenalin is to highlight as a role model for the development of therapeutics for multi-resistant cancer cells.

REFERENCES

7 REFERENCES

1. Saelens, X., Festjens, N., Vande Walle, L., van Gurp, M., van Loo, G., and Vandenamee, P. 2004. Toxic proteins released from mitochondria in cell death. *Oncogene* 23:2861-2874.
2. Frenzel, A., Grespi, F., Chmielewski, W., and Villunger, A. 2009. Bcl2 family proteins in carcinogenesis and the treatment of cancer. *Apoptosis* 14:584-596.
3. Letai, A. 2005. Pharmacological manipulation of Bcl-2 family members to control cell death. *J Clin Invest* 115:2648-2655.
4. Lee, K.H., Hall, I.H., Mar, E.C., Starnes, C.O., ElGebaly, S.A., Waddell, T.G., Hadgraft, R.I., Ruffner, C.G., and Weidner, I. 1977. Sesquiterpene antitumor agents: inhibitors of cellular metabolism. *Science* 196:533-536.
5. Schmidt, T.J. 1999. Toxic activities of sesquiterpene lactones: Structural and biochemical aspects. *Current Organic Chemistry* 3:577-608.
6. Kupchan, S.M., Eakin, M.A., and Thomas, A.M. 1971. Tumor Inhibitors .69. Structure-Cytotoxicity Relationships among Sesquiterpene Lactones. *Journal of Medicinal Chemistry* 14:1147-8.
7. Lee, K.H., Huang, E.S., Piantadosi, C., Pagano, J.S., and Geissman, T.A. 1971. Cytotoxicity of sesquiterpene lactones. *Cancer Res* 31:1649-1654.
8. Zhang, S., Won, Y.K., Ong, C.N., and Shen, H.M. 2005. Anti-cancer potential of sesquiterpene lactones: bioactivity and molecular mechanisms. *Curr Med Chem Anticancer Agents* 5:239-249.
9. Lyss, G., Knorre, A., Schmidt, T.J., Pahl, H.L., and Merfort, I. 1998. The anti-inflammatory sesquiterpene lactone helenalin inhibits the transcription factor NF-kappaB by directly targeting p65. *J Biol Chem* 273:33508-33516.
10. Gertsch, J., Sticher, O., Schmidt, T., and Heilmann, J. 2003. Influence of helenanolide-type sesquiterpene lactones on gene transcription profiles in Jurkat T cells and human peripheral blood cells: anti-inflammatory and cytotoxic effects. *Biochem Pharmacol* 66:2141-2153.
11. Klaas, C.A., Wagner, G., Laufer, S., Sosa, S., Della Loggia, R., Bomme, U., Pahl, H.L., and Merfort, I. 2002. Studies on the anti-inflammatory activity of phytopharmaceuticals prepared from Arnica flowers. *Planta Med* 68:385-391.
12. Hall, I.H., Starnes, C.O., Jr., Lee, K.H., and Waddell, T.G. 1980. Mode of action of sesquiterpene lactones as anti-inflammatory agents. *J Pharm Sci* 69:537-543.
13. Siedle, B., Gustavsson, L., Johansson, S., Murillo, R., Castro, V., Bohlin, L., and Merfort, I. 2003. The effect of sesquiterpene lactones on the release of human neutrophil elastase. *Biochem Pharmacol* 65:897-903.
14. Siedle, B., Garcia-Pineros, A.J., Murillo, R., Schulte-Monting, J., Castro, V., Rungeler, P., Klaas, C.A., Da Costa, F.B., Kisiel, W., and Merfort, I. 2004. Quantitative structure-activity relationship of sesquiterpene lactones as inhibitors of the transcription factor NF-kappaB. *J Med Chem* 47:6042-6054.
15. Picman, A.K. 1986. Biological-Activities of Sesquiterpene Lactones. *Biochemical Systematics and Ecology* 14:255-281.
16. Schmidt, T.J. 1997. Helenanolide-type sesquiterpene lactones--III. Rates and stereochemistry in the reaction of helenalin and related helenanolides with sulfhydryl containing biomolecules. *Bioorg Med Chem* 5:645-653.
17. Ghantous, A., Gali-Muhtasib, H., Vuorela, H., Saliba, N.A., and Darwiche, N. 2010. What made sesquiterpene lactones reach cancer clinical trials? *Drug Discov Today* 15:668-678.
18. Pettit, G.R. 1996. Progress in the discovery of biosynthetic anticancer drugs. *J Nat Prod* 59:812-821.
19. Grippo, A.A., Hall, I.H., Kiyokawa, H., Muraoka, O., Shen, Y.C., and Lee, K.H. 1992. The cytotoxicity of helenalin, its mono and difunctional esters, and related sesquiterpene lactones in murine and human tumor cells. *Drug Des Discov* 8:191-206.
20. Lee, K.H., Ibuka, T., Sims, D., Muraoka, O., Kiyokawa, H., Hall, I.H., and Kim, H.L. 1981. Antitumor agents. 44. Bis(helenaliny) esters and related derivatives as novel potent antileukemic agents. *J Med Chem* 24:924-927.
21. Dirsch, V.M., Stuppner, H., and Vollmar, A.M. 2001. Helenalin triggers a CD95 death receptor-independent apoptosis that is not affected by overexpression of Bcl-x(L) or Bcl-2. *Cancer Res* 61:5817-5823.

22. Lee, K.H., Huang, E.S., and Furukawa, H. 1972. Antitumor Agents .3. Synthesis and Cytotoxic Activity of Helenalin Amine Adducts and Related Derivatives. *Journal of Medicinal Chemistry* 15:609-618.
23. Jordan, J., d'Arcy Doherty, M., and Cohen, G.M. 1987. Effects of glutathione depletion on the cytotoxicity of agents toward a human colonic tumour cell line. *Br J Cancer* 55:627-631.
24. Heilmann, J., Wasescha, M.R., and Schmidt, T.J. 2001. The influence of glutathione and cysteine levels on the cytotoxicity of helenanolide type sesquiterpene lactones against KB cells. *Bioorg Med Chem* 9:2189-2194.
25. Auld, C.A., Hopkins, R.G., Fernandes, K.M., and Morrison, R.F. 2006. Novel effect of helenalin on Akt signaling and Skp2 expression in 3T3-L1 preadipocytes. *Biochem Biophys Res Commun* 346:314-320.
26. Huang, P.R., Yeh, Y.M., and Wang, T.C. 2005. Potent inhibition of human telomerase by helenalin. *Cancer Lett* 227:169-174.
27. Fernandes, K.M., Auld, C.A., Hopkins, R.G., and Morrison, R.F. 2008. Helenalin-mediated post-transcriptional regulation of p21(Cip1) inhibits 3T3-L1 preadipocyte proliferation. *J Cell Biochem* 105:913-921.
28. Hall, I.H., Lee, K.H., Starnes, C.O., Sumida, Y., Wu, R.Y., Waddell, T.G., Cochran, J.W., and Gerhart, K.G. 1979. Anti-inflammatory activity of sesquiterpene lactones and related compounds. *J Pharm Sci* 68:537-542.
29. Tornhamre, S., Schmidt, T.J., Nasman-Glaser, B., Ericsson, I., and Lindgren, J.A. 2001. Inhibitory effects of helenalin and related compounds on 5-lipoxygenase and leukotriene C(4) synthase in human blood cells. *Biochem Pharmacol* 62:903-911.
30. Boulanger, D., Brouillette, E., Jaspar, F., Malouin, F., Mainil, J., Bureau, F., and Lekeux, P. 2007. Helenalin reduces *Staphylococcus aureus* infection in vitro and in vivo. *Vet Microbiol* 119:330-338.
31. Berges, C., Fuchs, D., Opelz, G., Daniel, V., and Naujokat, C. 2009. Helenalin suppresses essential immune functions of activated CD4+ T cells by multiple mechanisms. *Mol Immunol* 46:2892-2901.
32. Lyss, G., Schmidt, T.J., Merfort, I., and Pahl, H.L. 1997. Helenalin, an anti-inflammatory sesquiterpene lactone from Arnica, selectively inhibits transcription factor NF-kappaB. *Biol Chem* 378:951-961.
33. Garcia-Pineros, A.J., Castro, V., Mora, G., Schmidt, T.J., Strunck, E., Pahl, H.L., and Merfort, I. 2001. Cysteine 38 in p65/NF-kappaB plays a crucial role in DNA binding inhibition by sesquiterpene lactones. *J Biol Chem* 276:39713-39720.
34. Hehner, S.P., Hofmann, T.G., Droge, W., and Schmitz, M.L. 1999. The antiinflammatory sesquiterpene lactone parthenolide inhibits NF-kappa B by targeting the I kappa B kinase complex. *J Immunol* 163:5617-5623.
35. Buchele, B., Zugmaier, W., Lunov, O., Syrovets, T., Merfort, I., and Simmet, T. 2010. Surface plasmon resonance analysis of nuclear factor-kappaB protein interactions with the sesquiterpene lactone helenalin. *Anal Biochem* 401:30-37.
36. Antignani, A., and Youle, R.J. 2006. How do Bax and Bak lead to permeabilization of the outer mitochondrial membrane? *Curr Opin Cell Biol* 18:685-689.
37. Reed, J.C. 2006. Proapoptotic multidomain Bcl-2/Bax-family proteins: mechanisms, physiological roles, and therapeutic opportunities. *Cell Death Differ* 13:1378-1386.
38. Youle, R.J., and Strasser, A. 2008. The BCL-2 protein family: opposing activities that mediate cell death. *Nat Rev Mol Cell Biol* 9:47-59.
39. Deng, X.M., Gao, F.Q., Mai, H.Q., and May, W.S. 2001. Multiple-site Bcl2 phosphorylation in the flexible loop domain (FLD) unexpectedly enhances anti-apoptotic function. *Blood* 98:796a-796a.
40. Hockenbery, D.M., Oltvai, Z.N., Yin, X.M., Millman, C.L., and Korsmeyer, S.J. 1993. Bcl-2 functions in an antioxidant pathway to prevent apoptosis. *Cell* 75:241-251.
41. Deng, X.M., Gao, F.Q., and May, W.S. 2003. Bcl2 retards G1/S cell cycle transition by regulating intracellular ROS. *Blood* 102:3179-3185.
42. Yamamoto, K., Ichijo, H., and Korsmeyer, S.J. 1999. BCL-2 is phosphorylated and inactivated by an ASK1/Jun N-terminal protein kinase pathway normally activated at G(2)/M. *Mol Cell Biol* 19:8469-8478.
43. Agostinis, P. 2003. Bcl2 phosphorylation: a tie between cell survival, growth, and ROS. *Blood* 102:3079-3079.
44. Degterev, A., and Yuan, J. 2008. Expansion and evolution of cell death programmes. *Nat Rev Mol Cell Biol* 9:378-390.
45. de Bruin, E.C., and Medema, J.P. 2008. Apoptosis and non-apoptotic deaths in cancer development and treatment response. *Cancer Treat Rev* 34:737-749.

46. Elliott, M.R., and Ravichandran, K.S. 2010. Clearance of apoptotic cells: implications in health and disease. *J Cell Biol* 189:1059-1070.
47. Gyrd-Hansen, M., and Meier, P. 2010. IAPs: from caspase inhibitors to modulators of NF-kappaB, inflammation and cancer. *Nat Rev Cancer* 10:561-574.
48. Samejima, K., and Earnshaw, W.C. 2005. Trashing the genome: the role of nucleases during apoptosis. *Nat Rev Mol Cell Biol* 6:677-688.
49. Peacock, J.W., Palmer, J., Fink, D., Ip, S., Pietras, E.M., Mui, A.L., Chung, S.W., Gleave, M.E., Cox, M.E., Parsons, R., et al. 2009. PTEN loss promotes mitochondrially dependent type II Fas-induced apoptosis via PEA-15. *Mol Cell Biol* 29:1222-1234.
50. Hotchkiss, R.S., Strasser, A., McDunn, J.E., and Swanson, P.E. 2009. Cell death. *N Engl J Med* 361:1570-1583.
51. Luke, C.J., Pak, S.C., Askew, Y.S., Naviglia, T.L., Askew, D.J., Nobar, S.M., Vetica, A.C., Long, O.S., Watkins, S.C., Stolz, D.B., et al. 2007. An intracellular serpin regulates necrosis by inhibiting the induction and sequelae of lysosomal injury. *Cell* 130:1108-1119.
52. Edinger, A.L., and Thompson, C.B. 2004. Death by design: apoptosis, necrosis and autophagy. *Curr Opin Cell Biol* 16:663-669.
53. Krysko, D.V., Vanden Berghe, T., D'Herde, K., and Vandenabeele, P. 2008. Apoptosis and necrosis: detection, discrimination and phagocytosis. *Methods* 44:205-221.
54. Lotze, M.T., and Tracey, K.J. 2005. High-mobility group box 1 protein (HMGB1): nuclear weapon in the immune arsenal. *Nat Rev Immunol* 5:331-342.
55. Degterev, A., Huang, Z., Boyce, M., Li, Y., Jagtap, P., Mizushima, N., Cuny, G.D., Mitchison, T.J., Moskowitz, M.A., and Yuan, J. 2005. Chemical inhibitor of nonapoptotic cell death with therapeutic potential for ischemic brain injury. *Nat Chem Biol* 1:112-119.
56. Holler, N., Zaru, R., Micheau, O., Thome, M., Attinger, A., Valitutti, S., Bodmer, J.L., Schneider, P., Seed, B., and Tschopp, J. 2000. Fas triggers an alternative, caspase-8-independent cell death pathway using the kinase RIP as effector molecule. *Nat Immunol* 1:489-495.
57. Duprez, L., Wirawan, E., Vanden Berghe, T., and Vandenabeele, P. 2009. Major cell death pathways at a glance. *Microbes Infect* 11:1050-1062.
58. Degenhardt, K., Mathew, R., Beaudoin, B., Bray, K., Anderson, D., Chen, G., Mukherjee, C., Shi, Y., Gelinas, C., Fan, Y., et al. 2006. Autophagy promotes tumor cell survival and restricts necrosis, inflammation, and tumorigenesis. *Cancer Cell* 10:51-64.
59. Guidicelli, G., Chaigne-Delalande, B., Dilhuydy, M.S., Pinson, B., Mahfouf, W., Pasquet, J.M., Mahon, F.X., Pourquier, P., Moreau, J.F., and Legembre, P. 2009. The necrotic signal induced by mycophenolic acid overcomes apoptosis-resistance in tumor cells. *PLoS One* 4:e5493.
60. Olofsson, M.H., Ueno, T., Pan, Y., Xu, R., Cai, F., van der Kuip, H., Muerdter, T.E., Sonnenberg, M., Aulitzky, W.E., Schwarz, S., et al. 2007. Cytokeratin-18 is a useful serum biomarker for early determination of response of breast carcinomas to chemotherapy. *Clin Cancer Res* 13:3198-3206.
61. Maiuri, M.C., Zalckvar, E., Kimchi, A., and Kroemer, G. 2007. Self-eating and self-killing: crosstalk between autophagy and apoptosis. *Nat Rev Mol Cell Biol* 8:741-752.
62. Fulda, S., Gorman, A.M., Hori, O., and Samali, A. 2010. Cellular stress responses: cell survival and cell death. *Int J Cell Biol* 2010:214074.
63. Kroemer, G., and White, E. 2010. Autophagy for the avoidance of degenerative, inflammatory, infectious, and neoplastic disease. *Curr Opin Cell Biol* 22:121-123.
64. Gozuacik, D., and Kimchi, A. 2004. Autophagy as a cell death and tumor suppressor mechanism. *Oncogene* 23:2891-2906.
65. Mizushima, N. 2004. Methods for monitoring autophagy. *Int J Biochem Cell Biol* 36:2491-2502.
66. Eisenberg-Lerner, A., Bialik, S., Simon, H.U., and Kimchi, A. 2009. Life and death partners: apoptosis, autophagy and the cross-talk between them. *Cell Death Differ* 16:966-975.
67. Orrenius, S., Zhivotovsky, B., and Nicotera, P. 2003. Regulation of cell death: the calcium-apoptosis link. *Nat Rev Mol Cell Biol* 4:552-565.
68. Szegezdi, E., Macdonald, D.C., Ni Chonghaile, T., Gupta, S., and Samali, A. 2009. Bcl-2 family on guard at the ER. *Am J Physiol Cell Physiol* 296:C941-953.
69. Hoyer-Hansen, M., and Jaattela, M. 2007. Connecting endoplasmic reticulum stress to autophagy by unfolded protein response and calcium. *Cell Death Differ* 14:1576-1582.
70. Ullman, E., Fan, Y., Stawowczyk, M., Chen, H.M., Yue, Z., and Zong, W.X. 2008. Autophagy promotes necrosis in apoptosis-deficient cells in response to ER stress. *Cell Death Differ* 15:422-425.
71. Boya, P., and Kroemer, G. 2009. Beclin 1: a BH3-only protein that fails to induce apoptosis. *Oncogene* 28:2125-2127.

72. Patingre, S., Tassa, A., Qu, X., Garuti, R., Liang, X.H., Mizushima, N., Packer, M., Schneider, M.D., and Levine, B. 2005. Bcl-2 antiapoptotic proteins inhibit Beclin 1-dependent autophagy. *Cell* 122:927-939.
73. He, C.C., and Levine, B. 2010. The Beclin 1 interactome. *Current Opinion in Cell Biology* 22:140-149.
74. Pinton, P., Giorgi, C., Siviero, R., Zecchini, E., and Rizzuto, R. 2008. Calcium and apoptosis: ER-mitochondria Ca²⁺ transfer in the control of apoptosis. *Oncogene* 27:6407-6418.
75. Sakaki, K., Wu, J., and Kaufman, R.J. 2008. Protein kinase C θ is required for autophagy in response to stress in the endoplasmic reticulum. *J Biol Chem* 283:15370-15380.
76. Hoyer-Hansen, M., Bastholm, L., Szyniarowski, P., Campanella, M., Szabadkai, G., Farkas, T., Bianchi, K., Fehrenbacher, N., Elling, F., Rizzuto, R., et al. 2007. Control of macroautophagy by calcium, calmodulin-dependent kinase kinase- β , and Bcl-2. *Mol Cell* 25:193-205.
77. Kim, I., Xu, W., and Reed, J.C. 2008. Cell death and endoplasmic reticulum stress: disease relevance and therapeutic opportunities. *Nat Rev Drug Discov* 7:1013-1030.
78. Nguyen, M., Millar, D.G., Yong, V.W., Korsmeyer, S.J., and Shore, G.C. 1993. Targeting of Bcl-2 to the mitochondrial outer membrane by a COOH-terminal signal anchor sequence. *J Biol Chem* 268:25265-25268.
79. Lithgow, T., Vandriel, R., Bertram, J.F., and Strasser, A. 1994. The Protein Product of the Oncogene Bcl-2 Is a Component of the Nuclear-Envelope, the Endoplasmic-Reticulum, and the Outer Mitochondrial-Membrane. *Cell Growth & Differentiation* 5:411-417.
80. Adams, J.M., and Cory, S. 2007. The Bcl-2 apoptotic switch in cancer development and therapy. *Oncogene* 26:1324-1337.
81. Sasi, N., Hwang, M., Jaboin, J., Csiki, I., and Lu, B. 2009. Regulated cell death pathways: new twists in modulation of BCL2 family function. *Mol Cancer Ther* 8:1421-1429.
82. Tsujimoto, Y., and Shimizu, S. 2007. Role of the mitochondrial membrane permeability transition in cell death. *Apoptosis* 12:835-840.
83. Odnokova, I.V., Sung, K.F., Mareninova, O.A., Hermann, K., Gukovsky, I., and Gukovskaya, A.S. 2008. Mitochondrial mechanisms of death responses in pancreatitis. *J Gastroenterol Hepatol* 23 Suppl 1:S25-30.
84. Odnokova, I.V., Sung, K.F., Mareninova, O.A., Hermann, K., Evtodienko, Y., Andreyev, A., Gukovsky, I., and Gukovskaya, A.S. 2009. Mechanisms regulating cytochrome c release in pancreatic mitochondria. *Gut* 58:431-442.
85. Reed, J.C. 2008. Bcl-2-family proteins and hematologic malignancies: history and future prospects. *Blood* 111:3322-3330.
86. Strasser, A., Harris, A.W., Huang, D.C., Krammer, P.H., and Cory, S. 1995. Bcl-2 and Fas/APO-1 regulate distinct pathways to lymphocyte apoptosis. *EMBO J* 14:6136-6147.
87. Huang, D.C., Hahne, M., Schroeter, M., Frei, K., Fontana, A., Villunger, A., Newton, K., Tschopp, J., and Strasser, A. 1999. Activation of Fas by FasL induces apoptosis by a mechanism that cannot be blocked by Bcl-2 or Bcl-x(L). *Proc Natl Acad Sci U S A* 96:14871-14876.
88. Scorrano, L., Oakes, S.A., Opferman, J.T., Cheng, E.H., Sorcinelli, M.D., Pozzan, T., and Korsmeyer, S.J. 2003. BAX and BAK regulation of endoplasmic reticulum Ca²⁺: a control point for apoptosis. *Science* 300:135-139.
89. Choi, J., Choi, K., Benveniste, E.N., Rho, S.B., Hong, Y.S., Lee, J.H., Kim, J., and Park, K. 2005. Bcl-2 promotes invasion and lung metastasis by inducing matrix metalloproteinase-2. *Cancer Res* 65:5554-5560.
90. Del Bufalo, D., Biroccio, A., Leonetti, C., and Zupi, G. 1997. Bcl-2 overexpression enhances the metastatic potential of a human breast cancer line. *FASEB J* 11:947-953.
91. Biroccio, A., Candiloro, A., Mottolese, M., Sapora, O., Albini, A., Zupi, G., and Del Bufalo, D. 2000. Bcl-2 overexpression and hypoxia synergistically act to modulate vascular endothelial growth factor expression and in vivo angiogenesis in a breast carcinoma line. *FASEB J* 14:652-660.
92. Iervolino, A., Trisciuglio, D., Ribatti, D., Candiloro, A., Biroccio, A., Zupi, G., and Del Bufalo, D. 2002. Bcl-2 overexpression in human melanoma cells increases angiogenesis through VEGF mRNA stabilization and HIF-1-mediated transcriptional activity. *FASEB J* 16:1453-1455.
93. Kim, R., Emi, M., Matsuura, K., and Tanabe, K. 2007. Antisense and nonantisense effects of antisense Bcl-2 on multiple roles of Bcl-2 as a chemosensitizer in cancer therapy. *Cancer Gene Ther* 14:1-11.

94. Gabrilovich, D.I., Chen, H.L., Girgis, K.R., Cunningham, H.T., Meny, G.M., Nadaf, S., Kavanaugh, D., and Carbone, D.P. 1996. Production of vascular endothelial growth factor by human tumors inhibits the functional maturation of dendritic cells. *Nat Med* 2:1096-1103.
95. Lickliter, J.D., Cox, J., McCarron, J., Martinez, N.R., Schmidt, C.W., Lin, H., Nieda, M., and Nicol, A.J. 2007. Small-molecule Bcl-2 inhibitors sensitise tumour cells to immune-mediated destruction. *Br J Cancer* 96:600-608.
96. Fulda, S. 2009. Tumor resistance to apoptosis. *Int J Cancer* 124:511-515.
97. Tsujimoto, Y., Yunis, J., Onorato-Showe, L., Erikson, J., Nowell, P.C., and Croce, C.M. 1984. Molecular cloning of the chromosomal breakpoint of B-cell lymphomas and leukemias with the t(11;14) chromosome translocation. *Science* 224:1403-1406.
98. McDonnell, T.J., and Korsmeyer, S.J. 1991. Progression from lymphoid hyperplasia to high-grade malignant lymphoma in mice transgenic for the t(14; 18). *Nature* 349:254-256.
99. Traver, D., Akashi, K., Weissman, I.L., and Lagasse, E. 1998. Mice defective in two apoptosis pathways in the myeloid lineage develop acute myeloblastic leukemia. *Immunity* 9:47-57.
100. Vaux, D.L., Cory, S., and Adams, J.M. 1988. Bcl-2 gene promotes haemopoietic cell survival and cooperates with c-myc to immortalize pre-B cells. *Nature* 335:440-442.
101. Strasser, A., Harris, A.W., Bath, M.L., and Cory, S. 1990. Novel primitive lymphoid tumours induced in transgenic mice by cooperation between myc and bcl-2. *Nature* 348:331-333.
102. Chonghaile, T.N., and Letai, A. 2008. Mimicking the BH3 domain to kill cancer cells. *Oncogene* 27 Suppl 1:S149-157.
103. Kang, M.H., and Reynolds, C.P. 2009. Bcl-2 inhibitors: targeting mitochondrial apoptotic pathways in cancer therapy. *Clin Cancer Res* 15:1126-1132.
104. Vogler, M., Dinsdale, D., Dyer, M.J., and Cohen, G.M. 2009. Bcl-2 inhibitors: small molecules with a big impact on cancer therapy. *Cell Death Differ* 16:360-367.
105. Walczak, H., Bouchon, A., Stahl, H., and Krammer, P.H. 2000. Tumor necrosis factor-related apoptosis-inducing ligand retains its apoptosis-inducing capacity on Bcl-2- or Bcl-xL-overexpressing chemotherapy-resistant tumor cells. *Cancer Res* 60:3051-3057.
106. Nicoletti, I., Migliorati, G., Pagliacci, M.C., Grignani, F., and Riccardi, C. 1991. A rapid and simple method for measuring thymocyte apoptosis by propidium iodide staining and flow cytometry. *J Immunol Methods* 139:271-279.
107. Leist, M., Volbracht, C., Fava, E., and Nicotera, P. 1998. 1-Methyl-4-phenylpyridinium induces autocrine excitotoxicity, protease activation, and neuronal apoptosis. *Mol Pharmacol* 54:789-801.
108. Bradford, M.M. 1976. Rapid and Sensitive Method for Quantitation of Microgram Quantities of Protein Utilizing Principle of Protein-Dye Binding. *Analytical Biochemistry* 72:248-254.
109. Laemmli, U.K. 1970. Cleavage of structural proteins during the assembly of the head of bacteriophage T4. *Nature* 227:680-685.
110. Kurien, B.T., and Scofield, R.H. 2003. Protein blotting: a review. *J Immunol Methods* 274:1-15.
111. Lassus, P., Opitz-Araya, X., and Lazebnik, Y. 2002. Requirement for caspase-2 in stress-induced apoptosis before mitochondrial permeabilization. *Science* 297:1352-1354.
112. Park, M.T., Kim, M.J., Kang, Y.H., Choi, S.Y., Lee, J.H., Choi, J.A., Kang, C.M., Cho, C.K., Kang, S., Bae, S., et al. 2005. Phytosphingosine in combination with ionizing radiation enhances apoptotic cell death in radiation-resistant cancer cells through ROS-dependent and -independent AIF release. *Blood* 105:1724-1733.
113. Pullar, J.M., Thomson, S.J., King, M.J., Turnbull, C.I., Midwinter, R.G., and Hampton, M.B. 2004. The chemopreventive agent phenethyl isothiocyanate sensitizes cells to Fas-mediated apoptosis. *Carcinogenesis* 25:765-772.
114. Thomson, S.J., Brown, K.K., Pullar, J.M., and Hampton, M.B. 2006. Phenethyl isothiocyanate triggers apoptosis in Jurkat cells made resistant by the overexpression of Bcl-2. *Cancer Res* 66:6772-6777.
115. Martinou, J.C., and Youle, R.J. 2006. Which came first, the cytochrome c release or the mitochondrial fission? *Cell Death Differ* 13:1291-1295.
116. Scorrano, L., Ashiya, M., Buttle, K., Weiler, S., Oakes, S.A., Mannella, C.A., and Korsmeyer, S.J. 2002. A distinct pathway remodels mitochondrial cristae and mobilizes cytochrome c during apoptosis. *Dev Cell* 2:55-67.
117. Germain, M., Mathai, J.P., McBride, H.M., and Shore, G.C. 2005. Endoplasmic reticulum BIK initiates DRP1-regulated remodelling of mitochondrial cristae during apoptosis. *EMBO J* 24:1546-1556.
118. Li, J., Ni, M., Lee, B., Barron, E., Hinton, D.R., and Lee, A.S. 2008. The unfolded protein response regulator GRP78/BiP is required for endoplasmic reticulum integrity and stress-induced autophagy in mammalian cells. *Cell Death Differ* 15:1460-1471.

119. Degterev, A., Hitomi, J., Germscheid, M., Ch'en, I.L., Korkina, O., Teng, X., Abbott, D., Cuny, G.D., Yuan, C., Wagner, G., et al. 2008. Identification of RIP1 kinase as a specific cellular target of necrostatins. *Nat Chem Biol* 4:313-321.
120. Miao, B., and Degterev, A. 2009. Methods to analyze cellular necroptosis. *Methods Mol Biol* 559:79-93.
121. Ricca, A., Biroccio, A., Del Bufalo, D., Mackay, A.R., Santoni, A., and Cippitelli, M. 2000. bcl-2 over-expression enhances NF-kappaB activity and induces mmp-9 transcription in human MCF7(ADR) breast-cancer cells. *Int J Cancer* 86:188-196.
122. Kiessling, M.K., Klemke, C.D., Kaminski, M.M., Galani, I.E., Krammer, P.H., and Gulow, K. 2009. Inhibition of constitutively activated nuclear factor-kappaB induces reactive oxygen species- and iron-dependent cell death in cutaneous T-cell lymphoma. *Cancer Res* 69:2365-2374.
123. Burke, J.R., Pattoli, M.A., Gregor, K.R., Brassil, P.J., MacMaster, J.F., McIntyre, K.W., Yang, X., Iotzova, V.S., Clarke, W., Strnad, J., et al. 2003. BMS-345541 is a highly selective inhibitor of I kappa B kinase that binds at an allosteric site of the enzyme and blocks NF-kappa B-dependent transcription in mice. *J Biol Chem* 278:1450-1456.
124. Franke, T.F. 2008. PI3K/Akt: getting it right matters. *Oncogene* 27:6473-6488.
125. Guzman, M.L., Rossi, R.M., Neelakantan, S., Li, X., Corbett, C.A., Hassane, D.C., Becker, M.W., Bennett, J.M., Sullivan, E., Lachowicz, J.L., et al. 2007. An orally bioavailable parthenolide analog selectively eradicates acute myelogenous leukemia stem and progenitor cells. *Blood* 110:4427-4435.
126. Kim, J.H., Liu, L., Lee, S.O., Kim, Y.T., You, K.R., and Kim, D.G. 2005. Susceptibility of cholangiocarcinoma cells to parthenolide-induced apoptosis. *Cancer Res* 65:6312-6320.
127. Steele, A.J., Jones, D.T., Ganeshaguru, K., Duke, V.M., Yogashangary, B.C., North, J.M., Lowdell, M.W., Kottaridis, P.D., Mehta, A.B., Prentice, A.G., et al. 2006. The sesquiterpene lactone parthenolide induces selective apoptosis of B-chronic lymphocytic leukemia cells in vitro. *Leukemia* 20:1073-1079.
128. Dirsch, V.M., Stuppner, H., and Vollmar, A.M. 2001. Cytotoxic sesquiterpene lactones mediate their death-inducing effect in leukemia T cells by triggering apoptosis. *Planta Med* 67:557-559.
129. Lopez-Anton, N., Hermann, C., Murillo, R., Merfort, I., Wanner, G., Vollmar, A.M., and Dirsch, V.M. 2007. Sesquiterpene lactones induce distinct forms of cell death that modulate human monocyte-derived macrophage responses. *Apoptosis* 12:141-153.
130. Shen, H.M., and Liu, Z.G. 2006. JNK signaling pathway is a key modulator in cell death mediated by reactive oxygen and nitrogen species. *Free Radic Biol Med* 40:928-939.
131. Weston, C.R., and Davis, R.J. 2007. The JNK signal transduction pathway. *Curr Opin Cell Biol* 19:142-149.
132. Ogino, T., Ozaki, M., Hosako, M., Omori, M., Okada, S., and Matsukawa, A. 2009. Activation of c-Jun N-terminal kinase is essential for oxidative stress-induced Jurkat cell apoptosis by monochloramine. *Leuk Res* 33:151-158.
133. Krilleke, D., Ucur, E., Pulte, D., Schulze-Osthoff, K., Debatin, K.M., and Herr, I. 2003. Inhibition of JNK signaling diminishes early but not late cellular stress-induced apoptosis. *Int J Cancer* 107:520-527.
134. Li, D.D., Wang, L.L., Deng, R., Tang, J., Shen, Y., Guo, J.F., Wang, Y., Xia, L.P., Feng, G.K., Liu, Q.Q., et al. 2009. The pivotal role of c-Jun NH2-terminal kinase-mediated Beclin 1 expression during anticancer agents-induced autophagy in cancer cells. *Oncogene* 28:886-898.
135. Park, K.J., Lee, S.H., Lee, C.H., Jang, J.Y., Chung, J., Kwon, M.H., and Kim, Y.S. 2009. Upregulation of Beclin-1 expression and phosphorylation of Bcl-2 and p53 are involved in the JNK-mediated autophagic cell death. *Biochem Biophys Res Commun* 382:726-729.
136. Djavaheri-Mergny, M., Amelotti, M., Mathieu, J., Besancon, F., Bauvy, C., Souquere, S., Pierron, G., and Codogno, P. 2006. NF-kappaB activation represses tumor necrosis factor-alpha-induced autophagy. *J Biol Chem* 281:30373-30382.
137. Ron, D., and Walter, P. 2007. Signal integration in the endoplasmic reticulum unfolded protein response. *Nat Rev Mol Cell Biol* 8:519-529.
138. Boyce, M., and Yuan, J. 2006. Cellular response to endoplasmic reticulum stress: a matter of life or death. *Cell Death Differ* 13:363-373.
139. Pelletier, N., Casamayor-Palleja, M., De Luca, K., Mondiere, P., Saltel, F., Jurdic, P., Bella, C., Genestier, L., and Defrance, T. 2006. The endoplasmic reticulum is a key component of the plasma cell death pathway. *J Immunol* 176:1340-1347.
140. Morishima, N., Nakanishi, K., Takenouchi, H., Shibata, T., and Yasuhiko, Y. 2002. An endoplasmic reticulum stress-specific caspase cascade in apoptosis. Cytochrome c-independent activation of caspase-9 by caspase-12. *J Biol Chem* 277:34287-34294.

141. Merrill, J., Kim, H.L., and Safe, S. 1986. Helenalin: mechanism of toxic action. *Adv Exp Med Biol* 197:891-896.
142. Jodynis-Liebert, J., Murias, M., and Bloszyk, E. 1999. Effect of several sesquiterpene lactones on lipid peroxidation and glutathione level. *Planta Med* 65:320-324.
143. Powis, G., Gallegos, A., Abraham, R.T., Ashendel, C.L., Zalkow, L.H., Grindey, G.B., and Bonjouklian, R. 1994. Increased intracellular Ca²⁺ signaling caused by the antitumor agent helenalin and its analogues. *Cancer Chemother Pharmacol* 34:344-350.
144. Olofsson, M.H., Havelka, A.M., Brnjic, S., Shoshan, M.C., and Linder, S. 2008. Charting calcium-regulated apoptosis pathways using chemical biology: role of calmodulin kinase II. *BMC Chem Biol* 8:2.
145. Liou, Y.F., Hall, I.H., Lee, K.H., Williams, W.L., Jr., and Chaney, S.G. 1983. Investigation of sesquiterpene lactones as protein synthesis inhibitors of P-388 lymphocytic leukemia cells. *Biochim Biophys Acta* 739:190-196.
146. Bell, B.D., Leverrier, S., Weist, B.M., Newton, R.H., Arechiga, A.F., Luhrs, K.A., Morrisette, N.S., and Walsh, C.M. 2008. FADD and caspase-8 control the outcome of autophagic signaling in proliferating T cells. *Proc Natl Acad Sci U S A* 105:16677-16682.
147. Ghosh, S., and Hayden, M.S. 2008. New regulators of NF-kappaB in inflammation. *Nat Rev Immunol* 8:837-848.
148. Baud, V., and Karin, M. 2009. Is NF-kappaB a good target for cancer therapy? Hopes and pitfalls. *Nat Rev Drug Discov* 8:33-40.
149. Viatour, P., Bentires-Alj, M., Chariot, A., Deregowski, V., de Leval, L., Merville, M.P., and Bours, V. 2003. NF- kappa B2/p100 induces Bcl-2 expression. *Leukemia* 17:1349-1356.
150. Braun, T., Carvalho, G., Fabre, C., Grosjean, J., Fenaux, P., and Kroemer, G. 2006. Targeting NF-kappaB in hematologic malignancies. *Cell Death Differ* 13:748-758.
151. Karin, M. 2006. Nuclear factor-kappaB in cancer development and progression. *Nature* 441:431-436.
152. Aggarwal, B.B. 2004. Nuclear factor-kappaB: the enemy within. *Cancer Cell* 6:203-208.
153. de Moissac, D., Zheng, H., and Kirshenbaum, L.A. 1999. Linkage of the BH4 domain of Bcl-2 and the nuclear factor kappaB signaling pathway for suppression of apoptosis. *J Biol Chem* 274:29505-29509.
154. Regula, K.M., Ens, K., and Kirshenbaum, L.A. 2002. IKK beta is required for Bcl-2-mediated NF-kappa B activation in ventricular myocytes. *J Biol Chem* 277:38676-38682.
155. Mortenson, M.M., Galante, J.G., Gilad, O., Schlieman, M.G., Virudachalam, S., Kung, H.J., and Bold, R.J. 2007. BCL-2 functions as an activator of the AKT signaling pathway in pancreatic cancer. *J Cell Biochem* 102:1171-1179.
156. Heckman, C.A., Mehew, J.W., and Boxer, L.M. 2002. NF-kappaB activates Bcl-2 expression in t(14;18) lymphoma cells. *Oncogene* 21:3898-3908.
157. Kurland, J.F., Kodym, R., Story, M.D., Spurgers, K.B., McDonnell, T.J., and Meyn, R.E. 2001. NF-kappaB1 (p50) homodimers contribute to transcription of the bcl-2 oncogene. *J Biol Chem* 276:45380-45386.
158. Kurland, J.F., Voehringer, D.W., and Meyn, R.E. 2003. The MEK/ERK pathway acts upstream of NF kappa B1 (p50) homodimer activity and Bcl-2 expression in a murine B-cell lymphoma cell line. MEK inhibition restores radiation-induced apoptosis. *J Biol Chem* 278:32465-32470.
159. Trachootham, D., Zhou, Y., Zhang, H., Demizu, Y., Chen, Z., Pelicano, H., Chiao, P.J., Achanta, G., Arlinghaus, R.B., Liu, J., et al. 2006. Selective killing of oncogenically transformed cells through a ROS-mediated mechanism by beta-phenylethyl isothiocyanate. *Cancer Cell* 10:241-252.
160. Clement, M.V., Hirpara, J.L., and Pervaiz, S. 2003. Decrease in intracellular superoxide sensitizes Bcl-2-overexpressing tumor cells to receptor and drug-induced apoptosis independent of the mitochondria. *Cell Death Differ* 10:1273-1285.
161. Chen, Z.X., and Pervaiz, S. 2009. BCL-2: pro-or anti-oxidant? *Front Biosci (Elite Ed)* 1:263-268.
162. Mirkovic, N., Voehringer, D.W., Story, M.D., McConkey, D.J., McDonnell, T.J., and Meyn, R.E. 1997. Resistance to radiation-induced apoptosis in Bcl-2-expressing cells is reversed by depleting cellular thiols. *Oncogene* 15:1461-1470.
163. Kamata, H., Honda, S., Maeda, S., Chang, L., Hirata, H., and Karin, M. 2005. Reactive oxygen species promote TNFalpha-induced death and sustained JNK activation by inhibiting MAP kinase phosphatases. *Cell* 120:649-661.
164. Bubici, C., Papa, S., Dean, K., and Franzoso, G. 2006. Mutual cross-talk between reactive oxygen species and nuclear factor-kappa B: molecular basis and biological significance. *Oncogene* 25:6731-6748.

165. Pham, C.G., Bubici, C., Zazzeroni, F., Papa, S., Jones, J., Alvarez, K., Jayawardena, S., De Smaele, E., Cong, R., Beaumont, C., et al. 2004. Ferritin heavy chain upregulation by NF-kappaB inhibits TNFalpha-induced apoptosis by suppressing reactive oxygen species. *Cell* 119:529-542.
166. Roderick, H.L., and Cook, S.J. 2008. Ca²⁺ signalling checkpoints in cancer: remodelling Ca²⁺ for cancer cell proliferation and survival. *Nat Rev Cancer* 8:361-375.
167. Melino, G., Bernassola, F., Knight, R.A., Corasaniti, M.T., Nistico, G., and Finazzi-Agro, A. 1997. S-nitrosylation regulates apoptosis. *Nature* 388:432-433.
168. Leist, M., Single, B., Naumann, H., Fava, E., Simon, B., Kuhnle, S., and Nicotera, P. 1999. Inhibition of mitochondrial ATP generation by nitric oxide switches apoptosis to necrosis. *Exp Cell Res* 249:396-403.
169. Tsujimoto, Y., Shimizu, S., Eguchi, Y., Kamiike, W., and Matsuda, H. 1997. Bcl-2 and Bcl-xL block apoptosis as well as necrosis: possible involvement of common mediators in apoptotic and necrotic signal transduction pathways. *Leukemia* 11 Suppl 3:380-382.

APPENDIX

8 APPENDIX

8.1 Abbreviations

AIF	Apoptosis inducing factor
ALL	Acute lymphocytic leukemia
AML	Acute myelogenous leukemia
ANOVA	Analysis of variance between groups
ANT	Adenine nucleotide translocator
AP 1	Activator protein 1
Apaf-1	Apoptotic protease-activating factor-1
APS	Ammonium persulfate
ASK1	Apoptosis signal-regulating kinase 1
ATF6	Activating transcription factor 6
ATP/dATP	Adenosine-5'-triphosphate/2'-desoxyadenosine-5'-triphosphate
Bcl	B-cell lymphoma
BH	Bcl-2 homology
BIR	Baculoviral IAP repeats
BSA	Bovine serum albumin
CAD	Caspase-activated DNase
CaMKK β	Calcium/calmodulin-dependent kinase kinase- β
CAPS	3-(Cyclohexylamino)-1-propanesulfonic acid
CARD	Caspase recruitment domain
CDK	Cyclin-dependent kinase
cIAP	Cellular inhibitor of apoptosis
CLL	Chronic lymphocytic leukemia
CPRG	Chlorophenol Red- β -D-galactoside
CypD	Cyclophilin D
DAMP	Damage-associated molecular pattern
DAP kinase	Death-associated protein kinase
DD	Death domain
DED	Death effector domain
DIABLO	Direct IAP binding protein with low pI
DISC	Death inducing signaling complex
DMSO	Dimethyl sulfoxide
DNA	Deoxyribonucleic acid
DTT	Dithiothreitol

ECL	Enhanced chemiluminescence
EDTA	Ethylenediaminetetraacetic acid
EGTA	Ethylene glycol-bis(2-aminoethylether)tetraacetic acid
eIF2 α	Eukaryotic translocation initiation factor-2
EMSA	Electromobility shift assay
EndoG	Endonuclease G
ER	Endoplasmatic reticulum
FACS	Fluorescence-activated cell sorter
FADD	Fas-associated death domain
FasL	Fas ligand
FCS g	Fetal calf serum gold
Fig	Figure
FL	Fluorescence
FSC	Forward scatter
GRP78	Glucose-related protein 78
GTP/GDP	Guanosine-5'-tri/diphosphate
h	Hour(s)
Hele	Helenalin
HEPES	N-(2-hydroxyethyl)piperazine-N'-(2-ethanesulfonic acid)
HFS	Hypotonic fluorochrome solution
HMGB1	high-mobility group box 1
HRP	Horseradish peroxidase
HtrA2	High temperature requirement protein A2
IAP	Inhibitor of apoptosis protein
IKK	I κ B kinase
IMM	Inner mitochondrial membrane
IP ₃	Inositol triphosphate
IP ₃ R	Inositol triphosphate receptor
IRE	Inositol-requiring enzyme
IRES	Internal ribosome entry site
JNK	c-Jun N-terminal kinase
kDa	Kilo Dalton
Lamp2	Lysosomal-associated membrane protein 2
MAPK	Mitogen-activated protein kinase
MMP	Mitochondrial membrane potential
MMP-9	Matrix metalloproteinase 9
MOMP	Mitochondrial outer membrane permeabilization
MPT	Mitochondrial membrane permeability transition

mRNA	Messenger RNA
NAC	N-acetyl-L-cysteine
NaF	Sodium fluoride
NCI	National Cancer Institute
NEAA	Non essential amino acids
Nec-1	Necrostatin-1
NF- κ B	Nuclear factor-kappa B
nt	Non-targeting
OMM	Outer mitochondrial membrane
p-	Phospho-
PAA	Polyacrylamide
PARP	poly-ADP-ribose polymerase
PBS	Phosphate buffered saline
PBS-T	Phosphate buffered saline with Tween
PE	Phosphatidylethanolamine
PERK	PKR-like ER kinase
pI	Isoelectric point
PI	Propidium iodide
PKC θ	Protein kinase C θ
PMSF	Phenylmethylsulphonylfluoride
PS	Phosphatidylserine
PT	Permeability transition
PTEN	Phosphatidylinositol(3,4,5)-triphosphate phosphatase
PTP	Permeability transition pore
Q-VD-OPh	N-(2-Quinolyl)valyl-aspartyl-(2,6-difluorophenoxy)methylketone
RIP1	Receptor interacting protein 1
RNA	Ribonucleic acid
ROS	Reactive oxygen species
rpm	Rotations per minute
SDS	Sodium dodecyl sulfate
SDS-PAGE	Sodium dodecyl sulfate polyacrylamide gel electrophoresis
SEM	Standard error of mean
Ser	Serine
siRNA	Small interfering RNA
Smac	Second mitochondria derived activator of caspases
SSC	Sideward scatter
T/E	Trypsin/EDTA
Tax	Paclitaxel

t-Bid	Truncated Bid
TEMED	N,N,N',N' tetramethylethylene diamine
TG	Thapsigargin
Thr	Threonine
TNFR1	TNF receptor1
TNF α	Tumor necrosis factor α
TRAF2	TNF receptor-associated factor 2
TRAIL	TNF-related apoptosis inducing ligand
Tris	Trishydroxymethylaminomethane
UPR	Unfolded protein response
UVRAG	UV irradiation resistance-associated tumor suppressor gene
VDAC	Voltage dependent anion channel
WM	Wortmannin
XIAP	X-chromosome linked IAP

8.2 Publications

8.2.1 Original Publications

Hoffmann R, López Antón N, Wanner G, von Schwarzenberg K, Dirsch V, Rudy A and Vollmar AM; Helenalin bypasses Bcl-2-mediated cell death resistance by inhibiting NF- κ B and promoting reactive oxygen species generation. JBC. Submitted.

Strasser R, Schorr S, Glas A, Reißner T, Hoffmann R, Vollmar AM and Carell T. Rad14 confers specificity for bulky adducts in nucleotide excision repair. In preparation.

Schmidt C, Messmer R, Bracher F and Krauss J. A new approach to furan-containing macrolactones. Turk. J. Chem. 2007 June;31(3):251-256.

8.2.2 Abstracts

Meßmer R, López Antón N, Dirsch VM, Rudy A, Vollmar AM. Characterisation of helenalin-induced apoptosis in Bcl-2 overexpressing Jurkat cells. ApopTrain Summer School, July 2008, Ulm, Germany.

Hoffmann R, López Antón N, Dirsch VM, Vollmar AM, Rudy A. The antiapoptotic protein Bcl-2 is not able to prevent helenalin-induced cell death. 50. Frühjahrstagung der DGPT, March 2009, Mainz, Germany.

Hoffmann R, López Antón N, Dirsch VM, Vollmar AM, Rudy A. The antiapoptotic protein Bcl-2 is not able to prevent helenalin-induced cell death. <interact>2009, March 2009, Munich, Germany.

8.3 Curriculum vitae

Personal data

Name	Ruth Hoffmann, maiden name Meßmer
Date of birth	14 th June 1982
Place of birth	Spaichingen
Nationality	German

Academic education

09/07-10/10	PhD thesis at the department of pharmacy, pharmaceutical biology, LMU Munich, Prof. Dr. A.M. Vollmar
01/07-05/07	Department of pharmacy, pharmaceutical biology, LMU Munich, Prof. Dr. A.M. Vollmar
07/07	Licensed pharmacist
10/01-06/07	Study of pharmacy at the LMU Munich <ul style="list-style-type: none">• 06/07: 3rd state examination• 02/06: 2nd state examination• 08/03: 1st state examination
01/07-05/07	Department of pharmacy, pharmaceutical biology, LMU Munich, Prof. Dr. A.M. Vollmar

School education

1992-2001	Gymnasium Spaichingen, Spaichingen
1988-1992	Rupert-Mayer-Schule, primary school, Spaichingen

Work experience

11/06-01/07	Hexal AG, Holzkirchen
05/06-10/06	Internationale Ludwigs-Apotheke, Munich

8.4 Acknowledgements

First and foremost, I would like to thank Prof. Dr. Angelika M. Vollmar for giving me the opportunity to perform my Ph.D. studies in her laboratories. Her expert and excellent supervision and mentorship always motivated me. I also highly appreciate that she trusted in my ideas and my opinion. She always and in any situation had time for me.

Further I would like to thank all members of the thesis committee. Special thanks go to PD Dr. Manfred Ogris for his time and effort as second advisor for this thesis.

I am seriously grateful to my two postdoctoral supervisors Dr. Anita Rudy and Dr. Karin von Schwarzenberg and also to Dr. Robert Fürst for their support throughout this work.

I would especially like to thank all my colleagues for their helpfulness and the warm and friendly atmosphere. I am very indebted to Jana, Bianca and Frau Schnegg, Rita and Bernadette for their great help whenever I needed it. For numerous discussions, helpful advices not only concerning work and of course leisure time activities like the “sushi meetings”, I want to thank Ulla, Bettina, Nina, Christine, Hanna and Bianca. Thank you for being more than just colleagues.

Gratitude goes as well to Florian and Bettina for proof-reading the manuscript.

I am especially indebted to my two families, the ‘Meßmers’ and the ‘Hoffmanns’. I am sincerely grateful for their blessings and constant moral support!

And Florian, there are no words to express how much your endless support, encouragement, patience and love have helped me.